

2012

## IDENTIFICATION OF SUMOYLATED PROTEINS AND INVESTIGATION OF PROTEIN UBIQUITINATION IN THE NF- $\kappa$ B PATHWAY

Xiaoyan Liu

University of Kentucky, xliua@uky.edu

[Right click to open a feedback form in a new tab to let us know how this document benefits you.](#)

### Recommended Citation

Liu, Xiaoyan, "IDENTIFICATION OF SUMOYLATED PROTEINS AND INVESTIGATION OF PROTEIN UBIQUITINATION IN THE NF- $\kappa$ B PATHWAY" (2012). *Theses and Dissertations--Molecular and Cellular Biochemistry*. 4.

[https://uknowledge.uky.edu/biochem\\_etds/4](https://uknowledge.uky.edu/biochem_etds/4)

This Doctoral Dissertation is brought to you for free and open access by the Molecular and Cellular Biochemistry at UKnowledge. It has been accepted for inclusion in Theses and Dissertations--Molecular and Cellular Biochemistry by an authorized administrator of UKnowledge. For more information, please contact [UKnowledge@lsv.uky.edu](mailto:UKnowledge@lsv.uky.edu).

## **STUDENT AGREEMENT:**

I represent that my thesis or dissertation and abstract are my original work. Proper attribution has been given to all outside sources. I understand that I am solely responsible for obtaining any needed copyright permissions. I have obtained and attached hereto needed written permission statements(s) from the owner(s) of each third-party copyrighted matter to be included in my work, allowing electronic distribution (if such use is not permitted by the fair use doctrine).

I hereby grant to The University of Kentucky and its agents the non-exclusive license to archive and make accessible my work in whole or in part in all forms of media, now or hereafter known. I agree that the document mentioned above may be made available immediately for worldwide access unless a preapproved embargo applies.

I retain all other ownership rights to the copyright of my work. I also retain the right to use in future works (such as articles or books) all or part of my work. I understand that I am free to register the copyright to my work.

## **REVIEW, APPROVAL AND ACCEPTANCE**

The document mentioned above has been reviewed and accepted by the student's advisor, on behalf of the advisory committee, and by the Director of Graduate Studies (DGS), on behalf of the program; we verify that this is the final, approved version of the student's dissertation including all changes required by the advisory committee. The undersigned agree to abide by the statements above.

Xiaoyan Liu, Student

Dr. Haining Zhu, Major Professor

Dr. Kevin D. Sarge, Director of Graduate Studies

IDENTIFICATION OF SUMOYLATED PROTEINS AND INVESTIGATION OF  
PROTEIN UBIQUITINATION IN THE NF- $\kappa$ B PATHWAY

---

DISSERTATION

---

A dissertation submitted in partial fulfillment of the  
requirements for the degree of Doctor of Philosophy in the  
College of Medicine at the University of Kentucky

By

Xiaoyan Liu  
Lexington, Kentucky  
Director: Dr. Haining Zhu, Professor of Biochemistry  
Lexington, Kentucky  
2012

Copyright © Xiaoyan Liu 2012

## ABSTRACT OF DISSERTATION

### IDENTIFICATION OF SUMOYLATED PROTEINS AND INVESTIGATION OF PROTEIN UBIQUITINATION IN THE NF- $\kappa$ B PATHWAY

SUMOylation and ubiquitination are important post-translational modifications. While ubiquitination is well known for targeting proteins for degradation, SUMOylation often regulates the intracellular localization of substrates. In the first project of this dissertation, we developed proteomic strategies to identify novel SUMOylated proteins in mammalian cells. In the second project, we investigated the regulation of protein ubiquitination in the NF- $\kappa$ B signaling pathway in the context of Paget's disease of bone (PDB).

Identification of SUMOylated proteins has been a challenge because of low abundance of SUMOylation substrates. Here, we utilized a mass spectrometry (MS)-based proteomic approach to identify novel SUMOylated proteins in mammalian cells. Seventy-four unique proteins were commonly identified in the collection of four SUMO-1 plasmids, thus considered candidate SUMOylated proteins. Many of these proteins are associated with the nucleus. The results were validated by confirming SUMOylation of a novel substrate Drebrin and a well known substrate Ran-GAP1. Furthermore, the potential SUMOylation sites in Drebrin have been identified and confirmed using site-directed mutagenesis.

PDB is a disorder characterized by increased bone turnover containing hyperactive osteoclasts. Mutations in Sequestosome 1 (p62) are associated with 40% of familial PDB. P62 is a scaffold protein and plays a critical role in regulating ubiquitination of TRAF family signaling molecules and mediating the activation of NF- $\kappa$ B by RANK and TNF $\alpha$  ligands. P62 also plays a critical role in shuttling substrates for autophagic degradation. The objective of this project is to determine the effects of PDB-associated p62 mutants on NF- $\kappa$ B signaling and autophagy. We compared the effect of wild-type (WT) p62 and PDB mutations (A381V, M404V and P392L) on the TNF $\alpha$ -induced NF- $\kappa$ B signaling using an NF- $\kappa$ B luciferase assay. Our results show that these p62 mutations increased the NF- $\kappa$ B signaling. In addition, we found that the PDB mutations did not change the interaction between p62 and the autophagy marker protein LC3. In summary, the PDB mutations in p62 are likely gain-of-function mutations that

can increase NF- $\kappa$ B signaling and potentially contribute to disease progression. Based on the results, we proposed a model to speculate the synergetic role of p62 PDB mutant on NF- $\kappa$ B signaling and autophagy.

**KEYWORDS:** SUMOylation; ubiquitination; Paget's disease of bone (PDB); p62; NF- $\kappa$ B signaling

---

Xiaoyan Liu

---

05/12/2012

---

IDENTIFICATION OF SUMOYLATED PROTEINS AND INVESTIGATION OF  
PROTEIN UBIQUITINATION IN THE NF- $\kappa$ B PATHWAY

By

Xiaoyan Liu

Haining Zhu, Ph.D.  
Director of Dissertation

Kevin D. Sarge, Ph.D.  
Director of Graduate Studies

05/12/2012

*To my dear parents Xingfu Liu and Cui-E Zhan*

## ACKNOWLEDGEMENTS

Someone said that a Doctor of Philosophy (PhD) is not achieved by one person, but a lot of people. I totally agree with this opinion. At this time, as I get closer to obtaining the PhD, I also would like to give my deepest and most sincere appreciation to a lot of people who helped me during graduate school. Without these people, I could never complete the program.

First of all, I would like to thank my mentor Dr. Haining Zhu. I learned a lot from him, such as critical analysis, independent thinking and presentation skills. Haining always encouraged me and helped me to make progress of projects by talking with me weekly. Haining is also a great mentor by sharing his experiences with us often. For instance, he suggested me to keep up with the literature and make a balance of “big picture” and “small details”. He also challenged me by asking lots of questions in my group meeting and journal club, which drove me to think deeper about the data and be more knowledgeable about the background. I also want to thank Haining for giving me to opportunity to attend the 55<sup>th</sup> and 57<sup>th</sup> ASMS conferences. It is my great pleasure to work with him and learn from him.

Next, I want to thank all my committee members, Dr. Louis Hersh, Dr. Sidney Whiteheart, Dr. Brett Spear and Dr. Tianyan Gao. My last project did not go on smoothly at first, therefore my committee members asked for a committee meeting every 6 months, instead of one year. These frequent committee meetings pushed me to work harder and made good progresses of my projects. They are always supportive and gave me numerous great advices and input. For example, they suggested checking the p62 expression level before the luciferase assay, which turned out to be important. I also talked with them individually for updating my progress, and they were always willing to listen and generously shared their thoughts and reagents for experiments. I am fortunate to have such a wonderful committee. In addition, I want to give my sincere thanks to Dr. James Geddes for not only being my outside-examiner, but also kind help for my student seminar and IBS coursework.

Besides, I would like to thank all the previous and current lab members. To begin with, I want to give my sincere thanks to Dr. Jianjun Zhai, a former post-doc in our lab. He is not only a great teacher, but also a great friend in my life. It is my fortunate to learn from him, not only the knowledge, but also personal characteristics. Next, I would like to give my special thanks to Dr. Fujian Zhang, the first graduate student of Haining. Although I have never met him, Fujian helped me a lot in my first project. I would also like to thank another former post-doc, Dr. Anna-Lena Ström for teaching me techniques and helping revising my qualifying proposal. To point out, I would like to thank Dr. Jozsef Gal, a Research Associate in our lab. He helped me a lot in DNA cloning and confocal microscopy, especially these last days in my graduate studies, which greatly helped me to finish up my projects. Again, I would like to give my sincere thanks to Dr. Ping Shi for always supporting and encouraging me, and she is also a good friend of mine. I also would like to thank Dr. Jiayu Zhang, a post-doc in our lab for teaching me confocal techniques and her encouragements. Additionally, I would like to thank Yanming Wei, an exchange student in our lab. His motivation often encouraged me to work as hard as him. Besides, I want to give my thanks to the technician in our lab, Li Liu. She could always make me laugh and make my day happier. Plus, I want to give thanks to a graduate student Liuqing Yang, for his



encouragements and help. I also want to thank former post-docs including Dr. You-jun Fu and Dr. Xiaohu Tang who always encouraged me. Again, I want to thank new post-docs Dr. Lei Shi and Dr. Jing Chen for their support. In addition, I want to thank David Kwinter for helping me with image analysis. Plus, I want to thank the previous exchange student Dr. Rujuan Liu, the previous technician Renee Kilty for their care and help. In addition, I give my special thanks to Dr. Anli Jiang for experiment details and the advices about finding jobs. Again, I would like to give my special thanks to Dr. Qingjun Wang for her great advices on my research, student seminars and personal life. Also, I'd like to thank Dr. Natasha Kyprianou for encouragements and help on finding jobs.

Additionally, I want to give my thanks to my student seminar advisors Dr. David Rodgers and Dr. Steve Schwarze. Dr. Rodgers is very supportive, and he even revised the words what I am going to say for the seminar. I also want to thank him for carefully revising my dissertation. Dr. Steve Schwarze is knowledgeable and he explained the things easy for understanding. I also want to thank him for helping me during the job interview. I would also like to thank Dr. Hans Bueler and Dr. Olivier Thibault for their knowledge and advices on my student seminar. In addition, I want to thank Robin Webb, Andres Chang, Brent Hackett, and David Meekins for being my student seminar committee members and their great advices.

Moreover, I want to thank a number of people from University of Kentucky or different countries worldwide, who generously shared the critical reagents and cells with us. Without their help, I could not make good progress of my projects. Firstly, I want to thank Dr. Lisa Cassis, Dr. Sean Thatcher, Dr. Deneys Van Der Westhuyzen and Dr. Lei Cai for kindly sharing Raw264.7 cells. Also, I would like to thank Dr. Matthew Gentry for sharing the HA-Ub constructs. I also want to thank Dr. Paul Murphy and Dr. Becky Dutch for sharing CHO cells. Most especially, I would like to give my great thanks to Dr. Jiake Xu and Dr. Jamie Tan (University of Western Australia, Australia) for generously sharing critical reagents (Raw264.7 cells stably expressing NF- $\kappa$ B luciferase reporter, NF- $\kappa$ B luciferase reporters and others). I'd also like to give my special thanks to Dr. Weimin Gong and Chunyan Niu in the Institute of Biophysics in Beijing for helping purifying the critical cytokine GST-rRANKL several times. I want to thank Dr. Maria Wooten (Auburn University) for sharing the HA-Ub constructs. In addition, I want to thank Dr. Sarch Rea (Sir Charles Gairdner Hospital, Australia) and Dr. Julie Crockett (University of Aberdeen, United Kingdom) for sharing HEK cells stably expressing RANK receptor. I also want to thank Dr. Tomas Brdicak (Charles University Prague, Czech Republic) for sharing Drebrin plasmid.

In addition, I would like to thank sincerely the Director of Graduate Studies of our department, Dr. Kevin Sarge for his contiguous encouragements and suggestion on my graduation. I also want to thank him for sharing the Ran-GAP1 antibody and his knowledge on SUMO study. I want to next give my thanks to Dr. David Watt who encouraged me that I have a gift of teaching. Plus, I want to thank Dr. Harry LeVine for revising my resumes for finding jobs. I also want to thank him for carefully revising my dissertation. I would also like to thank Dr. Skip Waechter for carefully revising my dissertation and his encouragements. Again, I would like to thank Doctor Hanna Mawad for his clinical information on Paget's disease of bone.

Plus, I would like to thank Dr. Jane Harrison and Jason Mitchell for giving me suggestions in the IBS program. Then, I would like to give my special thanks to Dr. Lorenzo Federico, one of my IBS classmates who helped me a lot in the coursework when I was in the

first year. I want to thank him for his continuous encouragements and support. Also I want to thank my classmate Dr. Michael Opata for his encouragements. I would also like to thank sincerely Dr. Guo-min Li and Dr. Liya Gu who gave me the opportunity to do the first rotation in their lab and help for fining jobs. I want to thank Dr. Fenghua Yuan and Yanbing Zhang for their help in Dr. Li's lab during my rotation. Plus, I'd like to thank my IBS classmate Dr. Erica Fleishaker for sharing the writing experience of dissertation.

Additionally, I would also like to thank all the previous and current Biochemistry staffs, especially, Marilou Johnson, Taha Al-jumaily, Maria Clark, Brenda Woods, Diana Griffieth, Philip Dickson, James Tribble, and Stephanie Viens.

Besides, I would like to give my special thanks to Dr. Chunxia Zhao and Dr. Lance Hellman. They are not only great scientists, but also great people from whom I could learn a lot. They both encouraged me a lot and believe that I am capable. I want to thank Lance also for revising my dissertation several times kindly. I would also like to thank my classmate Dr. Clint Smith for revising my dissertation carefully within a limited time and his encouragements.

In addition, I would like to thank all the previous and current post-doc, staffs and graduate students in our department. Especially, I would like to thank Dr. Hongyan Xing, Dr. Xiaoqing Tang, Dr. Manli Shen, Dr. Guangzuo Luo, Dr. Xinhe Huang, Dr. Latha Muniappan, Dr. Andreea Popa, Dr. Cyril Masante, Dr. Jamie Cantrell, Dr. Rachel Schowalter, Dr. Shaojing Ye, Dr. Weikang Cai, Dr. Perry Christian, Deepa Jonnalagadda, Dr. Wei Chen, Dr. Jason Ren, Jack Schmidt, Dr. Matin Chow, Mittul Patel, Dr. Deanna Morris, Dr. Senthil Karunakaran, Dr. Yu Zhong, Yunjie Huang, Jinchao Zhang, Kara Lawson, Xiaobo Li, Houfu Guo, Tianxin Yu, Dr. Marina Falaleeva, Olga Kelemen, and Xiu Xu.

Now, I would like to give my special thanks to my good friends Hui Ren, Fanmuyi Yang, Dr. Lei Tian, Dr. Chen Zhang, Dr. Zhaiyi Zhang, Dr. Xuan Zhang, and Dr. Chirie Sumanasekera. I really appreciate our friendship which gave me power and comfort when I had difficult times. It is my great fortunate to be a friend of them.

In addition, I would like to thank Dr. Dan Ni, Dr. Bei Dong, and Dr. Yulan Sun (May God bless her) for their care and encouragements. Next, I would also give my special thanks to Dr. Fang Zhu, Dr. Xiangrui Li, Dr. Qiang Wang, and Dr. Ying Xiong who always cared about me and gave me lots of encouragements. Also, I'd like to thank Jennifer Collins, Michelle Baber and Mo Dan for their support and care. Additionally, I want to thank Dr. Xiaoxue Li and Dr. Cindy Chen for their kind support and encouragements. I also want to thank my roommates and friends, Yan Li, Zhen Wang, Jinxiang Hu, Yuan Gao, and Lu Miao for their support and help.

Especially, I would like to give my sincere thanks to my American Host family Sarah and Jim Ryder, Sylvan, Mead, Peggy, and Puja Shah. I feel very fortunate to be a family member of them. I also want to thank many Christian friends I met in the church, especially Christa and Gorden Bingham, Bill Chen, Shuang Xu, and Baohui Song. Moreover, I would like to thank people in the UK Writing center to give my valuable suggestions. I also want to thank Xiaoliang Qi (PhD student in college of education, UK) and Amanda Konkle (PhD student in English department, UK) for carefully revising my dissertation. I would also like to thank Mr. Clark Kidwell for great suggestions on job interviews and communication skills.

In closing, I would like to thank my dear mother Cui-E Zhan and father Xingfu Liu for their unconditional love and support deeply and sincerely. They always encouraged me when I met difficulties, and they always believe that I am capable. They are the best parents I have even known. Also, I would like to thank my Uncle Dr. Chang-guo Zhan and Aunt Dr. Fang Zheng. They are the role models of the scientists for me, and they also cared about my study and personal life. I really appreciate their support and help during these years.

Without the names listed above, I could never ever finish this program. I really appreciate their help deeply and sincerely.

Thank you and I love you all.

## TABLE OF CONTENTS

ACKNOWLEDGEMENTS .....	iii
LIST OF FIGURES .....	x
LIST OF TABLES .....	xiii
Chapter 1. Background and introduction .....	1
Dissertation overview .....	1
SUMOylation .....	2
Paget's disease of bone (PDB) .....	10
P62 (Sequestosome 1) .....	14
NF- $\kappa$ B signaling .....	19
Autophagy .....	21
Chapter 2. Proteomic analysis of SUMOylated proteins in mammalian cells .....	32
Introduction .....	32
Materials and methods .....	33
Results .....	42
Generation of different versions of 3xFLAG-SUMO-1 fusion protein .....	42
Identification and classification of SUMOylated proteins from HEK293 cells overexpressing four different versions of SUMO-1 .....	43
Validation of Ran-GAP1 SUMOylation by MS/MS spectra and IP .....	44
Identification and validation of SUMOylation of a novel substrate named Drebrin .....	46
K185, K186, K270 and K271 are potential SUMOylation sites of Drebrin .....	47
Double mutation (K185R/K186R and K270R/K271R) in Drebrin separately did not appear to change protrusion formation .....	49
Discussion .....	50
An applicable proteomic method for identification of SUMO substrates .....	50
A novel substrate for SUMOylation, a cytosolic protein called Drebrin .....	51
Troubleshooting and further technique development .....	53
Significance of this study and future directions .....	54
Chapter 3. The role of PDB-associated p62 mutants in NF- $\kappa$ B signaling pathway .....	76

Introduction.....	76
Materials and methods .....	77
Results.....	83
Effect of the p62 PDB mutation on RANKL-induced NF- $\kappa$ B signaling in Raw264.7 cells.....	83
P62 contributes to TNF $\alpha$ -induced NF- $\kappa$ B signaling .....	85
P62 PDB mutants have a tendency to increase NF- $\kappa$ B signaling compared with WT p62 .....	86
P62 PDB mutant suppresses its binding with polyubiquitinated proteins in HEK293 cells.....	87
Overexpression of p62 in HEK293 cells leads to TRAF6 polyubiquitination in HEK293 cells .....	88
Mutant p62 impaired TRAF6 polyubiquitination compared with WT p62 in HEK293 cells.....	88
TNF $\alpha$ did not induce TRAF6 polyubiquitination in HEK293 cells.....	89
Overexpression of p62 in HEK293 cells leads to a TRAF6 polyubiquitination chain of different linkages .....	90
Discussion.....	91
Does p62 really facilitate TRAF6 to form a K63-linked polyubiquitin chain which activates NF- $\kappa$ B signaling? .....	91
Do p62 PDB mutants impair the TRAF6 polyubiquitination upon cytokine treatment?.....	92
Three workable cell models for studying the impact of PDB-associated p62 mutants on NF- $\kappa$ B signaling.....	93
Significance of this study and future directions .....	96
Chapter 4. The role of PDB-associated p62 mutants in autophagy .....	119
Introduction.....	119
Methods and materials .....	120
Results.....	122
Effect of the p62 PDB mutation on interaction with LC3 .....	122
Effect of the p62 PDB mutation on GFP-LC3 puncta formation.....	122
Effect of the p62 PDB mutant on LC3-II levels after rapamycin and NH <sub>4</sub> Cl treatment .....	123
Discussion.....	126
Challenges of current methods for studying the effect of PDB-associated p62 mutants on autophagy .....	126
Caution should be exercised when explaining LC3-II data .....	127
Significance of this study and future directions .....	128
Chapter 5. Discussion and future perspective.....	133
Significance of this research .....	133

Functional consequences of SUMOylation of Drebrin and other proteins .....	135
Mechanisms that PDB-associated p62 mutations increase NF- $\kappa$ B signaling .....	136
Autophagy in PDB .....	141
Other methods and models for studying the PDB.....	143
SUMOylation and NF- $\kappa$ B signaling .....	144
An integrated model: speculation about the role of PDB-associated p62 mutation.....	145
APPENDICES .....	147
Appendix I: List of all constructs.....	147
Appendix II: List of amplification primers and mutagenic primer sequences. ....	150
Appendix III: List of abbreviations.....	153
REFERENCES .....	155
VITA .....	167

## LIST OF FIGURES

Figure 1.1. SUMOylation conjugation pathway.....	25
Figure 1.2. Nuclear SUMOylation substrates and their functions.....	26
Figure 1.3. PDB is a disorder of bone remodeling. ....	27
Figure 1.4. Schematic domain structure of p62 and NMR structure of the p62 UBA domain.....	28
Figure 1.5. RANKL-induced and TNF $\alpha$ -induced NF- $\kappa$ B signaling. ....	29
Figure 1.6. P62 is proposed to involve in both ubiquitin proteasome system (UPS) and autophagy pathway.....	30
Figure 1.7. Autophagy pathway.....	31
Figure 2.1. Schematic diagrams of SUMO-1 constructs in our study. ....	57
Figure 2.2. Sypro Ruby staining SDS-PAGE gel of FLAG-SUMO-1 IP from cells overexpressing four versions of SUMO-1 constructs.....	58
Figure 2.3. Number of identified SUMOylated protein from HEK293 cells overexpressing four different versions of SUMO-1 constructs. ....	59
Figure 2.4. Classification of 74 identified common SUMOylated proteins. ....	60
Figure 2.5. MS/MS evidence of SUMOylated peptide from Ran-GAP1. ....	61
Figure 2.6. Validation of SUMOylated Ran-GAP1 by FLAG-SUMO-1 IP followed by Western blotting. ....	62
Figure 2.7. Predicted SUMOylation region of human Drebrin. ....	63
Figure 2.8. Validation of SUMOylated Drebrin by FLAG-SUMO-1 IP and HA-Drebrin IP followed by Western blotting.....	65
Figure 2.9. Identification of Drebrin SUMOylation sites by FLAG-SUMO-1 IP and HA-Drebrin IP.....	67
Figure 2.10. Immunostaining of Drebrin and actin filament in CHO cells. ....	69

Figure 3.1. A schematic diagram of NF- $\kappa$ B luciferase assay. ....	98
Figure 3.2. RANKL-induced NF- $\kappa$ B luciferase assay in Raw264.7 cells expressing WT p62 and p62 PDB mutants. ....	99
Figure 3.3. Comparison of the rate of I $\kappa$ B degradation in Raw264.7 cells expressing WT and mutant p62 induced by GST-rRANKL. ....	101
Figure 3.4. Immunostaining of p65 in Raw264.7 cells induced by GST-rRANKL. ....	102
Figure 3.5. Knockdown of the endogenous p62 in Raw264.7 cells by p62 siRNA. ....	103
Figure 3.6. TNF $\alpha$ -induced NF- $\kappa$ B luciferase assays in WT MEF and p62 KO MEF cells. ....	104
Figure 3.7. NF- $\kappa$ B luciferase assay induced by different concentration of TNF $\alpha$ in p62 KO MEF cells. ....	106
Figure 3.8. TNF $\alpha$ -induced NF- $\kappa$ B luciferase assay in p62 KO MEF cells expressing WT p62 or p62 PDB mutants. ....	107
Figure 3.9. Statistical analysis of fold increases in the TNF $\alpha$ -induced NF- $\kappa$ B luciferase assay in p62 KO MEF cells. ....	109
Figure 3.10. Statistical analysis of fold increases in the TNF $\alpha$ -induced NF- $\kappa$ B luciferase assay in HEK293 cells. ....	111
Figure 3.11. Comparison of immunoprecipitated polyubiquitinated proteins in HEK293 cells overexpressing WT and mutant p62. ....	113
Figure 3.12. Comparison of TRAF6 polyubiquitination in HEK293 cells overexpressing WT and mutant p62. ....	114
Figure 3.13. Comparison of the level of TRAF6 polyubiquitination in HEK293 cells overexpressing different amount of p62. ....	115
Figure 3.14. Comparison of TRAF6 polyubiquitination in HEK293 cells overexpressing WT and mutant p62 with and without TNF $\alpha$ treatment. ....	116
Figure 3.15. Comparison of TRAF6 polyubiquitination in HEK293 cells overexpressing p62 and a variety of different ubiquitin constructs. ....	117
Figure 4.1. Comparison of the effect of WT p62 or PDB mutant p62 on the interaction of LC3. ....	129



Figure 4.2. Immunostaining of p62 and LC3 in p62 KO MEF cells overexpressing p62 and GFP-LC3. ....	130
Figure 4.3. Comparison of the effect of WT p62 and p62 PDB mutant on LC3-II level after rapamycin or rapamycin/NH <sub>4</sub> Cl treatment. ....	131
Figure 5.1. A proposed model for the role of PDB mutant p62 in NF- $\kappa$ B signaling and autophagy. ....	146

## LIST OF TABLES

Table 2.1. Seventy-four proteins identified in cells expressing four different SUMO-1 constructs. ....	71
Table 2.2. Thirteen proteins with “GG”-tag identified by mass spectrometry from cells overexpressing SUMO-1 (“GG-T95R”). ....	75
Table 3.1. Comparison of three workable cell models for our study.....	118

## **Chapter 1. Background and introduction**

### **Dissertation overview**

SUMOylation and ubiquitination are two important post-translational modifications [1, 2]. This dissertation consists of two parts. In the first part (Chapter 2), we developed a relatively simple proteomic method to identify SUMOylated proteins in mammalian cells. We are also the first group to identify and validate that an actin-binding protein, Drebrin [3], could be SUMOylated. The second part (Chapter 3 and 4) of this dissertation is related to “ubiquitination” for the following reasons. Firstly, p62 is an ubiquitin-binding protein [4-6]. Secondly, most of the PDB-associated p62 mutations are in the ubiquitin-associated (UBA) domain [7]. Thirdly, in Chapter 3, we proposed that p62 PDB mutants increase the NF- $\kappa$ B signaling through increasing TRAF6 polyubiquitination. Fourthly, in Chapter 4, we studied the effect of p62 PDB mutants in autophagy. Autophagy is involved in degradation of polyubiquitinated proteins [8].

Currently, little is known about cellular consequences of PDB-associated p62 mutants currently [9]. To fill in this gap, we focused on studying the cellular consequences of PDB-associated p62 mutants on the NF- $\kappa$ B signaling and autophagy. We found that p62 PDB mutants increased TNF $\alpha$ -induced NF- $\kappa$ B signaling, but not through TRAF6 polyubiquitination (Chapter 3). Additionally, we showed that PDB mutants did not change the interaction between p62 and the autophagy marker protein LC3 (Chapter 4). Finally, an integrated model for the role of PDB mutant p62 in NF- $\kappa$ B signaling and autophagy is proposed (Fig. 5.1).

## **SUMOylation**

### ***Discovery of SUMO***

The small ubiquitin-like protein modifier (SUMO) was firstly discovered as reversible post-translational modification by several groups in the middle 1990s [10-12]. The first SUMOylated protein identified is Ran-GTPase-activating protein 1 (Ran-GAP1), which had been implicated in both nuclear transport and the control of mitosis [11, 12]. In 1997, the researchers found that cells contain two forms of RanGAP1, 70 kDa and 90 kDa [11]. Further analysis showed that the larger form contained a 97 amino acid protein, which is similar to ubiquitin in its shape, known as SUMO [12, 13].

Generally, three major SUMO paralogues, SUMO-1, SUMO-2 and SUMO-3 are expressed in cells [14]. It is not certain whether SUMO-4 protein is expressed in cells although a gene encoding SUMO-4 has been reported [15]. SUMO-2 and SUMO-3 are often referred to as SUMO-2/3 because they share 98% sequence similarity. However, SUMO-2/3 and SUMO-1 have only approximately 50% sequence identity [10, 16]. Human small ubiquitin-like modifier 1 (hSUMO-1) is a protein of 101 amino acids, similar to ubiquitin in 3D structure, even though they only share 17% homology at the amino acid level [17-19]. The SUMO-1 precursor has to be cleaved by SUMO-specific proteases to expose a C-terminal glycine-glycine (GG) functional group for subsequent SUMO activation and conjugation [1].

SUMOylation often regulates protein intracellular localization, protein-protein interactions or transcription regulator activity [2, 20]. SUMOylation is essential to normal

cellular behavior. Dysregulation of protein SUMOylation has been associated with a number of diseases such as cancer, neurodegenerative disease, viral infection, diabetes and developmental defects [2].

### ***SUMOylation vs. ubiquitination***

SUMOylation and ubiquitination are two important post-translational modifications in the cells. They share many similarities but they are also different in many aspects [21].

#### **(1) Similarity**

SUMO and ubiquitin have similar protein size, tertiary structure and a C-terminal di-glycine motif. Both SUMO and ubiquitin target the protein with the help of E1 (activating enzyme), E2 (conjugating enzyme) and E3 ligases. In addition, both SUMO and ubiquitin proteins are synthesized as immature precursors. These precursors are processed by the specific hydrolase for subsequent activation and conjugation [14, 22].

#### **(2) Difference**

Ubiquitination is well known for targeting substrates for degradation, whereas SUMOylation regulates a substrate's functions mainly by altering the intracellular localization, protein-protein interaction and transcription factor activity. In addition, the ubiquitin pathway has a large number of E2 s and E3 s, whereas the SUMO pathway only uses a single E2 and a few E3 s [17].

### ***SUMO conjugation, deSUMOylation and SUMO consensus sequence***

It is well known that ubiquitin conjugation requires E1 ubiquitin-activating enzyme, E2 ubiquitin-conjugating enzyme and E3 ubiquitin ligase [23]. SUMO conjugation is very similar to ubiquitin conjugation (Fig. 1.1). SUMO proteins are synthesized as inactive precursors, which must first undergo a C-terminal cleavage mediated by a family of sentrin/SUMO-specific protease (SENP) enzymes. This cleavage exposes a di-glycine motif, which is available for subsequent activation and conjugation [14]. In each conjugation cycle, SUMO is activated in an ATP-dependent manner by the E1 “activating” enzyme. SUMO is then passed to the active site of the conjugating enzyme Ubc9 (ubiquitin-conjugating 9). Finally, SUMO is covalently attached to lysine residues of the target protein through the isopeptide bond between the terminal glycine residue and the  $\epsilon$ -amino group of a lysine residue in the target protein by SUMO E3 ligase [1, 24, 25]. SUMOylation is a highly dynamic process that can be reversed by deconjugating enzymes such as the SENP enzymes [26]

The SUMO-1 consensus sequence is a motif of conserved residues next to the modified lysine residue and is found in many identified SUMO-1 substrates [27]. The sequence is  $\Psi$ KXE/D, where  $\Psi$  is a large hydrophobic residue (such as Val, Ile, Leu, Met, or Phe). K is the lysine to which SUMO-1 is conjugated and X is any amino acid, D is aspartic acid and E is glutamic acid. More than two-thirds of the known substrate proteins have at least one SUMOylation consensus sequence  $\Psi$ KXE/D [2, 28]. However, SUMOylation can also occur at lysine residues without this consensus motif, such as non-consensus SUMOylation sites. In addition, although not all lysine residues within the  $\Psi$ KXE/D motif are SUMOylated [1], SUMOylation consensus sequence  $\Psi$ KXE/D is still generally believed to be helpful for predicting SUMOylation sites.

### *Classification of SUMOylation substrates*

To date, more than 120 mammalian substrate proteins for SUMOylation have been identified [2]. Based on the subcellular localization of identified SUMOylation substrates, they could be classified as nuclear proteins, cytoplasmic proteins and transmembrane proteins. The majority of these substrates are nuclear proteins, indicating that SUMOylation is primarily involved in nuclear functions. However, a growing number of non-nuclear proteins have been identified, suggesting important non-nuclear roles of SUMOylation [29-31].

The nuclear SUMOylation substrates are well studied. These substrates could be further classified into nuclear pore complexes, transcription factors and coregulators, DNA replication and repair proteins, as well as kinetochore and centromere proteins [2, 32-34]. Functions of SUMOylation of these nuclear proteins are summarized in the Fig. 1.2.

A growing number of non-nuclear SUMOylation substrates have been identified, indicating more functions of SUMOylation beyond those related to the nucleus [2]. Ran-GAP1, the first identified SUMOylation substrate is a cytoplasmic protein. SUMOylation is clearly required for targeting Ran-GAP1 to the nuclear pore complex (NPC) [11]. Also, some identified SUMOylation substrates are transmembrane proteins, such as death receptors, Fas and TNFR1. SUMOylation of these receptors inhibits their apoptotic signaling [2, 35]. It is noted that a number of non-nuclear SUMOylation substrates are involved in signal transduction. SUMOylation of these proteins could change the activity, stability, or subcellular distribution of the proteins and eventually alter signaling events.

For example, SUMOylation protects inhibitor of NF- $\kappa$ B (I $\kappa$ B) from ubiquitination and degradation by 26S proteasome [2, 30].

### ***Functional consequences of SUMOylation***

The major functional consequences of SUMOylation include alteration of protein localization, protein-protein interactions and transcription regulator activity [2, 36].

#### ***(1) Protein localization***

As mentioned earlier, Ran-GAP1 is a cytosolic protein. Only SUMOylated Ran-GAP1 binds Ran-GTP binding protein (RanBP2), which mediates SUMOylated Ran-GAP1 translocation from the cytosol to the nuclear pore [11, 37]. Therefore, SUMOylation is critical for nuclear import of some proteins. In addition, SUMOylation could also target substrate proteins to specific locations within the cytoplasm. For example, DRP1 is a GTPase protein required for mitochondrial fission. SUMOylation of DRP1 facilitates its recruitment from the cytosol to the mitochondrial outer membrane [38].

#### ***(2) Protein-protein interactions***

SUMOylation of Ran-GAP1 is also an example of SUMOylation being involved in protein-protein interactions. As discussed earlier, only SUMOylated Ran-GAP1 can bind RanBP2. It is hypothesized that SUMO may serve as an interaction “hub” that recruits new interacting proteins to the substrate [1, 2]. For another example, it has been demonstrated that SUMOylation of transcription factor Elk1 could recruit the histone deacetylase 2 (HDAC2). This recruitment has been shown to result in decreased histone acetylation of Elk-1-regulated promoters and thus transcriptional repression of Elk-1 target genes [39].



### ***(3) Transcription regulator activity***

Most SUMOylation substrates are nuclear proteins. Particularly, the primary nuclear SUMOylation substrates are transcription factors and regulators. In most cases, SUMOylation negatively regulates gene expression by either enhancing the function of transcription repressors or inhibiting the function of transcription activators [34, 40, 41]. However, the opposite occurs occasionally. For example, heat shock factor 1 (HSF1) is SUMOylated in response to stress and HSF1 SUMOylation often leads to activation of its target genes [13, 42].

### ***SUMOylation and disease***

As described above, SUMOylation is a dynamic process that could be reversed by deconjugating enzymes such as the SENP enzymes [1, 26]. A delicate balance between SUMOylation and deSUMOylation is essential to normal cell functions (Fig. 1.2). Growing evidence has shown that the loss of this balance in SUMOylation and deSUMOylation can lead to diseases including cancer, diabetes and neurodegenerative diseases such as Alzheimer's disease, Parkinson's disease, familial amyotrophic sclerosis (fALS) and Huntington's disease [2, 14, 43]. For example, a recent study has shown that SUMOylation of amyloid precursor protein (APP) close to the  $\beta$ -secretase cleavage site is associated with a decrease of A $\beta$  aggregates, which is generally believed a probable cause of Alzheimer's disease [14, 29, 31]. The causative relationships between the deregulation of SUMOylation and pathogenesis of the diseases are still unclear and under active investigation. Studies so far have suggested that SUMO target proteins might be therapeutic targets for treating these diseases [14, 43].

In our study, we used a modified proteomic method to identify SUMOylated proteins in HEK293 cells. We also found that Drebrin is a novel substrate for SUMOylation. Background about Drebrin is described as below.

### ***Discovery, isoforms and domains of Drebrin***

Developmentally-regulated brain protein (Drebrin) is an actin-binding protein, involved in the regulation of actin filament organization. Drebrin plays an important role during the formation of neurites and cell protrusions of motile cells [44]. The expression level of Drebrin is very high in the cerebral cortex, hippocampus, thalamus and striatum [45]. Drebrin was originally discovered by Shirao *et al.* [46].

Drebrin has three isoforms including E1, E2 (embryonic) and A (adult) isoform, which are generated by alternative RNA splicing from a single *Drebrin* gene [47]. Drebrin E1 and E2 were first identified as developmentally regulated brain proteins by two-dimensional gel electrophoresis in 1985 [46]. Drebrin A was discovered using a monoclonal antibody against Drebrin E in 1986 [48]. A cDNA clone for a common domain of Drebrin E1, E2 and A was first isolated from brains of 10-day chick embryos in 1988 [3, 49]. All three isoforms are strongly expressed in neurons [44]. On SDS-PAGE gels, the molecular weight of Drebrin A is about 125 kDa and the molecular weight of Drebrin E is about 115 kDa [45].

The N-terminal domain of Drebrin is an actin-depolymerizing factor homology (ADF-H) domain which is highly conserved across vertebrate [50]. Also, there is an actin-binding domain close to ADF-H. In the C terminus of Drebrin, there are homer-

binding motifs [44]. Homer proteins are scaffold proteins at the post-synaptic density where they facilitate synaptic signaling and appear to be critical in learning and memory [51].

### ***Drebrin contributes to the formation of filopodia***

The formation and maintenance of an appropriate shape is fundamental to cells. It is also important for cells to modulate morphology in response to changing environmental stimuli. The cytoskeleton plays an important role to provide both a rigid scaffold and mechanical forces to move the cell [44]. Also, the cytoskeleton is regulated by many proteins which bind cytoskeletal components such as microtubules and actin filaments. Drebrin is one of these actin-binding protein [44], and growing evidence shows that Drebrin is important for controlling cell shape and function by its interaction with other proteins [44].

The most visualized function of Drebrin is that Drebrin contributes to filopodia formation in neurons and other cell types [52]. In 1992, it was firstly reported that exogenous GFP-Drebrin A accumulated within spines and elongated the length of spine [53-55]. Later, it was reported that overexpression of full length Drebrin, or truncations containing the actin-binding domain, induced the formation of numerous microspikes in fibroblasts and massive spines in cultured hippocampal neurons [44, 56, 57]. Also, it was shown that overexpression of Drebrin E2 in cultured epithelial cells resulted in a phenotype similar to that produced in neurons and fibroblasts [44, 58]. It was also shown that filopodia formation could also be inhibited by a reduced amount of Drebrin [52].

In our study, we used the proteomic method to first show that Drebrin could be SUMOylated. Additionally, we found the potential SUMOylation sites of Drebrin. We also try to investigate the functional consequence of Drebrin SUMOylation.

Next, we will talk about another post-translational modification, ubiquitination, which is similar with SUMOylation described above. Here, we firstly will introduce a disease called Paget's disease of bone (PDB) because mutation in the gene encoding an ubiquitin-binding protein, p62 is associated with PDB. Then, we will describe the protein p62 in detail. We also will introduce NF- $\kappa$ B signaling, in which ubiquitination of many proteins occur. In the end, we will describe autophagy, which is involved in degradation of polyubiquitinated proteins [8].

### **Paget's disease of bone (PDB)**

#### ***Prevalence and symptoms of PDB***

Paget's disease of bone is named after Sir James Paget who was a British Surgeon. In 1876, he published a scientific article describing cases of previously unrecognized chronic bone disease, which he called "osteitis deformans". Over 120 years after Sir Paget's finding, scientists and clinicians began to make significant progress in understanding the etiology of the condition we now know as Paget's disease of bone (PDB) [59], which is the second most common bone disease after osteoporosis [60].

PDB is most common in England, Western Europe, and North America. Very few cases have been reported in Asia and Africa [59]. Approximately 3% of individuals aged over 50 years are affected with PDB in Caucasian populations [7, 61]. PDB is not lethal, but a chronic disorder that typically results in deformed bones [9]. The symptoms include

bone pain, susceptibility to pathological fractures, osteoarthritis, headache, deafness and neurological complications [59, 62, 63]. Osteosarcoma often occurs in PDB patients [64]. An elevated level of alkaline phosphatase, bone scans, x-rays help the diagnosis [61]. Currently, the common drug for treating the PDB are bisphosphonates, a class of relatively non-selective compounds that target and induce apoptosis of osteoclasts [7].

### ***PDB is a disorder of bone remodeling***

Bone mass in human being is controlled by both osteoclasts (bone-resorbing cells) and osteoblasts (bone-forming cells) [65]. The opposing activities of these two cell types ensure that bone is constantly remodeled in a process essential to maintain adult bone structure and function [59].

PDB is characterized by focal areas of increased bone turnover containing enlarged hyperactive osteoclasts [7, 66]. Pagetic lesions contain increased numbers of osteoclasts compared with normal bone, which have increased size and contain more nuclei than normal osteoclasts [7]. The increased osteoclast activity leads subsequently to increases in osteoblast activity [59]. Although bone resorption (osteoclast) initially exceeds formation (osteoblast), bone formation greatly exceeds bone resorption in later stages. Therefore, the overall process of bone formation becomes accelerated and disorganized, ultimately resulting in abnormal bone structure.

### ***RANK plays an important role in the formation of osteoclast***

Receptor activator of nuclear factor kappa-B ligand (RANKL), also known as TNF-related activation-induced cytokine (TRANCE) or osteoprotegerin ligand (OPGL), is a member of the tumor necrosis factor superfamily. It is most abundantly expressed as a cell surface protein by bone marrow stromal cells [67-69]. In 1998, RANKL (OPGL) was shown to be the main osteoclastogenic cytokine both *in vitro* and *in vivo* [67, 70, 71].

Osteoclast precursors are monocyte/macrophages. It was reported that RANKL could transform the macrophages to osteoclasts [67, 70, 71]. RANKL could interact with its receptor RANK (Fig. 1.5) [72]. RANKL and RANK are encoded by *Tnfrsf11* and *Tnfrsf11a* genes, respectively [67]. It has been reported that both *Tnfrsf11*-knockout mice (without RANKL) and mice in which *Tnfrsf11a* has been deleted (RANK<sup>-/-</sup>) fail to generate osteoclasts [67, 71, 73]. However, *Tnfrsf11a* knockout mice (RANK<sup>-/-</sup>) could be rescued by RANK-expressing haematopoietic cells, which suggests that RANK plays an important role in osteoclast formation [67, 73].

#### ***Etiology of PDB: disordered RANKL-induced NF-κB signaling***

It has been generally accepted that disordered osteoclast RANKL-induced NF-κB signaling may be central to disease etiology [9]. RANKL-induced NF-κB signaling plays a role in regulating the transformation of osteoclast to activated osteoclast [67]. Therefore, hyperactivated osteoclasts identified in PDB patient might be due to the up-regulation of RANKL-induced NF-κB signaling [9].

There are other factors that also contribute to PDB. It is suggested that PDB etiology is also involved with slow virus [59]. It has been shown that the infection of osteoclasts with a paramyxovirus is a possible cause of PDB [74]. Exposure to

environmental toxin could be another factor affecting PDB incidence. PDB cases in Lancashire (county of historic origin in the North West of England) identified in a 1974 survey have been linked to the cotton industry. It was proposed that arsenic pesticide from cotton bales might be responsible for the high prevalence of disease [75].

Both viral infection and exposure to environmental toxins such as arsenic may upregulate the expression of SQSTM1 (p62), which is an important protein in RANKL-induced NF- $\kappa$ B signaling pathway [7, 9, 59].

### ***Genetics of PDB: p62 (SQSTM1) mutations***

The most common genetic mutations found in classical PDB patients are in the *SQSTM1* (*sequestosome1*) gene, located on chromosome 5 at the PDB3 locus [59, 76]. This gene encodes the SQSTM1 protein (also known as p62), which has diverse functional properties [59, 76]. In osteoclasts, p62 appears to be an important component in the RANKL-induced NF- $\kappa$ B signaling pathway [59, 77]. Mutations in p62 gene are a major cause of PDB, but do not account for all cases of PDB [7]. Mutations in p62 gene have also been associated with familial and sporadic disease in up to 40% of cases [7].

To date, over 20 PDB-associated p62 mutations have been identified. Most of the p62 PDB mutations are either missense or truncating mutations in the ubiquitin-associated (UBA) domain, the C terminus of the p62 protein. A few p62 PDB mutations are outside of UBA domain [9].

Recent studies have supported the idea that p62 PDB mutations including P392L, P384S and K378X, are associated with increased RANKL-induced NF- $\kappa$ B signaling compared with wild-type p62 [9, 78-81]. While p62 mutations are linked to most cases of

PDB, mutations in genes encoding other proteins including VCP and RANK, are linked to PDB- related syndromes [59].

In our study, we are interested in cellular consequences of PDB-associated p62 mutations. Thus, we investigated the impact of these p62 mutations on NF- $\kappa$ B signaling and autophagy.

## **P62 (Sequestosome 1)**

### ***The domain structures of p62***

P62 is also called sequestosome 1 or SQSTM1 [82]. It is a conserved multifunctional protein that is mainly involved in cellular signaling, protein degradation, protein aggregation and apoptosis [5, 83-85]. Plus, p62 is a cellular protein which is found in almost all mammalian cell types [86]. It was identified as a common component of cytoplasmic inclusions in protein aggregation diseases including amyotrophic lateral sclerosis (ALS) [87] and other neurodegenerative diseases [88].

The p62 gene has 8 exons and encodes a protein of 440 amino acids [89]. The diverse functions of p62 could be reflected by its domain structure (Fig. 1.4 A) [90]. Generally, p62 consists of six domains/motifs: Phox and Bem1 (PB1) domain, ZZ-type zinc finger, the SOD1 mutant interaction region (SMIR), TRAF6 binding (TB) motif, the microtubule-associated protein 1 light chain 3B (LC3) interaction region (LIR) and an ubiquitin binding-associated (UBA) domain [5, 83].



### ***(1) PB1 domain***

The N-terminal Phox and Bem1 (PB1) domains of p62 could form heterodimers with other PB1 domains, and could also form homodimers and homooligomers of p62 [83, 91, 92]. The PB1 domain of p62 interacts with the PB1 domain of a number of proteins including atypical protein kinase C (aPKC), MAPK/ERK kinase 5 (MEK5), extracellular responsive kinase (ERK) and neighbor of BRCA1 gene 1 (NBR1). Particularly, the interaction of p62 and aPKC plays an important role in NF- $\kappa$ B signaling described below [5].

### ***(2) ZZ-type zinc finger***

The ZZ-type zinc finger mediates the interaction of p62 with receptor-interacting protein kinase 1 (also called RIP, RIP1 or RIPK1) [83, 93]. This interaction also plays an important role in the TNF $\alpha$ -induced NF- $\kappa$ B signaling pathway.

### ***(3) SMIR motif***

We identified a motif that is essential for the interaction of p62 with mutants of the Cu/Zn superoxide dismutase (SOD1) linked to familial ALS [83]. The SOD1 mutant interaction region (SMIR, residues 178-224) is the actual sequence that interacts with mutant SOD1. In particular, the conserved W184, H190 and the positively charged R183, R186, K187 and K189 residues within the SMIR are critical for the interaction because substitution of these residues with alanine significantly impaired the p62-mutant SOD1 interaction. In addition, oligomerization of p62 via the PB1 domain also plays an indispensable role in the p62-mutant SOD1 interaction [83]. The ubiquitin-independent recognition of misfolded proteins by SMIR is illustrated in Figure 2.

### ***(4) TB motif***

P62 binds to the TNF receptor-associated factor 6 (TRAF6) through the TRAF6 binding (TB) motif. TRAF6 is an E3 ubiquitin ligase in the RANKL-induced NF- $\kappa$ B signaling pathway. The interaction of p62 with TRAF6 could promote K63 linked polyubiquitination of TRAF6, which could further activate NF- $\kappa$ B [5]. The interaction of p62 with the E3 ubiquitin ligase TRAF6 promotes K63-linked polyubiquitination of TRAF6 and of other substrates such as Trk A and IKK $\gamma$  [94-96].

#### ***(5) LC3 interaction region (LIR)***

The microtubule-associated protein 1 light chain 3B (LC3) is a protein essential to autophagosome formation [83, 97]. The LC3 interaction region (LIR) of p62 can directly interact with LC3 [83, 97]. Particularly, one PDB-associated p62 mutation, D335E, is found in this LIR region [98].

#### ***(6) Ubiquitin binding-associated (UBA) domain***

The C-terminus of ubiquitin binding-associated (UBA) domain of p62 is responsible for ubiquitin binding [82, 99, 100]. It is proposed that p62 interacts with polyubiquitinated proteins through the UBA domain. Once the polyubiquitin chain of a substrate protein binds to the UBA domain of p62, the substrate can be either translocated to the proteasome or autophagosome for degradation (see below).

#### ***The role of p62 in protein degradation***

P62 plays a critical role in both ubiquitin-proteasome system (UPS) and autophagy, the two major known protein degradation pathways in mammalian cells (Fig. 1.6). P62 was reported to be a shuttling factor to the proteasome [4, 82, 101]. Accumulating evidence suggests that the involvement of p62 in autophagy is likely more important. Moreover, p62 can mediate the cross-talk between the UPS and autophagy. It

was proposed that p62 accumulation after autophagy inhibition could further suppress the clearance of ubiquitinated proteins destined for proteasomal degradation [102].

The p62 protein plays a critical role in autophagy as a cargo receptor. P62 is frequently detected in protein inclusions related to human diseases [88, 103-105]. The depletion of p62 inhibited autophagic degradation of aggregation-prone polyglutamine-expanded huntingtin inclusions while p62 protected cells from cell death induced by polyglutamine-expanded huntingtin [89]. Inhibition of autophagy caused elevated levels of p62 and induced more and larger p62 inclusions [89, 106, 107]. It was found that p62 actually regulates the formation and autophagic removal of protein inclusions [89, 106]. p62 binds directly to LC3 through its “LC3 interaction region” (LIR) [89, 97] that is critical to its ability to shuttle substrates to autophagosomes for degradation [97, 108, 109]. The C-terminal UBA domain can interact with polyubiquitin chains [100]. It was proposed that p62 targets ubiquitinated protein aggregates to autophagy through an interaction between its UBA domain and polyubiquitin [97]. However, our lab found that the UBA domain of p62 was dispensable for the recognition of familial ALS-related mutant SOD1 [83]. Instead, an internal sequence motif, the SMIR plays a critical role in mutant SOD1 recognition, suggesting that p62 might also target protein cargos for autophagic degradation via ubiquitin-independent mechanisms [83].

### ***PDB-associated p62 mutations and phenotype***

The most common genetic mutations found in classical PDB patients are in the p62 gene, located on chromosome 5 at the PDB3 locus [59, 76]. To date, over 20 PDB-

associated p62 mutations have been identified [9]. Most of the p62 PDB mutations are in the UBA domain [110]. A few p62 PDB mutations are outside of UBA domain [9].

### ***(1) p62 UBA domain mutations***

In 2003, the three-dimensional structure of the p62 UBA domain (residues 387-436) was determined by protein NMR (Fig. 1.4 B) [99, 111]. Identified p62 UBA domain mutations include P387L [112], P392L [113, 114], L394X [115], E396X [112], S399P [116], M404V [115, 117], G411S [115], G425R [115, 117], M404T [116] and others. Moreover, it was demonstrated that all of these mutations impaired K48-linked polyubiquitin binding by p62 *in vitro* [116]. Therefore, it was proposed that the disease mechanism in PDB involves a common loss of ubiquitin binding of p62. Interestingly, the mutations found in the UBA domain, P392L, G411S and G425R were also recently reported in ALS patients [118]. These findings suggest that p62 mutations might represent a causative or risk factor in ALS too.

### ***(2) p62 non-UBA domain mutations***

In recent years, more PDB-associated p62 mutations have been found in the non-UBA domain. A D335E missense mutation located in the LC3-interacting region (LIR) of p62, 50 amino acids away from UBA domain was identified [9]. Other non-UBA mutations include P364S [79], A381V [78, 98], Y383X [98] and others.

In our study, we mainly investigated the effect of PDB-associated p62 mutations on NF- $\kappa$ B signaling and possible mechanisms. We selected three p62 UBA domain

mutations (P392L, M404V and G411S) and two p62 non-UBA domain mutations (D335E and A381V) in our work.

### **NF- $\kappa$ B signaling**

Nuclear factor  $\kappa$ B (NF- $\kappa$ B) is a transcription factor found in almost all mammalian cell types [119, 120]. NF- $\kappa$ B is well known for regulation of immune responses and inflammation [119, 121]. Growing studies have shown that NF- $\kappa$ B is also involved in the oncogenesis [121], bone diseases [65] and cell death [122].

Currently, the numerous studies of NF- $\kappa$ B consist of website ([www.nf-kb.org](http://www.nf-kb.org)), patent and around 25,000 publications [120]. Here, we only focus on introducing RANKL-induced and TNF $\alpha$ -induced NF- $\kappa$ B signaling pathways which are related to our research topic.

### ***RANKL-induced NF- $\kappa$ B signaling***

RANKL is a cytokine that is highly expressed in bone marrow [67]. RANKL-induced NF- $\kappa$ B activity controls normal osteoclastogenesis and also plays an important role in the bone resorbing function of mature osteoclasts [59, 67, 123]. Therefore, upregulation of RANKL-induced NF- $\kappa$ B signaling could at least in part explain the increase in osteoclastic activity in PDB [59].

The binding of RANKL and RANK receptor induces receptor trimerization and recruitment of TRAF6 to bind RANK receptor [124, 125]. P62 subsequently binds to TRAF6 through its TB motif, and facilitates TRAF6 Lys63-linked polyubiquitination [126], since TRAF6 is an RING domain-containing E3 ligases [127, 128]. In addition,

TRAF6 could catalyze the K63-linked polyubiquitination of TAB1-TAB2-TAK1 complex [129], which activates the I $\kappa$ B kinase (IKK). Moreover, atypical protein kinase C (aPKC) is activated by interaction with p62 through its PB1 domain, and further activates the IKK [95]. Activated IKK further phosphorylates I $\kappa$ B, and I $\kappa$ B will be degraded by 26 S proteasome. Transcription factor NF- $\kappa$ B is then released from I $\kappa$ B and translocates from the cytosol to the nucleus, activating the transcription of target genes related to the osteoclast formation [130]. The pathway is illustrated in Fig. 1.5. In addition, Osteoprotegerin (OPG) negatively regulate RANKL-induced NF- $\kappa$ B signaling by competitive binding of RANKL with RANK receptor [131].

In our study, we studied the impact of PDB-associated p62 mutants on RANKL-induced NF- $\kappa$ B signaling. However, the lack of appropriate cell lines prevented us from further investigation.

### ***TNF $\alpha$ -induced NF- $\kappa$ B signaling***

Tumor necrosis factor  $\alpha$  (TNF $\alpha$ ) is an important cytokine involved in inflammation, cellular homeostasis and tumor progression and apoptosis [132, 133]. TNF $\alpha$ -induced NF- $\kappa$ B activation is similar to RANKL-induced NF- $\kappa$ B signaling discussed above, but also has its own characteristics.

TNF $\alpha$  functions through two receptors, TNF-R1 and TNF-R2 [134]. TNF-R2 is exclusively expressed only on endothelial and immune cells. TNF-R1 is universally expressed in many cell types, and has been studied more extensively than TNF-R2 [135]. TNF $\alpha$  binds TNF-R1 and induces receptor trimerization and leading to the recruitment of

the adaptor protein TNF-R1-associated death domain protein (TRADD) which binds to the death domain (DD) of TNF-R1[135]. TRADD protein also recruits TNF receptor-associated factor 2 (TRAF2), a family protein with TRAF6 mentioned above. TRAF2 is an E3 ligase and it could undergo auto-polyubiquitination and ubiquitinates RIP through K63-linked polyubiquitin chains. RIP polyubiquitination binds to TAB2/TAB3 complex, and recruit TAK1, which phosphorylates IKK, leading to the activation of the IKK complex [72]. Moreover, p62 interacts with RIP through its ZZ finger. P62 could also interact with aPKC through PB1 domain, and thereby activate IKK [72]. Activated IKK further phosphorylates I $\kappa$ B, and I $\kappa$ B will be degraded by the 26S proteasome. Transcription factor NF- $\kappa$ B is then released from I $\kappa$ B and translocates from the cytosol to the nucleus, activating the transcription of target genes [135]. TNF $\alpha$ -induced NF- $\kappa$ B signaling is illustrated in the Fig. 1.5.

In our study, we investigated the impact of PDB-associated p62 mutations on TNF $\alpha$ -induced NF- $\kappa$ B signaling. We found that p62 PDB mutants increased TNF $\alpha$ -induced NF- $\kappa$ B signaling compared with WT p62. Additionally, we tried to determine the molecular mechanisms of the role of p62 PDB mutant in signaling.

## **Autophagy**

In Greek, “autophagy” means “self-eating” [136]. It is another way of protein degradation, in addition to ubiquitin proteasome system (UPS) [137]. Autophagy is a process for degradation of cellular contents, organelles, misfolded proteins and invading bacteria through the lysosomal machinery [138-143]. It contains several different forms, including macroautophagy, microautophagy and chaperone-mediated autophagy [85].

Autophagy has emerged as a very active area of investigation as it closely regulates many cellular functions. Autophagy is also implicated in many diseases, including alcoholic liver disease, neurodegenerative disease and cancer [138, 144-146].

### ***Inducers and inhibitors of macroautophagy***

We focus on macroautophagy in our study. The soluble materials and organelles in the cytoplasm are sequestered by an isolation membrane (also termed “phagophore”). Autophagosomes are formed by expansion of the isolation membrane. The autophagosome then fuses with the lysosome to become an autophagolysosome (also termed “autolysosome”) where the enclosed substrates are degraded (Fig. 1.7 A) [85]. Currently, several autophagy inducers and inhibitors have been widely used (Fig. 1.7 A) [147]. For example, rapamycin is an inhibitor of the mTOR pathway which negatively regulates autophagy. Therefore, rapamycin is an inducer for autophagy.  $\text{NH}_4\text{Cl}$  and Bafilomycin A inhibit the fusion of lysosome and autophagosome, thereby inhibiting autophagy. Another common strategy to induce autophagy is starvation [148]. The class III phosphatidylinositol 3-kinase (PI3K-III) activates autophagy and 3-MA inhibits PI3K-III. Therefore 3-MA is another inhibitor for autophagy. In contrast, beclin-1 activates PI3K-III. Thus beclin-1 is an inducer for autophagy. Other autophagy inhibitors include E64d and pepstatin A, which inhibit the protease activity in the autophagolysosome (Fig. 1.7 A).

### ***LC3-II is a marker for autophagosome***

LC3 is widely used as an autophagy marker. In yeast, Atg 8 is the homolog of LC3 in human [149, 150]. There are two forms of LC3, LC3-I and LC3-II, in yeast and



mammalian cells. LC3-I is cytosolic, whereas LC3-II is conjugated with phosphatidylethanolamine (PE) and is mainly present in isolation membranes, autophagosomes and much less on autolysosomes. Therefore, LC3-II serves as a marker for autophagosomes. The conversion of LC3-I to LC3-II requires the Atg5-Atg12 complex (Fig. 1.7 B) [151].

It seems that the increase of LC3-II indicates more autophagosome and higher autophagic activity. However, LC3-II is also degraded by autophagy, making it difficult to interpret autophagy activity solely based on LC3-II level. Therefore, lysosomal protease inhibitors (E64d and pepstatin A) and inhibitors for the fusion of lysosome and autophagosomes (NH<sub>4</sub>Cl and Bafilomycin A) are commonly used in the studies to help determine whether autophagic activity is truly increased [152]. It is important to compare the amount of LC3-II in the presence and absence of these inhibitors.

Methods for studying autophagy also include counting the number of GFP-LC3 puncta in cells overexpressing GFP-LC3.

### ***P62 is both a substrate and regulator of autophagy***

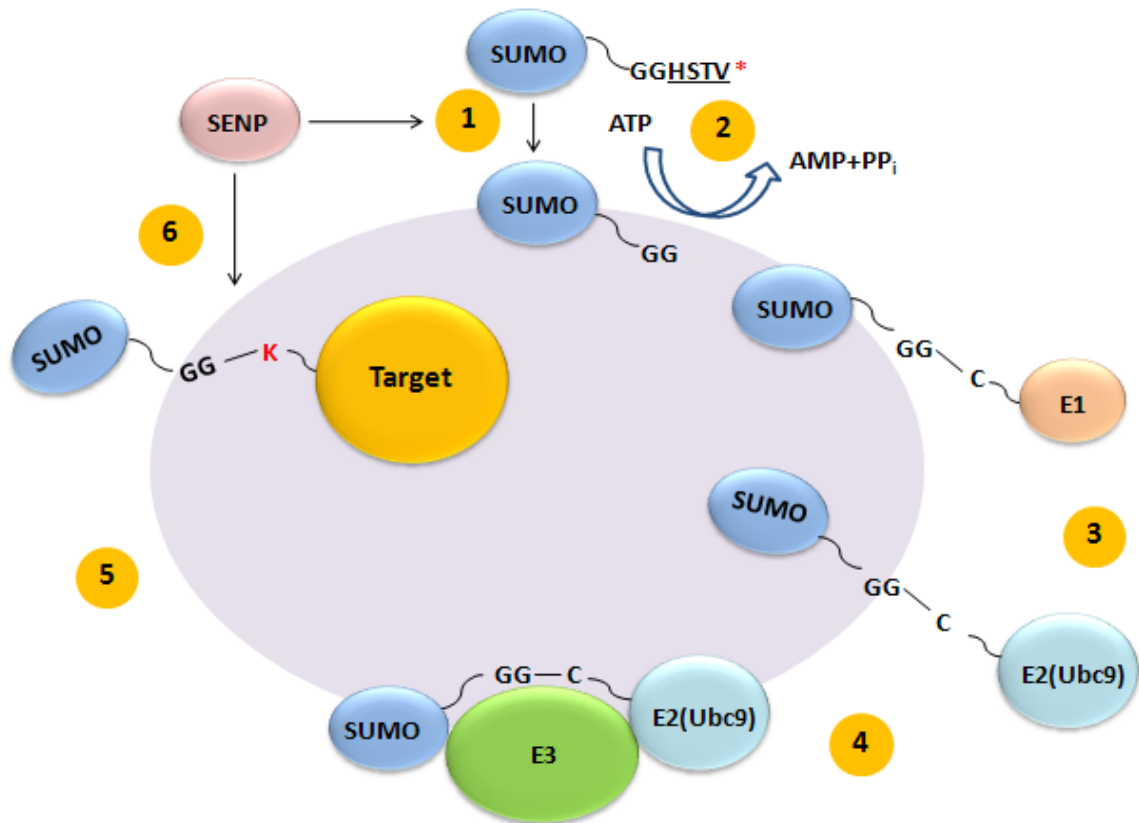
P62 is a specific substrate of autophagy [153]. It can bind LC3 on the autophagosome through LIR domain (Fig. 1.4 A) [152]. P62 proteins which have mutations in LIR region are not degraded by autophagy, result in their accumulation followed by inclusion formation [8]. Therefore, it is suggested that p62 is degraded by autophagy through interaction with LC3 directly. In addition, p62 mutations in PB1 domain are defective in oligomerization. Lower autophagic degradation of these p62 mutants indicates that oligomerization of p62 through PB1 are critical for their

degradation by autophagy [8]. Besides, the level of p62 is upregulated in Atg5 <sup>-/-</sup> MEFs, suggesting that accumulation of p62 could serve as an indicator of autophagy suppression [152]. The steady-state level of p62 has recently been used as a marker of autophagic degradation activity. For instance, an elevated level of p62 would be interpreted as inhibition or failure of autophagic activity [154]. However, this involves the critical assumption that p62 biosynthesis is not itself regulated. It has been reported that p62 can be induced at the transcriptional level by various stresses including oxidative stress [155, 156] or proteasome inhibition [157]. Thus, caution should be exercised when using the p62 level as a marker of autophagic activity.

On the other hand, p62 is also a regulator of autophagy. P62 binds the polyubiquitinated protein aggregates through its UBA domain. P62, which binds polyubiquitinated proteins, could also oligomerize through PB1 domains. It is indicated that the interaction of p62 and LC3 is involved in linking polyubiquitinated protein aggregates to autophagy [8, 106, 158] (Fig. 1.6). Therefore, p62 is not only a substrate for autophagy, but it also regulates the autophagic activity of other proteins.

In our study, we mainly investigated the impact of PDB-associated p62 mutations in autophagy.

**Figure 1.1. SUMOylation conjugation pathway.** SUMO conjugation needs E1 SUMO-activating enzyme, E2 SUMO-conjugating enzyme (Ubc9) and E3 SUMO ligase, which is similar to ubiquitin conjugation. SUMO could also be removed by deconjugating enzymes such as the SENP enzymes. This pictures is modified from a review paper written by Wilkinson *et al.* [1].



\* SUMO-1: "HSTV"; SUMO-2: "VY"; SUMO-3: "VPESLAGHSF"

**Figure 1.2. Nuclear SUMOylation substrates and their functions.** The well studied nuclear SUMOylation substrates could be further classified into nuclear pore complexes, transcription factors & coregulators, DNA replication & repair proteins and kinetochore & centromere proteins. A delicate balance between SUMOylation and deSUMOylation is essential to normal cell functions. This picture is modified from a review paper written by Zhao [2].

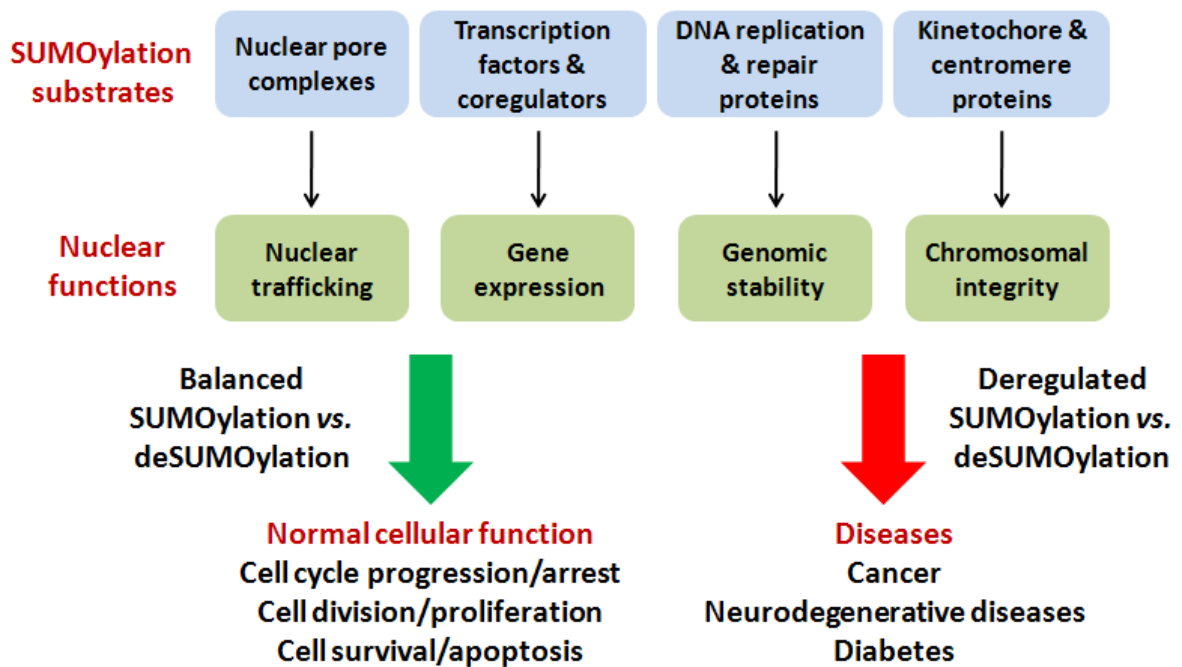


**Figure 1.3. PDB is a disorder of bone remodeling.** Bone mass in human being is controlled by both osteoclasts (bone-resorbing cells) and osteoblasts (bone-forming cells). The opposing activities of these two cell types ensure bone is constantly remodeled in a process essential for maintaining adult bone structure and function [59]. PDB is characterized by focal areas of increased bone turnover containing enlarged hyperactive osteoclasts [7, 59]. This picture is taken from a review paper written by Layfield (2007) [59]. This picture is used with a license agreement between Xiaoyan Liu and Cambridge University Press, with a license number 2822601263692.

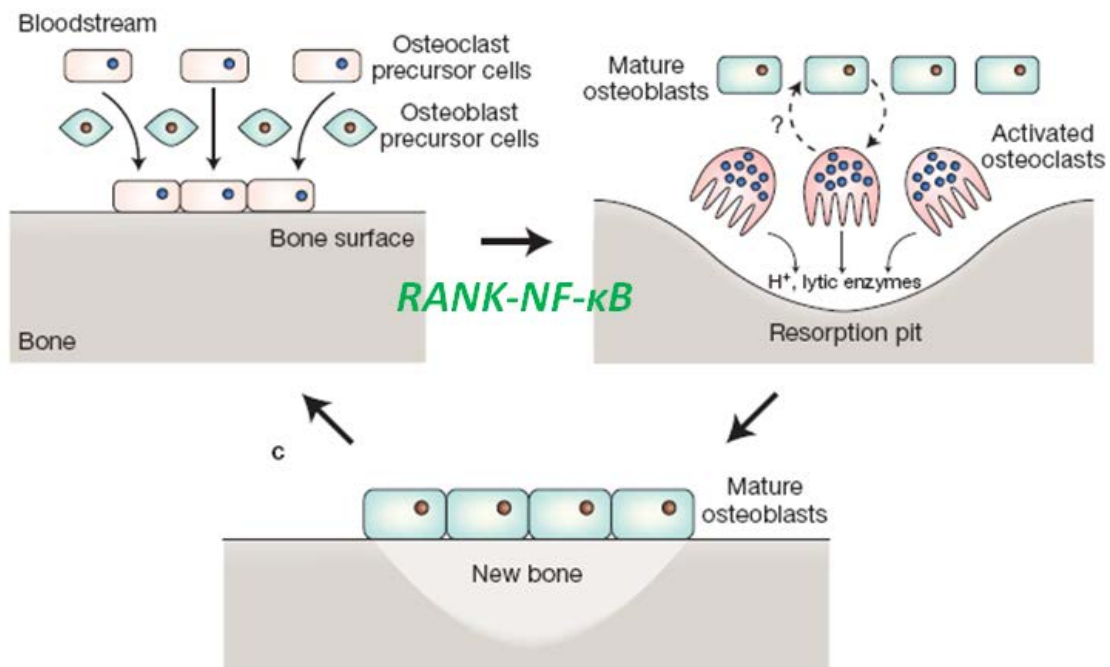
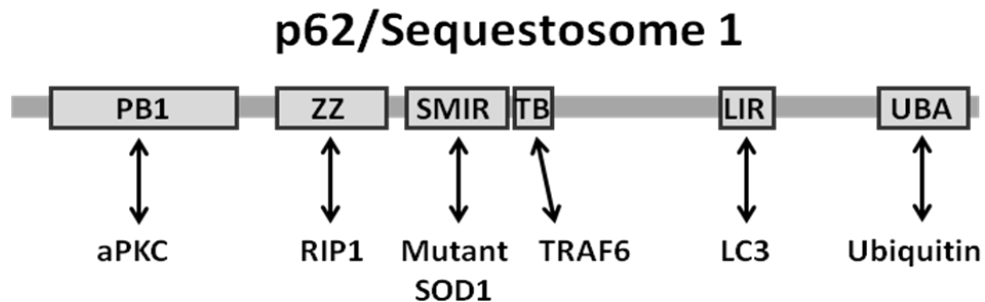


**Figure 1.4. Schematic domain structure of p62 and NMR structure of the p62 UBA domain.** (A) P62 has different domains which exhibit diverse functions by interacting with a number of key proteins. This pictures is modified from a review paper written by Moscat *et al.* [90]. (B) Surface representation of the p62 UBA domain determined by protein NMR. Several representative p62 PDB mutations are shown here. This pictures is taken from a review paper written by Layfield *et al.* [111]. Fig. 1.4 B is used with a license agreement between Xiaoyan Liu and Springer provided by Copyright Clearance Center, with a license number 2822600493041.

(A)



(B)

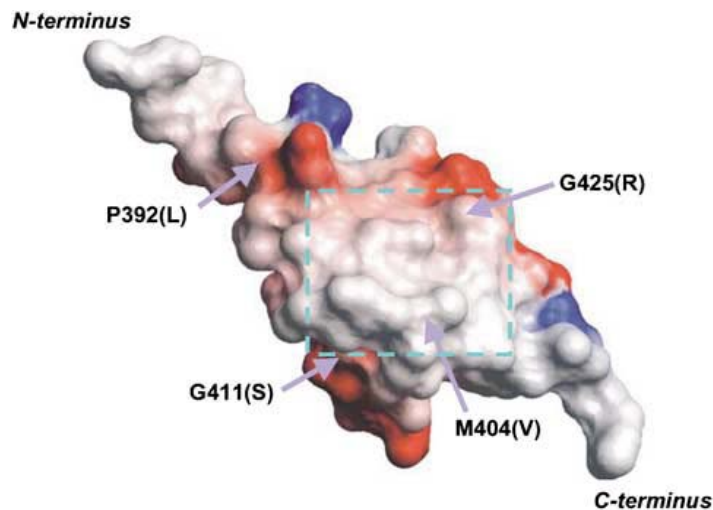


**Figure 1.5. RANKL-induced and TNF $\alpha$ -induced NF- $\kappa$ B signaling.** Upon RANKL or TNF $\alpha$  stimulation, TNF-R and RANK receptor undergo trimerization and recruit TRAFs to membrane. Briefly, NF- $\kappa$ B signaling is involved in TRAFs polyubiquitination, IKK activation, I $\kappa$ B degradation and NF- $\kappa$ B translocation from cytosol to nucleus and following target genes expressions. This diagram was drawn in light of a number of papers [65, 93-95, 130, 135, 159].

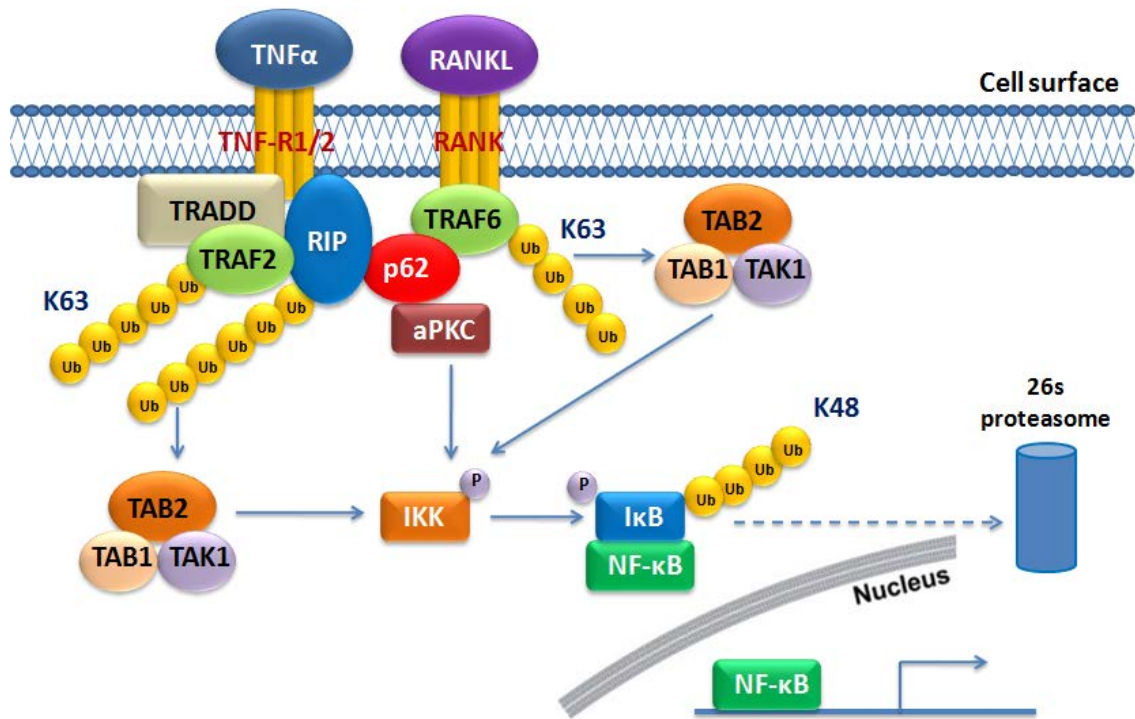


**Figure 1.6. P62 is proposed to involve in both ubiquitin proteasome system (UPS) and autophagy pathway.** P62 involves in targeting polyubiquitinated proteins for degradation by both UPS and autophagy. This picture is modified from a review paper written by Komatsu *et al.* [8] with permission. The use of this picture is also permitted by the *FEBS Letters*.

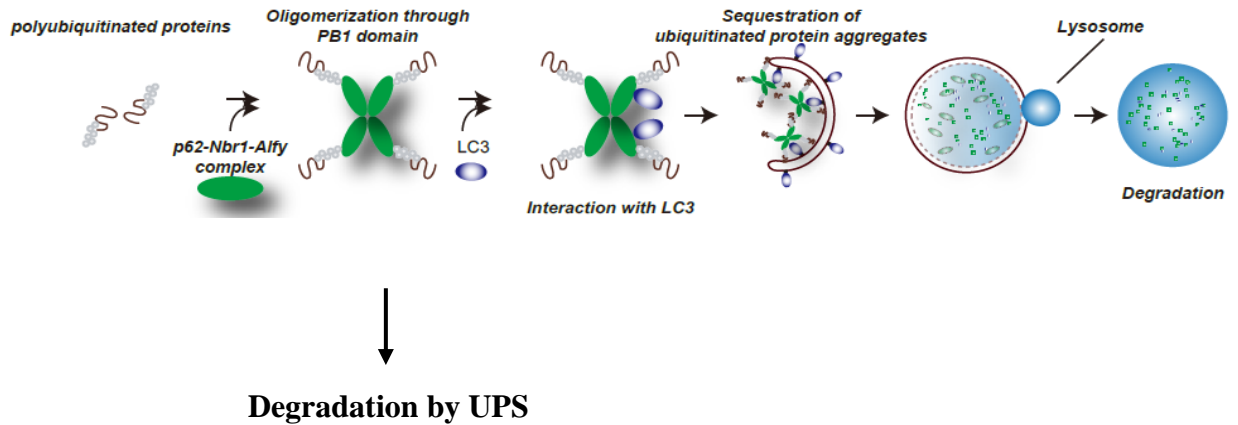
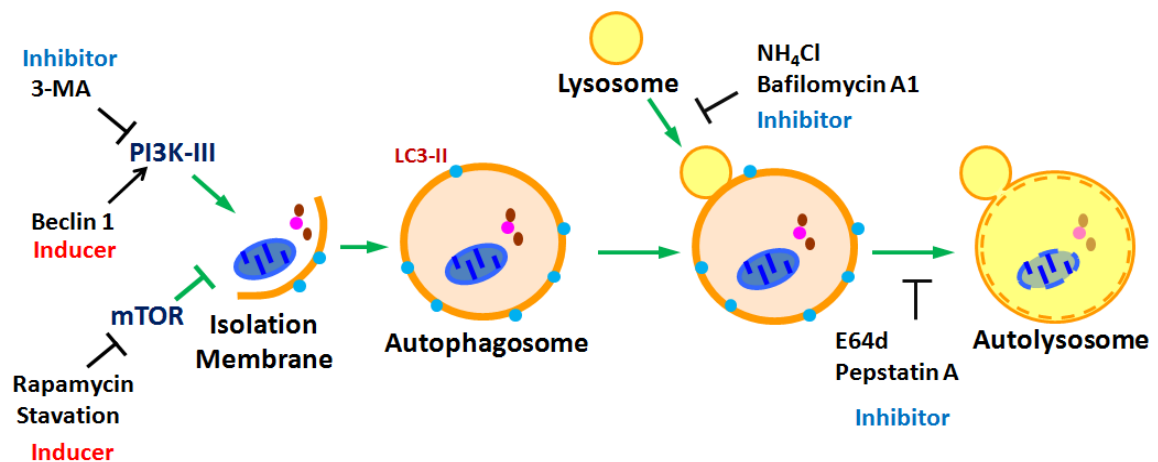


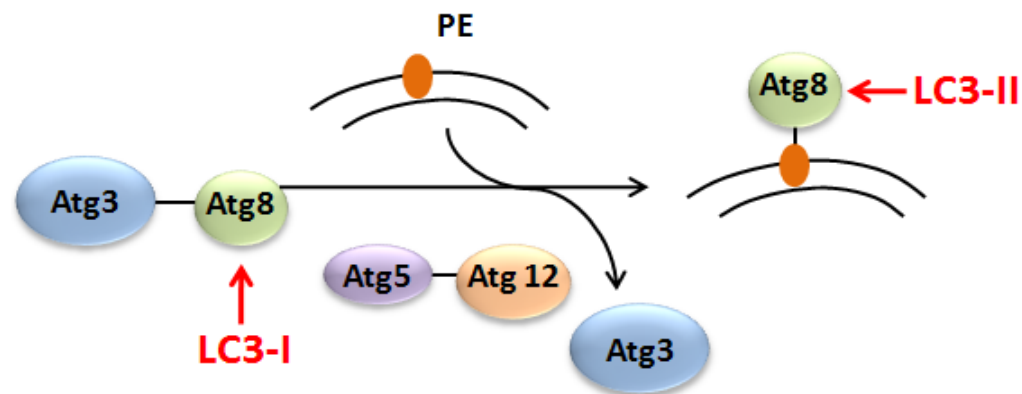


**Figure 1.7. Autophagy pathway.** (A) The process of autophagy. Autophagy inducers (shown in red) and autophagy inhibitors (shown in blue) are presented here. This picture is modified from Dr. Ping Shi's dissertation in Dr. Haining Zhu's lab. (B) The conversion of LC3-I to LC3-II requires the Atg5-Atg12 complex. This picture is modified from a review paper written by Nedelsky *et al.* [151].

(A)



(B)



## Chapter 2. Proteomic analysis of SUMOylated proteins in mammalian cells

### Introduction

As described in Chapter 1, SUMOylation of proteins are involved in a number of diseases including neurodegenerative diseases, cancer and diabetes [14, 160]. Therefore, it is important to identify the SUMOylation substrates and investigate the functional consequences of SUMOylation of these substrates, which might shed light on finding the therapeutic target for treating these diseases. Identification of SUMOylated proteins has remained a challenge because of the low abundance of SUMOylation substrates, a small portion of SUMOylated proteins, in addition to the high activity of SUMO deconjugating enzymes such as SENP [161]. Quantitative proteomics, using isotope labeling-based methods, have been used to identify SUMOylation substrates [162]. Knuesel *et al.* [163] showed that the SUMO-1(T95R) mutant can be used for the identification of the SUMOylation site by mass spectrometry *in vitro* [163]. In light of this study, we introduced a relatively simple proteomic method without isotope labeling for identification of SUMOylated proteins, which had not been previously reported. Furthermore, Knuesel *et al.* [163] was unable to determine whether this hSUMO-1(T95R) mutant was still functional *in vivo*. In our current study, we demonstrated whether that this mutant retained its functionality in HEK cells.

Most reported substrates for SUMOylation are nuclear proteins, though a few cytosolic proteins have been shown to be substrates [24, 36, 164]. Given this lack of knowledge about cytosolic SUMOylation targets, we were particularly interested in novel cytosolic protein targets.

In this Chapter, we aim to identify novel SUMOylation substrates in mammalian cells by using our newly developed proteomic method. The most important advantage of our strategy is that, it is an isotope-labeling free method, which is easier compared with isotope-labeling method. Especially, we expect to identify novel cytosolic protein as SUMOylation substrates. For the potential novel SUMOylation substrates identified by mass spectrometry analysis, we should firstly validate SUMOylation of these proteins by other methods, such as immunoprecipitation and Western blotting. Next, we need to find the potential SUMOylation sites of these novel substrates. Finally, we would like to investigate the functional consequences of these novel SUMOylation substrates.

## **Materials and methods**

### **cDNA cloning of human *SUMO-1* gene**

Total RNA was extracted from HEK293 cells using Qiagen RNA extraction kit following the manufacturer's instruction. Human SUMO-1 full-length cDNA ("SUMO-1-FL") was amplified with the following two primers containing two restriction sites at each end: 5' -GC GGA TCC ATG TCT GAC CAG GAG GCA AAA CC-3' and 5'-GC GCGGCCGC CTA AAC TGT TGA ATG ACC CCC TCT TTG- 3' using cDNA RT-PCR amplification kit (Invitrogen). Human SUMO-1 cDNA lacking the last four amino acids with GG bases at the C-terminal end, was amplified with the following two primers containing two restriction sites at each end: 5'-GC GGA TCC ATG TCT GAC CAG GAG GCA AAA CC-3' and 5'-GC GCGGCCGC CTA AAC TGT TGA ATG ACC CCC TCT TTG -3' using cDNA RT-PCR amplification kit (Invitrogen) ("SUMO-1-GG"). The

amplified PCR products were recovered using a PCR purification kit (Qiagen), digested with *HindIII* and *BamHI* and then ligated into the p3xFLAG-CMV-10 expression vector (Sigma, St Louis, MO, USA) digested with *HindIII* and *BamHI*. The positive clones containing the correct inserts were sequenced, and were named pCMV-3xFLAG-SUMO-1-FL (“SUMO-1 FL” or “FL”, full length) and pCMV-3xFLAG-SUMO-1-GG (“SUMO1-GG” or “GG”, last four amino acids truncated), respectively.

### **Plasmids construction**

SUMO-1 FL plasmid with the T95R mutation was amplified from the pCMV-3xFLAG-SUMO-1-FL construct by PCR using two primers containing the following sequences: 5'-GC AAG CTT ATG TCT GAC CAG GAG GCA AAA CC-3' and 5'-GC GCGGCCGC CTA AAC TGT TGA ATG ACC CCC TCT TTG-3'. SUMO-1 GG (last four amino acids truncated) with the T95R mutation was amplified from the pCMV-3xFLAG-SUMO-1-GG construct by PCR using two primers containing the following sequences: 5'-GC AAG CTT ATG TCT GAC CAG GAG GCA AAA CC-3' and 5'-GC GCGGCCGC CTA ACC CCC TCT TTG TTC CTG ATA-3'. The amplified DNA fragments were inserted into the *HindIII* and *NotI* sites of the pCMV-3xFLAG-10 vector (Sigma). The positive clones were named “SUMO-1-FL-T95R” (or “FL-T95R”, full length with T95R mutation) and “SUMO-1-GG-T95R” (or “GG-T95R”, last four amino acids truncated, with T95R mutation), respectively.

The original Drebrin construct was a gift from Drs. Tomas Brdickac and Ondrej Hrusaka (Czech Republic) [165]. Drebrin was firstly amplified by PCR by using upper and lower primers GJ764 and GJ765 (Appendix II). The amplified DNA fragments were inserted into the *EcoRI* and *BamHI* sites of p3xHA-CMV-10, and the positive clones

containing the correct inserts were sequenced. The positive clones were named p3xHA-Drebrin (human full-length, WT Drebrin). Drebrin constructs containing various point mutations were generated using the QuikChange II Site-Directed Mutagenesis Kit (Stratagene), or Quikchange Multi Mutagenesis Kit (Stratagene) based on p3xHA-Drebrin (WT). The mutagenic primer sequences are summarized in Appendix II. These mutations included K185R, K186R, K192R, K270R, K271R, K185R/K186R, K270/K271R and the Drebrin mutant in which five Lys are mutated to Arg: K185R/K186R/K192R/K270R/K271R (“5-K mutant”).

### **Cell culture and transient transfection**

Human embryonic kidney 293 (HEK293) cells were maintained at 37°C with 5% CO<sub>2</sub> in Dulbecco's modified Eagle's medium (Invitrogen) containing 10% fetal bovine serum (FBS), 100 units/ml penicillin and 100 µg/ml streptomycin. Chinese hamster ovary (CHO) cells were cultured in classical liquid media: Hams nutrient mixture F12 (SH3052601; Thermo scientific, HyClone).

For protein identification by mass spectrometry, 50% confluent cells were transfected with the four different 3xFLAG-SUMO-1 constructs mentioned above, and the p3xFLAG-CMV-10 control vector using lipofectamine transfection reagent (Invitrogen) in a 10cm plate format. For Ran-GAP1 SUMOylation verification by FLAG immunoprecipitation (IP), 70% confluent cells were transfected with FLAG-SUMO-1 (FL) in a 6-well plate format. For Drebrin SUMOylation verification by FLAG and HA

IP, 70% confluent cells were transfected with 3xHA-Drebrin (WT) and the different mutant 3xHA-Drebrin constructs in a 6-well plate format.

### **In-gel digestion and gel extraction**

After FLAG-IP, enriched SUMOylated proteins were subjected to 10% SDS-PAGE. The gel was washed twice with fix buffer (50% methanol and 7% acidic acid), and was then stained with SYPRO Ruby (S-12000; Invitrogen) overnight (Fig. 2.2). The next day, the gel was washed twice with wash buffer (10% methanol and 7% acidic acid). Each lane of gel was cut into seven or eight bands, and these bands were subsequently cut into the small pieces. These gel pieces were then washed three times with 50% ACN, 25mM  $\text{NH}_4\text{HCO}_3$  (AMBIC) pH 8.0, dried with a SpeedVac and reduced with 10mM DTT/50mM AMBIC at 56°C for 45 minutes. Next, proteins were alkylated with 55mM IAA/50mM AMBIC at room temperature for 30 minutes in the dark. Following the wash with 25mM AMBIC, the gel pieces were dehydrated with 100% ACN and then dried using a SpeedVac for 10 minutes. The gels pieces were then incubated with 10ng/ $\mu\text{l}$  trypsin in 25mM AMBIC overnight at 37°C. The resulting peptides were extracted using 200 $\mu\text{l}$  50% ACN and 5% formic acid. The extraction liquid was subsequently transferred into a new 0.5ml low retention tube and concentrated to 20  $\mu\text{l}$ .

### **Mass spectrometry analysis**

The peptides were subjected to Liquid Chromatography/Mass Spectrometry/Mass Spectrometry (LC-MS/MS) analysis, and the electrospray MS/MS data were collected from a Q-Star XL quadrupole time-of-flight (TOF) mass spectrometer (ABI/MDS Sciex,

Foster City, CA, USA) using a nano-flow HPLC system (Eksigent, Dublin, CA, USA). For direct infusion electrospray ionisation- mass spectrometry (ESI-MS) analysis, the sample was diluted 10 times with 90% acetonitrile containing 0.1% formic acid and loaded to Au/Pd-coated spray emitter (Proxeon, Odense, Denmark). The electrospray voltage was 2100 V and the mass range of TOF MS was from 350 to 1600 (m/Z). Nano-flow LC-MS/MS was performed by exploiting the nano-HPLC system for sample pick-up and separation, where the desired volume of sample solution was injected by the autosampler, desalted on a trap column (300  $\mu$ m i.d. x 5 mm; LC Packings), and was then subsequently separated by reverse phase C18 column (75  $\mu$ m i.d. x 150mm; Vydac) at a flow rate of 200 nL/minutes. The HPLC gradient was linear from 5% to 75% in 55 minutes using mobile phase A (H<sub>2</sub>O, 0.1% formic acid) and B (80% acetonitrile, 0.1% formic acid). Data acquisition was performed using information-dependent mode, where each cycle typically consisted of a 1s TOF MS survey from 350 to 1600 (m/z) and two 2s MS/MS scans with mass range of 100-1600 (m/z).

### **Protein identification and data analysis**

LC-MS/MS data were subjected to database searches for protein identification using a local MASCOT search engine, and candidate proteins were generated by searching the Swiss-Prot database. LC-MS/MS data were also submitted to the MASCOT server for MS/MS ion search, and the peak lists from the LC-MS/MS spectra were generated by the MASCOT script embedded in the Analyst QS software using the following parameters: no smoothing, charge state determined from the MS scan, precursor ion charge states of 2+ and 3+, centroid MS/MS data, height percentage 50% and merge distance 0.02 Da. The typical parameters used in the MASCOT MS/MS ion

search are: *Homo sapiens*, maximum of three trypsin missed cleavages, “Ubi-GG-Lys” definition, cysteine carbamidomethylation, methionine oxidation, protein N-term Acetylation, a maximum of 100 ppm MS error tolerance and a maximum of 0.5 Da MS/MS error tolerance. For MS/MS ion search, proteins with one peptide ion scoring higher than 20 were considered an unambiguous identification without manual inspection. All other hits were manually verified by confirming the peptide sequences from the MS/MS spectra. Non-specific proteins from empty vector were eliminated from the protein list generated from other four different SUMO-1 samples.

### **Gene ontology (GO) database**

The identified common SUMOylated protein list was subjected to the Gene Ontology (GO) database, and these proteins were classified based on their location of the cell. These locations included nucleus, cellular membrane, cytosol, cytoskeleton, chromosome, mitochondrion, extracellular and unannotated location.

### **Immunoprecipitation**

Forty-eight hours after transfection, cells were washed with 1x phosphate-buffered saline (PBS) and lysed using 1x radio immunoprecipitation assay (RIPA) buffer (Millipore) supplemented with protease inhibitor cocktail (P-8340; Sigma, St Louis, MO, USA), 0.625 mg/mL N-ethylmaleimide (Sigma), 1 mM sodium *o*-vanadate (Sigma) and 0.2 mM phenylmethylsulfonyl fluoride (Sigma).



The FLAG immunoprecipitations were performed by anti-FLAG M2 affinity gel (F2426; Sigma) in a final volume of 500 µl containing 1 mg protein extract. The IP samples and the corresponding extracts were subjected to sodium dodecyl sulfate polyacrylamide gel electrophoresis (SDS-PAGE) followed by Western blotting using the following antibodies: anti-Ran-GAP1 (gift from Dr. Kevin Sarge, University of Kentucky), anti-FLAG (A8592; Sigma), anti-actin (sc-1616; Santa Cruz Biotechnology) and anti-HA (mouse, sc-7392; Santa Cruz Biotechnology).

The hemagglutinin (HA) IPs were performed by using 2 µg of a mouse monoclonal anti-HA antibody (mouse, sc-7392; Santa Cruz Biotechnology) and Protein-G Sepharose (17-0618-01; GE Healthcare). The IP samples and the corresponding extracts were then subjected to SDS-PAGE followed by Western blotting using the following antibodies: anti-FLAG (A8592; Sigma), anti-actin (sc-1616; Santa Cruz Biotechnology) and anti-HA (rabbit, sc-805; Santa Cruz Biotechnology).

### **Western blotting and quantification**

Nitrocellulose membrane was incubated in blocking solution, 5% milk in Tris-Buffered Saline and Tween 20 (TBST) for one hour. Then the membranes were incubated with primary antibody for more than three hours. After four washes with TBST for five minutes each, the membrane was incubated with the secondary antibody for more than one hour. After four washes again with TBST for five minutes each, proteins of interest were visualized by either normal or dura enhanced chemiluminescent (ECL) substrate (Thermo scientific) for detection of horseradish peroxidase (HRP) enzyme (Thermo scientific). The membrane was covered with the wrapping membrane and an autoradiography film (Denville Scientific) which was exposed to the membrane. The

exposure time varied from one second to 20 minutes depending on the signal intensity. Films were subsequently developed by a Kodak X- OMAT 2000 processor.

Software Image J was used for quantification of Western blotting bands on X-ray films. Since ECL signals of the Western blot were captured on X-ray films which are known to have a narrow linear range of detection, the quantification of the Western blot may be out of linear range for certain experiments. Enhanced chemofluorescence (ECF) substrate and Alkaline Phosphatase (AP)-conjugated secondary antibody are encouraged for use in the future.

### **Bioinformatic analysis**

SUMOylation sites were predicted using the online software SUMOsp 2.0 (<http://www.sumosp.biocuckoo.org/prediction.php>). This software was used to analyze all the candidate SUMOylated proteins in the list (Table 2.1). In addition, AlignX Module Vector NTI (Invitrogen) was used to align the predicted SUMOylated region of human (*Homo sapiens*), mouse (*Mus musculus*), rat (*Rattus norvegicus*), rabbit (*Oryctolagus cuniculus*), horse (*Equus caballus*), cattle (*Bos taurus*), african elephant (*Loxodonta africana*), giant panda (*Ailuropoda melanoleuca*), domestic dog (*Canis familiaris*), opossum (*Monodelphis domestica*), chicken (*Gallus gallus*), lizard (*Anolis carolinensis*), african clawed frog (*Xenopus laevis*) and zebrafish (*Daniorerio*) (Fig. 2.7 C).

### **Immunostaining and confocal microscopy**

Chinese hamster ovary (CHO) cells at 30%-40% confluency were transfected with HA-Drebrin (WT and mutants) using lipofectamine reagent (Invitrogen) on gelatin-coated coverslips. Twenty-four hours post-transfection, cells were fixed with 4% paraformaldehyde (PFA) at 37 °C for 15 minutes, permeabilized with PBS/0.1% Triton, and blocked with 3% bovine serum albumin (BSA) in PBS for 1 hour. All the primary and secondary antibodies were diluted in 3% BSA/PBS. Cells were first stained with primary antibody HA (mouse, sc-7392; Santa Cruz Biotechnology, 1:300) or Drebrin (ab11068; Abcam, 1:100) for 5.5 hours. The coverslips were then washed with PBS and incubated with 4',6-diamidino-2-phenylindole (DAPI) (D9542; Sigma, 2mg/ml, 1:2000), Oregon Green 488 phalloidin (Invitrogen, 1:50), secondary antibody Alexa Fluor 594 anti-mouse (A21203; Invitrogen 1:300), or Alexa Fluor 594 anti-rabbit, (A11012; Invitrogen 1:300) for 1 hour. Finally, the coverslips were mounted using Vectashield mounting medium (Vector Laboratories). Fluorescence microscopy was used by a Leica SP5 inverted confocal microscope with a 40X objective.

### **Protrusion quantification and statistical analysis**

For each sample, 10 view images with Z-stack were taken by a Leica SP5 inverted confocal microscope with a 40X objective. Each view contained about 20-30 cells. The numbers of protrusions were counted for each cell which has protrusions. The percentage of cells with protrusions was counted. The data were presented as mean with standard deviation (SD) based on these 10 view images. The significant differences in percentage of cells with protrusions between cells expressing WT Drebrin and mutant

Drebrin were analyzed by one-way ANOVA, with Tukey's post-test using the software GraphPad Prism 5 Demo.

## **Results**

### **Generation of different versions of 3xFLAG-SUMO-1 fusion protein**

The arginine residue at the C-terminus of ubiquitin could be recognized and cleaved by trypsin, leaving a diglycine signature peptide for identification of ubiquitination site by mass spectrometry [166, 167]. However, for human SUMO-1, the C-terminal end is "TGG" instead of "RGG", thus it is impossible to generate the diglycine signature peptide. In addition, the last lysine or arginine residues of SUMO-1 are considerably distant from the C-terminus end, generating a SUMO tag (ELGMEEEDVIEVYQEQTGG) that is too big for detection by tandem mass spectrometry.

To solve this problem, we mutated the Thr95 residue of SUMO-1 to Arg. Thus, if endogenous SENPs in HEK293 cells correctly recognize and process the mutant construct, the last four amino acids of SUMO-1 will be removed. This cleavage of SUMO-1 ("FL-T95R") would yield a 114.1Da diglycine signature tag ("GG-tag") following trypsin digestion, which could be used for identification of SUMOylation site with high confidence. Considering that endogenous SENP might not work efficiently to remove the last four amino acids of SUMO-1, we also removed the last four amino acids manually to generate the "SUMO-1-GG" ("GG", last four amino acids truncated) and

“SUMO-1-GG-T95R” (“GG-T95R”, last four amino acids truncated, with T95R mutation) (Fig. 2.1).

### **Identification and classification of SUMOylated proteins from HEK293 cells overexpressing four different versions of SUMO-1**

SUMOylated proteins were immunoprecipitated from cell lysates of HEK293 cells overexpressing four different FLAG tagged SUMO-1 plasmids including “FL” (full length), “FL-T95R” (full length with T95R mutation), “GG” (last four amino acids truncated) and “GG-T95R” (last four amino acids truncated, with T95R mutation). The enriched SUMOylated proteins were then subjected to in-gel digestion, and the resulting peptides were extracted and subjected to LC-MS/MS analysis. The LC-MS/MS data were subsequently subjected to MASCOT MS/MS ion search.

Proteins with one peptide ion scoring higher than 60 or two peptide ions scoring higher than 30 were considered unambiguous identification without manual inspection. The ion score filter is 20. All other hits were manually verified by confirming the peptide sequences from the MS/MS spectra. Non-specific proteins from control samples were eliminated from all other four samples. The number of proteins identified in cells expressing “FL” SUMO-1 (full length), “FL-T95R” SUMO-1 (full length with T95R mutation), “GG” SUMO-1 (last four amino acids truncated) and “GG-T95R” SUMO-1 (last four amino acids truncated, with T95R mutation) are 129, 213, 217 and 177, respectively (Fig. 2.3 A). There are 74 identified common SUMOylated proteins among these four samples (Table 2.1). In these 74 proteins, two proteins have GG-tag. One is

Ran GTPase-activating protein 1 (Ran-GAP1) (RAGP1\_HUMAN), the other is T-complex protein 1 subunit delta (TCP-1-delta) (TCPD\_HUMAN) (Table 2.2). Additionally, there are 88 common proteins identified from cells overexpressing “FL” SUMO-1 (full length) and “GG-T95R” SUMO-1 (last four amino acids truncated, with T95R mutation) (Fig. 2.3 B).

As described above, a total of 177 unique proteins were identified from the purified SUMOylated proteins in cells overexpressing “GG-T95R” SUMO-1 (last four amino acids truncated, with T95R mutation) (Fig. 2.3 A). There were 13 proteins identified with GG-tag from cells overexpressing “GG-T95R” SUMO-1 (last four amino acids truncated, with T95R mutation) when cutoff was 20 (Table 2.2).

The above 74 identified common SUMOylated proteins were classified by subcellular location using the Gene Ontology (GO) databases, and these proteins were classified into nucleus, membrane, cytosol, cytoskeleton, chromosome, mitochondrion, extracellular and unannotated (Fig. 2.4). Among these 74 identified common SUMOylated proteins, most protein (51.4%) were located in the nucleus, 28.4% protein were located into membrane, 21.6% protein were located in the cytosol, 16.2% protein were located in the cytoskeleton, 12.2% protein were located in the chromosome, 9.5% protein were located in the mitochondrion, 6.8% protein were extracellular and 6.8% protein were unannotated (Fig. 2.4).

### **Validation of Ran-GAP1 SUMOylation by MS/MS spectra and IP**

Ran-GAP1 was the first identified SUMOylated protein [12] and was also in our candidate SUMOylation protein list (Table 2.1). Thus, we have again validated Ran-GAP1 SUMOylation using MS/MS spectra (Fig. 2.5) and IP (Fig. 2.6). The successful validation of Ran-GAP1 could serve as a positive control for our proteomic method.

First, we validated Ran-GAP1 SUMOylation by MS/MS spectra. If Ran-GAP1 is SUMOylated, after trypsin digestion, it will generate a peptide with a GG-tag. Then after fragmentation, it will generate a lysine residue (128.09 Da) with two glycine residue (114.04 Da), a total 242.1379 Da. Indeed, here we found the MS/MS spectra of peptide LLVHMGLLK\*(GG)SEDK derived from digestion of Ran-GAP1. This peptide was fragmented into a, b, c, x, y and z series ions. The molecular weight of y4 ion is 478.1643 and molecular weight of y5 ion is 720.2861. The difference between y4 and y5 ion is 242.1218, which is exactly the molecular weight of lysine and two glycine mentioned above, representing the GG tag generated by trypsin digestion (Fig. 2.5). Therefore, it is shown that Ran-GAP1 is SUMOylated by MS/MS spectra.

Next, HEK293 cells were transfected with “FL” SUMO-1 (full length) or “GG-T95R” SUMO-1 (last four amino acids truncated, with T95R mutation). Forty-eight hours post-transfection, FLAG-SUMO-1 IP was performed, and IP products were subjected to SDS-PAGE. Western blotting was performed using antibodies against Ran-GAP1, FLAG and actin. SUMOylated Ran-GAP1 was shown in IP products from cells overexpressing either “FL” SUMO-1 or “GG-T95R” SUMO-1, but not in the control samples (Fig. 2.6). Therefore, it is again shown that Ran-GAP1 is SUMOylated by IP and Western blotting.

## **Identification and validation of SUMOylation of a novel substrate named Drebrin**

We also used the software SUMOsp 2.0 to predict SUMOylation sites for all the candidate SUMOylation proteins in our list (Table 2.1). Among these 74 common proteins, 40 proteins (54%) have SUMOylation consensus sequences, 61 proteins (82%) have predicted SUMOylation sites including both SUMOylation consensus sites and non-SUMOylation consensus sites (Table 2.1).

Our candidate SUMOylation protein list (Table 2.1) includes a protein called Drebrin. As described in Chapter 1, Drebrin is an actin-binding protein involved in the formation of neurites and cell protrusions [44]. Unlike nuclear proteins that comprise the majority of SUMOylation substrates, Drebrin is a cytosolic actin-binding protein [45, 56]. The SUMOsp2.0 software showed that Drebrin had four predicted SUMOylation sites, in which one is a SUMOylation consensus motif, and the other three are non-consensus type (Table 2.1 and Fig. 2.7 A). We also aligned this predicted SUMOylated region among different species. This region was shown to be highly conserved among vertebrate species, suggesting that this region is functionally important (Fig. 2.7 C). Consistently, a previous report states that the Drebrin protein is highly conserved, especially at the N-terminal (residues 1-315) [44].

We verified Drebrin SUMOylation by both FLAG-SUMO-1 IP and HA-Drebrin IP. In detail, we first verified Drebrin SUMOylation by FLAG-SUMO-1 IP. HEK293 cells were transfected with “FL” SUMO-1 (full length) or “GG-T95R” SUMO-1 (last four amino acids truncated, with T95R mutation). Forty-eight hours post-transfection, FLAG-



SUMO-1 IP was performed and IP products were subjected to SDS-PAGE. Western blotting was performed using antibodies against Drebrin with longer and short exposure time. SUMOylated Drebrin is shown in both cells expressing “FL” SUMO-1 and “GG-T95R” SUMO-1, not in the control cells (Fig. 2.8 A, long exposure), suggesting that Drebrin is SUMOylated by FLAG-SUMO-1 IP. Also, the SUMOylation level of Drebrin is higher in cells expressing “FL” SUMO-1 than “GG-T95R” SUMO-1 (Fig. 2.8 A).

In addition, we verified Drebrin SUMOylation by HA-Drebrin IP. HEK293 cells were transfected with HA-Drebrin (WT) and FLAG-SUMO-1 (full length). Forty-eight hours post-transfection, HA-Drebrin IP was performed and IP products were subjected to SDS-PAGE. Western blotting was performed using antibodies against FLAG, HA and actin. SUMOylated Drebrin was observed in cells expressing both HA-Drebrin and FLAG-SUMO-1, but not in control cells (Fig. 2.8 B), indicating that Drebrin is SUMOylated by HA-Drebrin IP.

### **K185, K186, K270 and K271 are potential SUMOylation sites of Drebrin**

We next aimed to find potential SUMOylation sites of Drebrin. According to the SUMOylation consensus sequence  $\Psi$ KXE/D [1], Drebrin has four predicted SUMOylation sites including one SUMOylation consensus site, AKKE (amino acid 184-187) and three non-consensus sites, which are KKEE (amino acid 185-188), RKEE (amino acid 191-194) and KKSE (amino acid 270-273) (Fig. 2.7 B). These sites are also conserved among a number of different species (Fig. 2.7 C).

By using the site-directed mutagenesis, we generated several Drebrin single mutants through changing the K185, K186, K192, K270 and K271 of Drebrin to R respectively. Also, we generated double mutants including K185R/K186R and K270R/K271R. Additionally, we generated a mutant in which all the five K are mutated to R, K185R/K186R/K192R/K270R/K271R, called “5-K mutant”.

Then, we performed both FLAG-SUMO-1 IP and HA-Drebrin IP in HEK293 cells overexpressing FLAG-SUMO-1 (full length) and a variety of different HA-Drebrin mutants including double mutations K185R/K186R, K270R/K271R, single mutant K192R and “5-K mutant” in which all the five K were mutated to R. IP products were subjected to SDS-PAGE and Western blotting was performed using antibodies against HA, FLAG and actin (Fig. 2.9 A and B). Interestingly, the SUMOylation level of mutant Drebrin (combined mutations K185R/K186R) was much less (50% reduction) than that of WT Drebrin (Fig. 2.9 B, lane 3). Also, the SUMOylation level of mutant Drebrin (combined mutations K270R/K271R) was slightly less (30% reduction) than that of WT Drebrin (Fig. 2.9 B, lane 5).

Therefore, these data suggest that potential Drebrin SUMOylation sites could be K185, K186, K270 and K271. To further clarify which K is SUMOylated, we performed the HA-Drebrin IP using the single Drebrin mutant, our preliminary data showed that no single lysine mutant (K185R, K186R, K270R or K271R) could abolish the SUMOylation level of Drebrin (data not shown). Clarification of this issue requires additional experiments.

### **Double mutation (K185R/K186R and K270R/K271R) in Drebrin separately did not appear to change protrusion formation**

As described in Chapter 1, previous studies have demonstrated that Drebrin plays an important role in the formation of filopodia [53, 54, 57]. Also, we have shown that mutant K185R/K186R and K270R/K271R impair Drebrin SUMOylation compared with WT Drebrin. The next questions would be whether these two mutants also change the formation of filopodia compared with WT Drebrin. In order to address this question, CHO cells were transfected with HA-Drebrin (WT, K185R/K186R or K270R/K271R). Twenty-four hours post-transfection, immunostaining was performed using either HA or Drebrin antibody for staining Drebrin, Oregon Green 488 phalloidin for staining actin and DAPI for staining nucleus. Confocal microscopy was used to observe cellular protrusions (Fig. 2.10 A).

Consistent with the literature [53, 54, 57], we observed obvious cellular protrusions in cells overexpressing Drebrin (WT and mutants) (Fig. 2.10 A). However, after we quantified the percentage of cells with protrusions from 10 view images (each image was selected from five Z-stack images) for each sample, we found that there was no significant change among cells expressing WT Drebrin and Drebrin mutants (Fig. 2.10 B). Therefore, our preliminary results suggested that mutation of these two sites (K185R/K186R and K270R/K271R) in Drebrin separately did not appear to change protrusion formation.

## Discussion

### **An applicable proteomic method for identification of SUMO substrates**

Previous proteomic method for identification of SUMO substrates is using isotope-labeling method, which is complex [162]. In this Chapter, we developed a relatively simple proteomic method to identify SUMOylated proteins in HEK293 cells based on previous studies [163, 167]. First, we generated a number of SUMO-1 constructs to facilitate identification of SUMOylated proteins by mass spectrometry. In detail, we mutated the Thr95 of SUMO-1 to Arg (“FL-T95R” SUMO-1, full length, with T95R mutation). Since endogenous SENPs remove the last four amino acids of SUMO-1, it could yield a GG-tag after trypsin digestion and facilitate the identification by mass spectrometry [163, 167]. Considering that SENPs may not work very efficiently, we further removed the last four amino acids manually, and generated “GG-T95R” SUMO-1 (last four amino acids truncated, with T95R mutation). For comparison, we also generated a SUMO-1 plasmid without the last four amino acids but retained Thr 95, called “GG” SUMO-1 (last four amino acids truncated). Together with full length SUMO-1 (“FL”), these four different versions of SUMO-1 are all FLAG tagged (Fig. 2.1), and served for enriching SUMOylated proteins by FLAG-IP. The IP products were subjected to in-gel digestion and mass spectrometry for analysis.

After eliminating the non-specific proteins, 74 common SUMOylated proteins were identified from cells expressing four different SUMO-1 constructs. These 74 proteins are considered as candidate SUMOylated proteins. In this protein list, three proteins were reported before as SUMOylation substrates including Ran-GAP1 [12],

nucleophosmin (NPM) [168] and proliferating cell nuclear antigen (PCNA) [169] (Table 2.1). Also, 16 proteins were found in the articles related to the SUMOylation in PubMed database. In addition, we predicted SUMOylation sites including SUMO consensus sites ( $\Psi$ KXE/D) and non-consensus sites for all these 74 proteins using software SUMOsp 2.0. The numbers of consensus and non-consensus sites of each protein are shown in Table 2.1. Among these 74 common proteins, 40 proteins (54%) have SUMOylation consensus sequences, and 61 proteins (82%) have predicted SUMOylation sites including SUMOylation consensus sites and non-SUMOylation consensus sites (Table 2.1). Additionally, 51.4% of these 74 identified common SUMOylated proteins are nuclear proteins, consistent with the observations that most identified SUMOylated proteins are located within the nucleus [2]. Moreover, we successfully verified the SUMOylation of Ran-GAP1, the first identified SUMOylation substrate [37] in our system by MS/MS spectra (Fig. 2.5) and IP (Fig. 2.6). The successful validation of Ran-GAP1 could serve as a positive control for our proteomic method. Altogether, we have developed an applicable proteomic method for identification of SUMO substrates.

### **A novel substrate for SUMOylation, a cytosolic protein called Drebrin**

Currently, not many cytosolic SUMOylation substrates have been found [24, 36]. To fill this gap, we identified and validated SUMOylation of a cytosolic protein, called Drebrin. In our study, we identified a novel cytosolic SUMO substrate, Drebrin. We verified Drebrin SUMOylation by both FLAG-IP and HA-IP in HEK293 cells overexpressing FLAG-SUMO-1 and HA-Drebrin (Fig. 2.8 A and B). Drebrin has four

predicted SUMOylation sites including one SUMOylation consensus site, AKKE (amino acids 184-187) and three non-consensus sites, which are KKEE (amino acids 185-188), RKEE (amino acids 191-194) and KKSE (amino acids 270-273) (Fig. 2.7 B). These sites are also conserved among a number of different species (Fig. 2.7 C).

In order to find potential SUMOylation sites of Drebrin, we generated several Drebrin single mutants through changing the K185, K186, K192, K270 and K271 to R respectively. Also, we generated double mutants including K185R/K186R and K270R/K271R. Additionally, we generated a mutant in which all the five K are mutated to R, K185R/K186R/K192R/K270R/K271R, called “5-K mutant”. Next, we compared the effect of SUMOylation in cells overexpressing these HA-Drebrin mutants and WT HA-Drebrin by HA-IP. Our data showed that the SUMOylation level of Drebrin K185R/K186R was much less than that of WT Drebrin (Fig. 2.9 B, lane 3), about 50% decrease. Plus, the SUMOylation level of Drebrin K270R/ K271R is slightly less than that of WT Drebrin (Fig. 2.9 B, lane 5), about 30% decrease.

We are also curious about the functional consequence of SUMOylated Drebrin. It was reported that overexpressing Drebrin in CHO cells could cause the formation of cellular membrane protrusions [53]. Therefore, we investigated the effect of SUMOylated Drebrin on these CHO cells by overexpressing either WT HA-Drebrin or double mutant HA-Drebrin (K185R/K186R and K270R/K271R). Consistent with the literature [53, 54, 57], we observed obvious membrane protrusions in cells overexpressing Drebrin (WT and mutants). However, after we quantified the percentage of cells with protrusions from 10 view images (each image was selected from five Z-stack images) for each sample, there was no significant change among cells expressing WT Drebrin and Drebrin mutants

(Fig. 2.10 B). Thus, our data suggests that mutation of these two sites (K185R/K186R and K270R/K271R) separately did not appear to change protrusion formation.

### **Troubleshooting and further technique development**

Although our proteomic method is applicable as discussed before, several problems still remain. Firstly, among the 177 unique proteins identified from the purified SUMOylated proteins in cells overexpressing SUMO-1 (GG-T95R) (Fig. 2.3 A), there were only 13 protein identified with GG-tag when cutoff was 20 (Table 2.2). Additionally, only two of these 13 proteins were in the 74 common protein list (Table 2.1 and 2.2). Moreover, the evidence of MS/MS spectra for GG-tag was not obvious except for Ran-GAP1 (Fig. 2.5). Therefore, GG-tag might not be easy for identification by current LC-MS/MS settings. It might due to majority identification of the GG-tags are below the current limit of detection. Potential ways to overcome this problem could be increasing the amount of enriched SUMOylated proteins subjected to LC-MS/MS by increasing cultured cells. Also, more advanced mass spectrometry might help to better identify the GG-tag.

Another potential problem of our method is that the FLAG-IP is not very specific for enrichment of SUMOylated proteins. Although proteins in control cells were eliminated, the enriched SUMOylated proteins by FLAG-IP might still be contaminated with proteins containing other post-translational modification, such as ubiquitination, which is very similar to SUMOylation. If so, it is difficult to distinguish SUMOylation

from ubiquitination in the identified proteins containing GG-tags because they both will have GG-tags following tryptic digestion. One way to get around this problem could be using tandem affinity purification (TAP) for better enrichment of SUMOylated proteins.

A third concern is that the “5-K mutant” Drebrin in which all the five Lys are mutated to Arg did not completely abolish SUMOylation compared with WT Drebrin by HA-IP (data not shown). Therefore our data suggest that other Lys outside of the predicted SUMOylation region (Fig. 2.7 B) might be present. Another possibility is that cells have “compensation mechanism”, thus SUMOylation could occur at some random Lys when all the SUMOylated Lys are mutated. In addition, the experiments shown in Fig. 2.9 B were repeated three times. SUMOylation of K185R/K186R mutant Drebrin decreased compared with WT p62 for all three experiments. However, K270R/271R mutant Drebrin did not decrease for all three experiments, suggesting again that SUMOylation sites might be outside of the predicted SUMOylation region. Clarification of this issue requires additional experiments.

### **Significance of this study and future directions**

Based on a previous study [163], we developed a relatively simple proteomic method to identify SUMOylated substrates. We have identified 74 SUMOylated proteins by our method, in which three proteins are reported to be SUMOylation substrates, 16 proteins are related to the SUMOylation substrates, 40 proteins have SUMOylation consensus sequences ( $\Psi$ KXE/D) and 61 proteins have predicted SUMOylation sites by



software. We also validated the first SUMOylated protein Ran-GAP1 in our system. Therefore, our method is applicable for identifying novel SUMOylation substrates.

In addition, we are the first group to report that an actin-binding protein, Drebrin, is a substrate for SUMOylation. It is interesting that Drebrin is not in the nucleus, and little is known about SUMO substrates located outside of nucleus [24, 36]. These data may expand our knowledge of non-nuclear SUMOylation substrates by studying the functional consequence of Drebrin. In our study, we verified Drebrin SUMOylation by IP and found that K185, K186, K270 and K271 might be Drebrin SUMOylation sites. Also, our data have shown that double mutation (K185R/K186R and K270R/K271R) separately did not appear to change protrusion formation (Fig. 2.10 B). Therefore, we could further explore the functional consequences of Drebrin in the future.

Moreover, in our protein list, there are several proteins that have a relatively high number of predicted SUMOylation sites (highlighted in Table 2.1). These proteins include general transcription factor II-I (four consensus and two non-consensus sites), heterogeneous nuclear ribonucleoproteins C1/C2 (two consensus and eight non-consensus sites), heterogeneous nuclear ribonucleoprotein U (three consensus and five non-consensus sites), heterogeneous nuclear ribonucleoprotein D0 (one consensus and three non-consensus sites), nucleolin (four consensus and four non-consensus sites), poly [ADP-ribose] polymerase 1 (five consensus and 11 non-consensus sites), 60S ribosomal protein L24 (two consensus and two non-consensus sites) and spectrin beta chain, brain 1 (three consensus and 13 non-consensus sites), Ras GTPase-activating-like protein IQGAP1 (four consensus and 11 non-consensus sites), ATP-dependent DNA helicase 2 subunit 1 (two consensus and four non-consensus sites) and myosin-10 (six consensus

and 10 non-consensus sites), another cytosolic protein. Future studies could validate whether these proteins above are SUMOylation substrates by IP and other methods.

**Figure 2.1. Schematic diagrams of SUMO-1 constructs in our study.** Schematic diagrams of four p3xFLAG-SUMO-1 constructs used in our study including “FL” (full length), “FL-T95R” (full length with T95R mutation), “GG” (last four amino acids truncated) and “GG-T95R” (last four amino acids truncated, with T95R mutation).

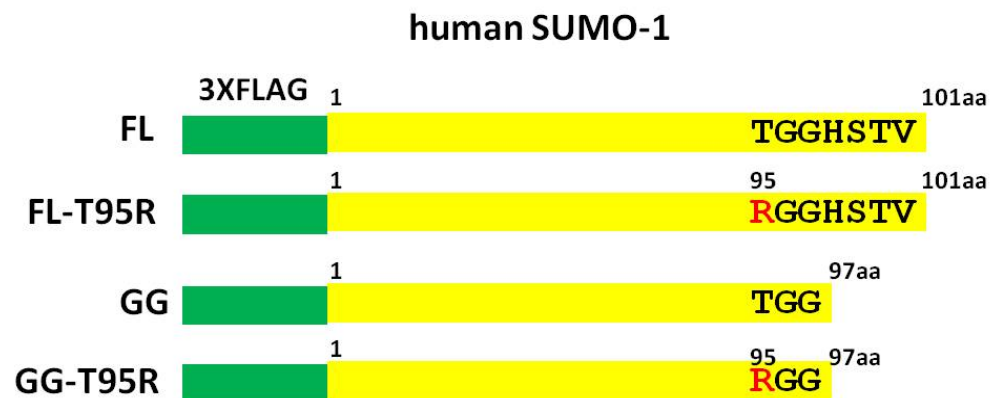


**Figure 2.2. Sypro Ruby staining SDS-PAGE gel of FLAG-SUMO-1 IP from cells overexpressing four versions of SUMO-1 constructs.** HEK293 cells were transfected with four different SUMO-1 constructs including “FL” (full length), “FL-T95R” (full length with T95R mutation), “GG” (last four amino acids truncated) and “GG-T95R” (last four amino acids truncated, with T95R mutation). Forty-eight hours post-transfection, FLAG-SUMO-1 IP was performed and IP products were subjected to SDS-PAGE. The gel was then stained with Sypro Ruby overnight. Each lane was cut into seven or eight bands and the gel was subjected to the in-gel digestion, gel extraction and LC-MS/MS.

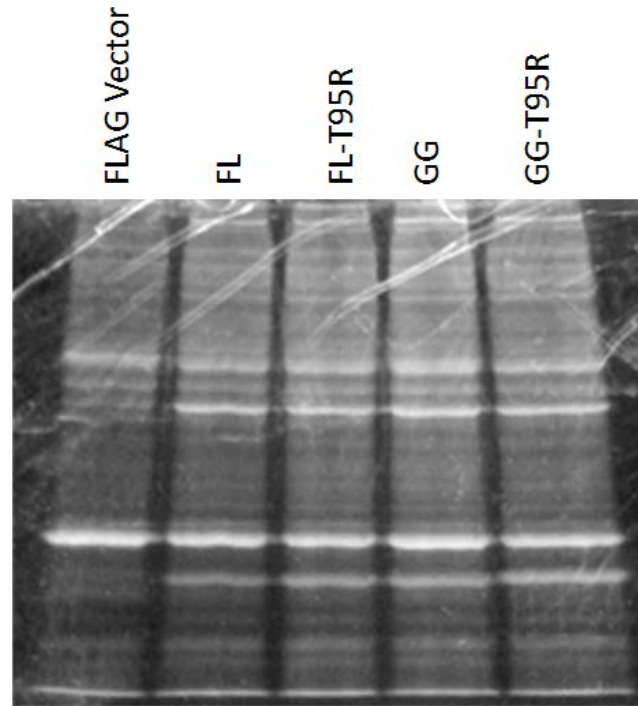
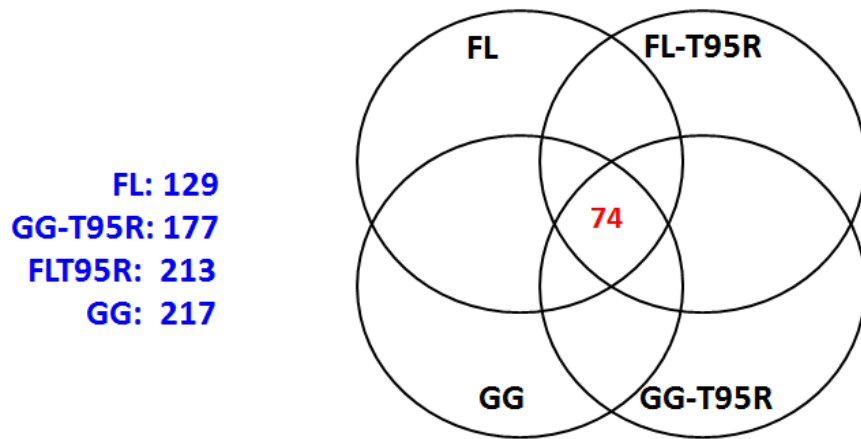


**Figure 2.3. Number of identified SUMOylated protein from HEK293 cells overexpressing four different versions of SUMO-1 constructs.** (A) Numbers of SUMOylated proteins identified with high confidence (ion score filter 20) from HEK293 cell overexpressing four different versions of SUMO-1 constructs including “FL” (full length), “FL-T95R” (full length with T95R mutation), “GG” (last four amino acids truncated) and “GG-T95R” (last four amino acids truncated, with T95R mutation). There are 74 common SUMOylated proteins. Non-specific proteins from control samples were eliminated from identified SUMOylated proteins. (B) Number of SUMOylated proteins identified with high confidence (Ion score filter 20) from HEK293 cell transfected with “FL” (full length) and “GG-T95R” (last four amino acids truncated, with T95R mutation). There are 88 common SUMOylated proteins.

(A)



(B)

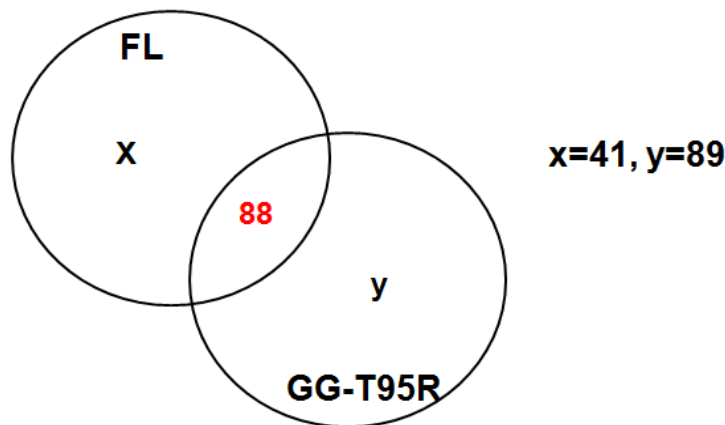


**Figure 2.4. Classification of 74 identified common SUMOylated proteins.** The 74 common proteins were classified based on the subcellular locations including nucleus, membrane, cytosol, cytoskeleton, chromosome, mitochondrion, extracellular and unannotated locations by Gene Ontology (GO) databases. The percentage of proteins belonging to each subcellular location is also shown.

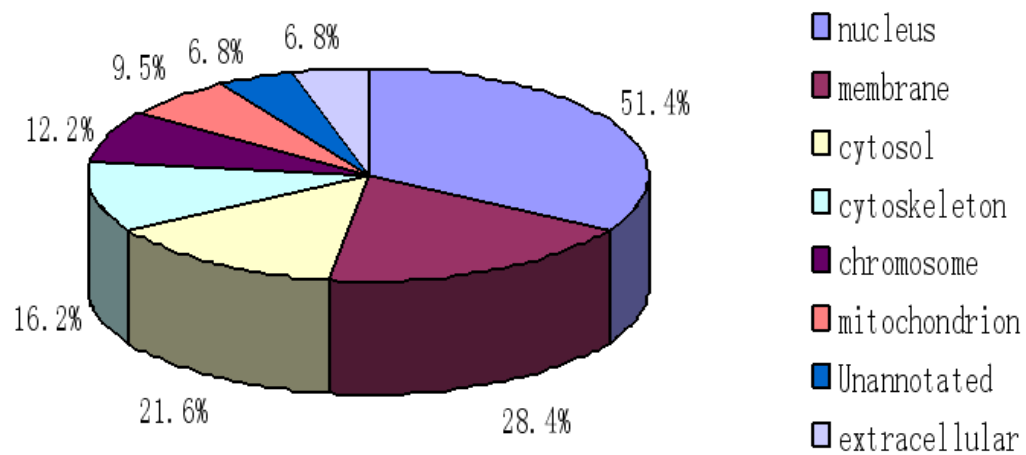


**Figure 2.5. MS/MS evidence of SUMOylated peptide from Ran-GAP1.** MS/MS spectrum of the peptide LLVHMGLL\*(GG)SEDK derived from digestion of Ran GTPase-activating protein 1 (Ran-GAP1). Validation of Ran-GAP1 serves as a positive control for our proteomic method.

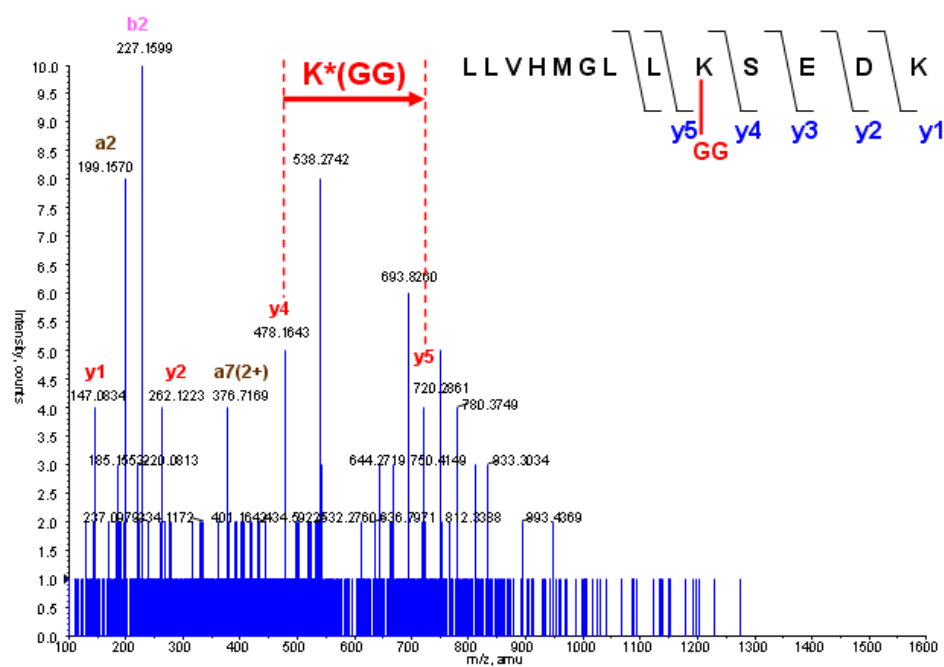


**Figure 2.6. Validation of SUMOylated Ran-GAP1 by FLAG-SUMO-1 IP followed by Western blotting.** HEK293 cells were transfected with “FL” SUMO-1 (full length) or “GG-T95R” SUMO-1 (last four amino acids truncated, with T95R mutation). Forty-eight hours post-transfection, FLAG-SUMO-1 IP was performed and IP products were subjected to SDS-PAGE. Western blotting was performed using antibodies against Ran-GAP1, FLAG and actin.

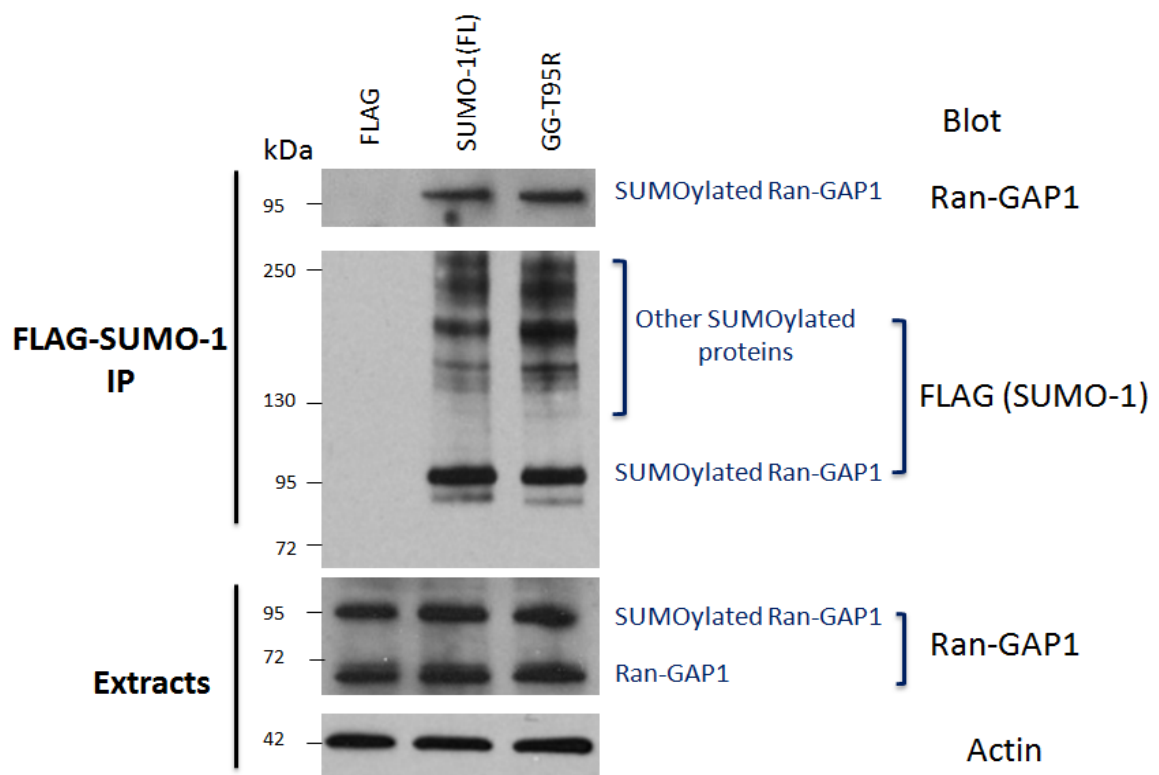




**Figure 2.7. Predicted SUMOylation region of human Drebrin.** (A) Predicted SUMOylation region of human Drebrin by software SUMOsp 2.0. (B) The predicted SUMOylation consensus site is highlighted and the predicted non-consensus SUMOylation sites are underlined. The predicted SUMOylated Lys residues are shown in red. (C) The sequence alignment of predicted SUMOylation region of Drebrin among different species including human (*Homo sapiens*), mouse (*Mus musculus*), rat (*Rattus norvegicus*), rabbit (*Oryctolagus cuniculus*), horse (*Equus caballus*), cattle (*Bos taurus*), african elephant (*Loxodonta africana*), giant panda (*Ailuropoda melanoleuca*), domestic dog (*Canis familiaris*), opossum (*Monodelphis domestica*), chicken (*Gallus gallus*), lizard (*Anolis carolinensis*), african clawed frog (*Xenopus laevis*) and zebrafish (*Danio rerio*).

(A)

Predicted Sites				
Position	Peptide	Score	Cutoff	Type
185	EQAKKEE	1.028	0.13	TypeI: Ψ-K-X-E
186	QAKKEEE	3.397	2.64	TypeII: Non-consensus
192	ELRKEEE	3.074	2.64	TypeII: Non-consensus
271	HMKKSES	3.088	2.64	TypeII: Non-consensus

(B)

185 186 192

**AKKEE**ELR**K**EEERKKALDERLRFEQERMEQERQEQ

EERERRYREREREQQIEEHRRKQQTLEAEEAKRRLKEQ

270 271

SIFGDHRDEEEETHMK**K**SESEV

185 186 192 270 271

Human WEQAKKEEELRKEEERKKALDERLRFQERMEQERQEEERERRREREQIEEHRKKQOTLEAEAAKRRLKEQSIFGDHRDEEETHMKKSESEVE

Mouse WEQAKKEEELRKEEERKKALDARLRFQERMEQERQEEERERRREREQIEEHRKKQOQSLAEAAKRRLKEQSIFGDORDEEESQMKKSESEVE

Rat WEQAKKEEELRKEEERKKALDARLRFQERMEQERQEEERERRREREQIEEHRKKQOQSLAEAAKRRLLDQSIFGDORDEEESQMKKSESEVE

Rabbit WEQAKKEEELRKEEERKKALDERLRFQERMEQERQEEERERRREREQIEEHRKKQOTLEAEAAKRRLKEQSIFGDQRDEEETQMKKSESEVE

Horse WEQAKKEEELRKEEERKKVLDERLRFQERMEQERMEQEEERERRREREQIEEHRKKQOTLEAEAAKRRLKEQSIFGDQDEEETQMKKSESEVE

Cattle WEQAKKEEELRKEEERKKALDERLRFQERMEQERQEEERERRREREQIEEHRKKQOTLEAEAAKRRLKEQSIFGDORDEEETQMKKSESEVE

Elephant WEQAKKEEELRKEEERKKALDERLRFQERMEQERQEEERERRREREQIEEHRKKQOTLEAEAAKRRLKEQSIFGDQDEEETQMKKSESEVE

Panda WEQAKKEEELRKEEERKKALDERLRFQERMEQERQEEERERRREREQIEEHRKKQOTLEAEAAKRRLKEQSIFGDORDEEETQMKKSESEVE

Dog WEQAKKEEELRKEEERKKALDERLRFQERMEQERQEEERERRREREQIEEHRKKQOTLEAEAAKRRLKEQSIFGDORDEEETQMKKSESEVE

Opossum WEQAKKEEELRKEEERKKALDERLRFQERMEQERLEQEEERKRYREREQIEEHRKKQOTLEAEAAKRLKEQSIFGDQDEEETQMKKSESEVE

Chicken WEQAKKEEELRKEEERKKALDARLRFQERMEQERLEQEEERKRYREREQIEEHRKKQOSMEAEAAKRLKEQSIFGEQEEDRQRLRKSESEVE

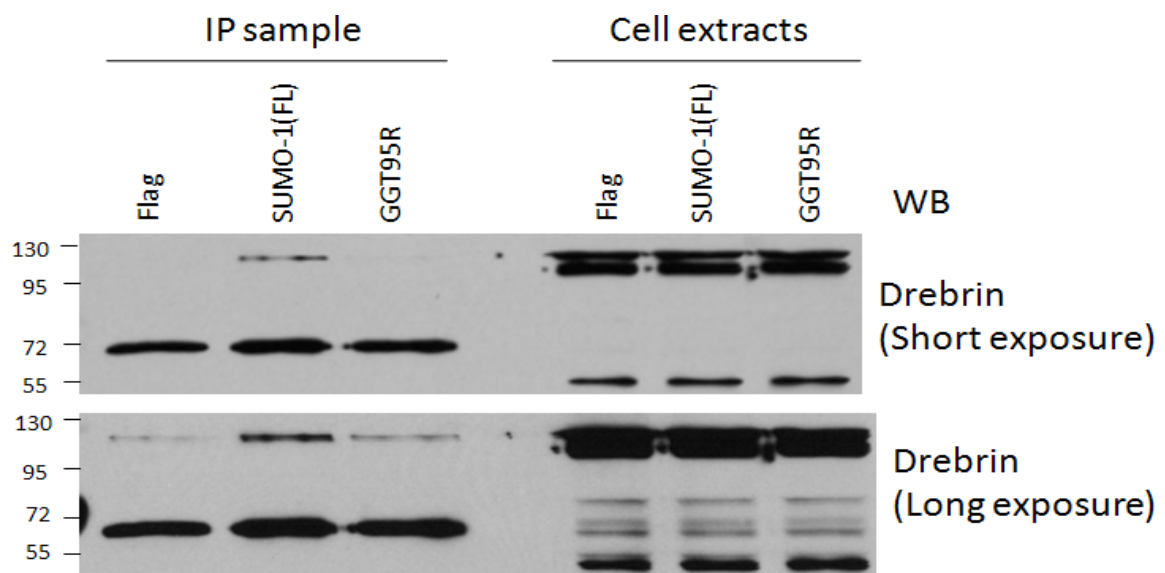
Lizard WEQAKKEEELRKEEERKKALDERLRFQERMEQERQEEERKRYREREQIEEHRKKQOQSLAEAAKRLKEQSIFGQDEEEDRQRPKKSESEVE

Frog WEQAKKEEELRKEEERKKALDERLRFQERMEQERKEQEEERKRYQEREQIEEHRKKLDQEEAEAAKQNS-SIFHQRDEEETATELKRTSESEVE

Zebrafish WEQAKKEEELRKEEERKKAAEERQFERNELERKEQEEERKRYREREQIEEHRKK--ILEEEAKERTNPOLITEPSDPSLE--KKESESEVE

**Figure 2.8. Validation of SUMOylated Drebrin by FLAG-SUMO-1 IP and HA-Drebrin IP followed by Western blotting. (A)** Validation of SUMOylated Drebrin by FLAG-SUMO1 IP. HEK293 cells were transfected with “FL” SUMO-1 (full length) or “GG-T95R” SUMO-1 (last four amino acids truncated, with T95R mutation). Forty-eight hours post-transfection, FLAG-SUMO-1 IP was performed and IP products were subjected to SDS-PAGE. Western blotting was performed using antibodies against Drebrin with longer and short exposure time. **(B)** Validation of SUMOylated Drebrin by HA-Drebrin IP. HEK293 cells were transfected with FLAG-SUMO-1 (full length) and HA-Drebrin (WT). Forty-eight hours post-transfection, HA-Drebrin IP was performed and IP products were subjected to SDS-PAGE. Western blotting was performed using antibodies against FLAG, HA and actin.

**(A)**



(B)

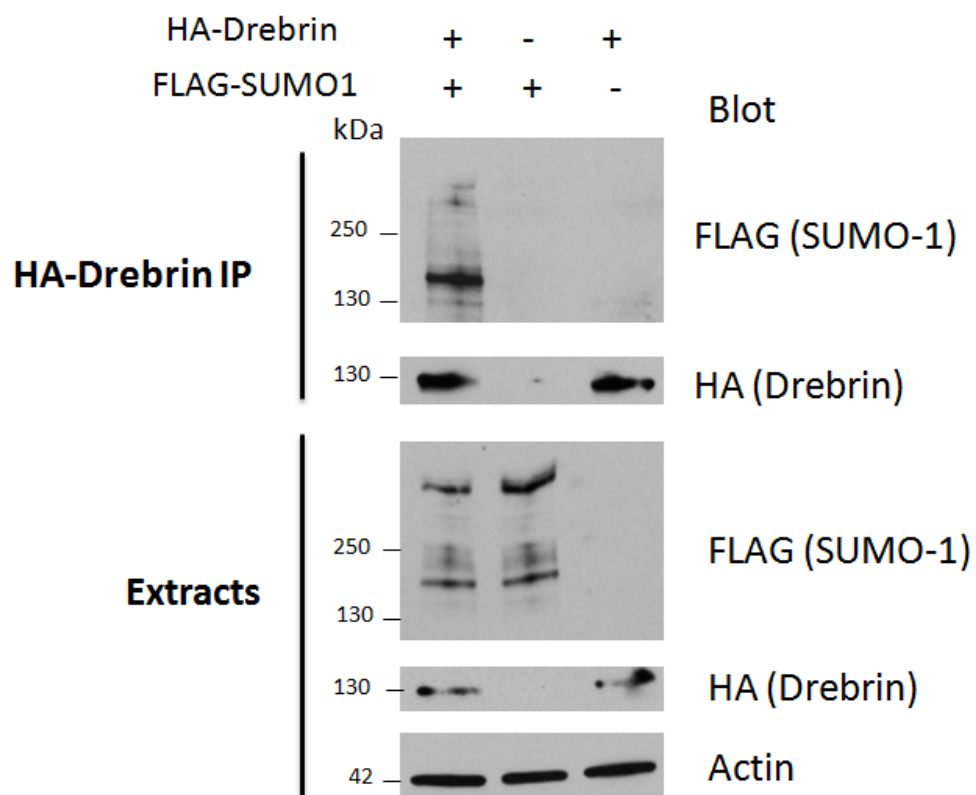
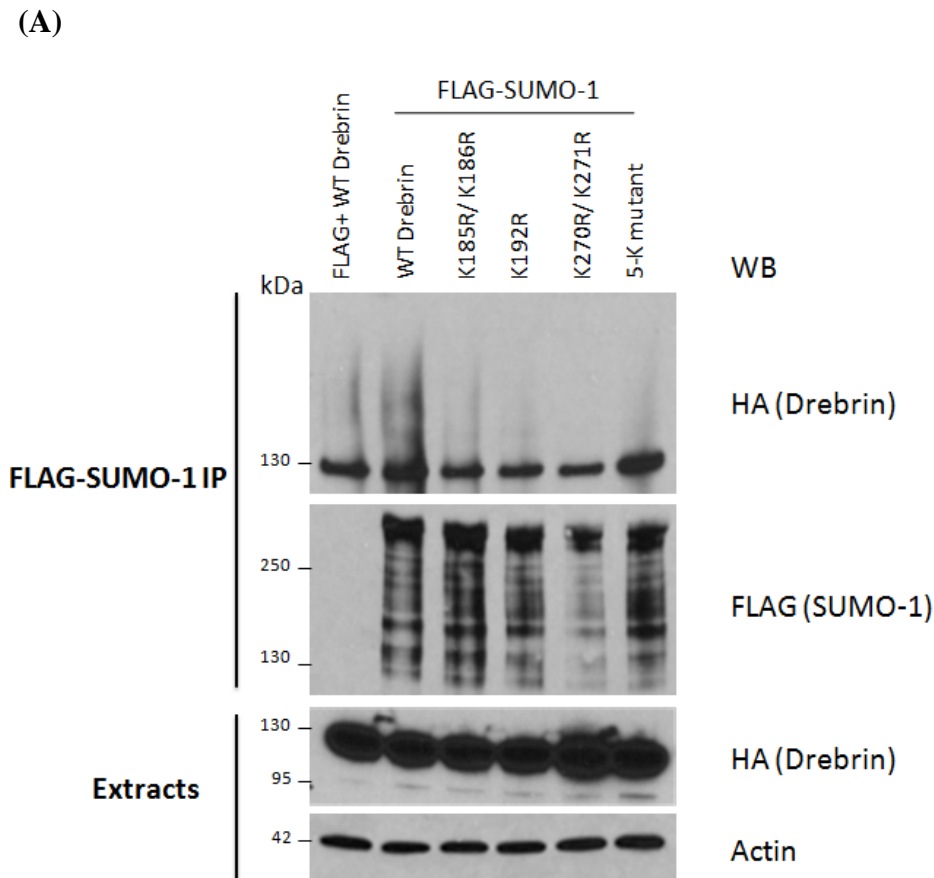


**Figure 2.9. Identification of Drebrin SUMOylation sites by FLAG-SUMO-1 IP and HA-Drebrin IP.** (A) Identification of Drebrin SUMOylation sites by FLAG-SUMO-1 IP. HEK293 cells were transfected with full length FLAG-SUMO-1 and HA-Drebrin (WT) or mutant HA-Drebrin including K185R/K186R, K192R, K270R/K271R and K185R /K186R/ K192R /K270R/K271R (“5-K mutant”). FLAG-SUMO-1 IP was performed and IP products were subjected to SDS-PAGE. Western blotting was performed using antibodies against HA, FLAG and actin. (B) Identification of Drebrin SUMOylation sites by HA-Drebrin IP. HEK293 cells were transfected with full length FLAG-SUMO-1 and HA-Drebrin (WT) or mutant HA-Drebrin including K185R/K186R, K192R and K270R/K271R. HA-Drebrin IP was performed and IP products were subjected to SDS-PAGE. Western blotting was performed using antibodies against HA, FLAG and actin. Quantification of SUMOylated Drebrin/Drebrin was done by Image J software. The relative amount of SUMOylated Drebrin was obtained by normalization of SUMOylated Drebrin to HA-Drebrin and this number for WT Drebrin was set to 1. All other mutants were normalized accordingly. The quantification data is shown in red.



(B)

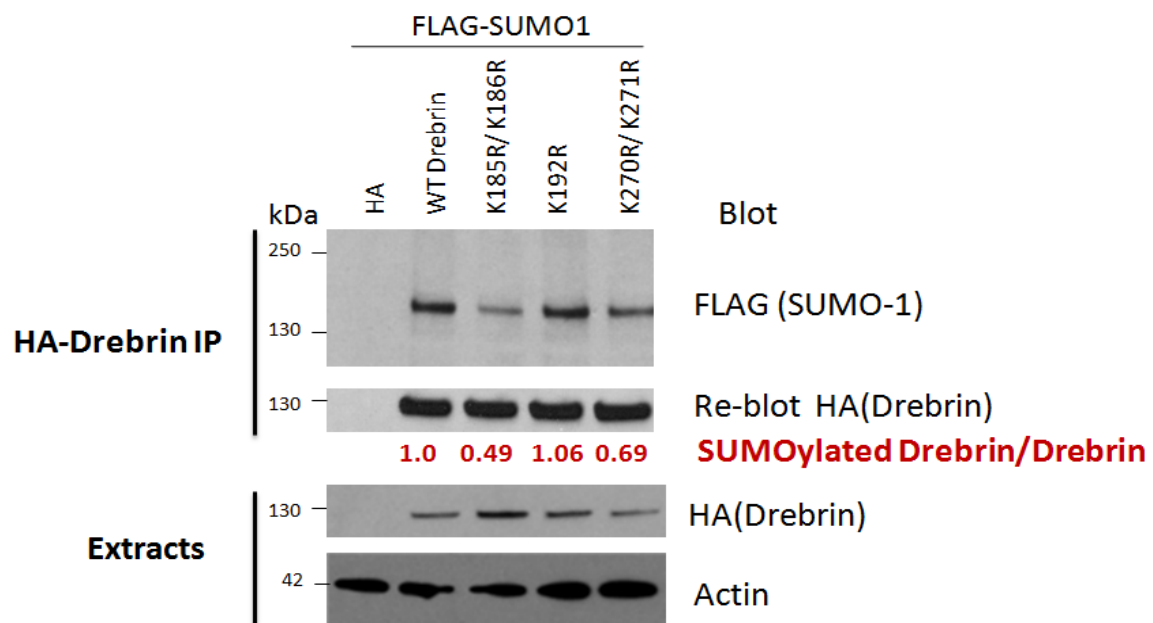
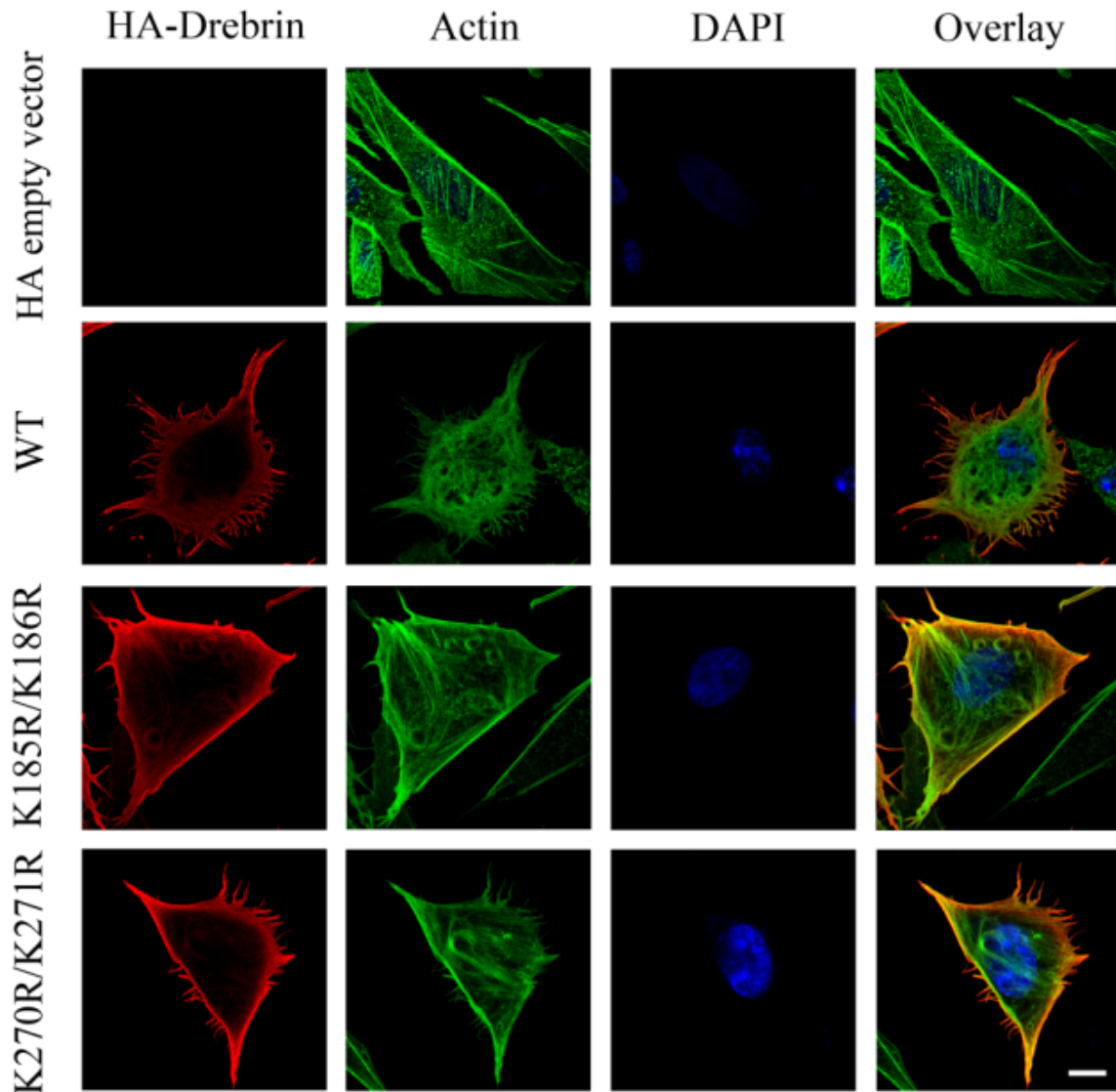


**Figure 2.10. Immunostaining of Drebrin and actin filament in CHO cells.** CHO cells were transfected with WT Drebrin or mutant Drebrin (K185R/K186R or K270R/K271R) or empty HA vector. Non-transfected CHO cells also were used as control cells. Twenty-four hours post-transfection, cells were fixed with 4% PFA and permeabilized with 0.1% Triton. Primary antibody HA (1:300) or Drebrin (1:50) and secondary antibody Alexa Fluoro 594 (mouse or rabbit) (red, 1:300), as well as DAPI (blue, 1:2000), Oregon Green 488 phalloidin (green, 1:50) were used. Confocal microscopy was applied for observation. Scale bars=10  $\mu$ m. **(A)** Immunostaining of Drebrin and actin. **(B)** Quantification of % of protrusions in each sample. The data were presented as mean  $\pm$  S.D., and one way ANOVA analysis with Tukey's test was used to analyze the differences between the individual experiments.

**(A)**



(B)

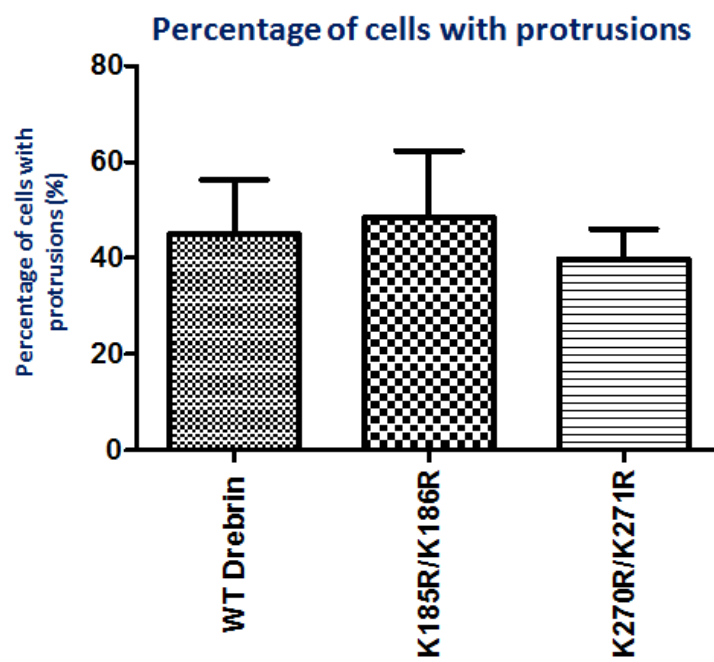




**Table 2.1. Seventy-four proteins identified in cells expressing four different SUMO-1 constructs.** Proteins were identified by nano-LC-MS/MS from in-gel tryptic digestion followed by MASCOT search. The number of SUMOylation consensus sites and predicted non-consensus SUMOylation sites were analyzed by SUMOsp 2.0 software. A number of proteins with higher number of predicted SUMOylation sites (large than four, at least one SUMO consensus site) were highlighted.

<i>Accession</i>	<i>Protein Description</i>	<i>SUMO consensus sites</i>	<i>Non-consensus sites</i>
ACTN4_HUMAN	Alpha-actinin-4	1	3
ALDOA_HUMAN	Fructose-bisphosphate aldolase A	0	2
ATPA_HUMAN	ATP synthase subunit alpha, mitochondrial precursor	1	0
ATPB_HUMAN	ATP synthase subunit beta, mitochondrial precursor	0	1
C1TC_HUMAN	C-1-tetrahydrofolate synthase, cytoplasmic (C1-THF synthase)	1	0
DDX3X_HUMAN	ATP-dependent RNA helicase DDX3X	1	1
DDX5_HUMAN	Probable ATP-dependent RNA helicase DDX5	1	2
DREB_HUMAN	Drebrin (Developmentally- regulated brain protein)	1	3
EF1D_HUMAN	Elongation factor 1-delta	0	1
EF1G_HUMAN	Elongation factor 1- gamma	1	1
EFTU_HUMAN	Elongation factor Tu, mitochondrial precursor	1	1
G3P_HUMAN	Glyceraldehyde-3- phosphate dehydrogenase	1	2
GSTM2_HUMAN	Glutathione S-transferase Mu 2	1	1
GTF2I_HUMAN	General transcription factor II-I (GTFII-I)	4	2
H4_HUMAN	Histone H4	0	0

Contd.

HNRH1_HUMAN	Heterogeneous nuclear ribonucleoprotein H (hnRNP H)	0	2
HNRPC_HUMAN	Heterogeneous nuclear ribonucleoproteins C1/C2	2	8
HNRPD_HUMAN	Heterogeneous nuclear ribonucleoprotein D0	1	3
HNRPU_HUMAN	Heterogeneous nuclear ribonucleoprotein U	3	5
IF4A1_HUMAN	Eukaryotic initiation factor 4A-I	1	1
IF5A1_HUMAN	Eukaryotic translation initiation factor 5A-1	0	1
IMA2_HUMAN	Importin alpha-2 subunit	0	2
IMB1_HUMAN	Importin beta-1 subunit	0	3
IQGA1_HUMAN	Ras GTPase-activating-like protein IQGAP1	4	11
KU70_HUMAN	ATP-dependent DNA helicase 2 subunit 1	2	4
MCM3_HUMAN	DNA replication licensing factor MCM3	0	5
MCM4_HUMAN	DNA replication licensing factor MCM4	1	2
MCM7_HUMAN	DNA replication licensing factor MCM7	0	4
MYH10_HUMAN	Myosin-10	6	10
MYL6_HUMAN	Myosin light polypeptide 6	0	0
NOLA1_HUMAN	H/ACA ribonucleoprotein complex subunit 1	0	0
NONO_HUMAN	Non-POU domain-containing octamer-binding protein	1	2
NPM_HUMAN	Nucleophosmin (NPM)	2	3
NUCL_HUMAN	Nucleolin (Protein C23)	4	4

Contd.

ODPA_HUMAN	Pyruvate dehydrogenase E1 component alpha subunit	0	1
PARP1_HUMAN	Poly [ADP-ribose] polymerase 1	5	11
PCBP1_HUMAN	Poly(rC)-binding protein 1	0	0
PCBP2_HUMAN	Poly(rC)-binding protein 2	0	1
PCNA_HUMAN	Proliferating cell nuclear antigen (PCNA)	1	0
PLST_HUMAN	Plastin-3 (T-plastin)	0	2
PPIA_HUMAN	Peptidyl-prolyl cis-trans isomerase A	1	0
PRPS1_HUMAN	Ribose-phosphate pyrophosphokinase I	0	0
RAN_HUMAN	GTP-binding nuclear protein Ran	0	0
RAGP1_HUMAN	Ran GTPase-activating protein 1	2	1
RL11_HUMAN	60S ribosomal protein L11	1	1
RL14_HUMAN	60S ribosomal protein L14	1	1
RL19_HUMAN	60S ribosomal protein L19	1	4
RL22_HUMAN	60S ribosomal protein L22	0	0
RL24_HUMAN	60S ribosomal protein L24	2	2
RL27_HUMAN	60S ribosomal protein L27	1	0
RL31_HUMAN	60S ribosomal protein L31	0	0
RL38_HUMAN	60S ribosomal protein L38	0	3
RL4_HUMAN	60S ribosomal protein L4 (L1)	0	2
RL9_HUMAN	60S ribosomal protein L9	0	1
ROA1_HUMAN	Heterogeneous nuclear ribonucleoprotein A1	0	3
Contd.			

RS14_HUMAN	40S ribosomal protein S14	0	2
RS15A_HUMAN	40S ribosomal protein S15a	0	0
RS3A_HUMAN	40S ribosomal protein S3a	2	0
RS4X_HUMAN	40S ribosomal protein S4	0	4
RS6_HUMAN	40S ribosomal protein S6	0	4
SFPQ_HUMAN	Splicing factor, proline- and glutamine-rich	2	1
SPTA2_HUMAN	Spectrin alpha chain, brain	2	9
SPTB2_HUMAN	Spectrin beta chain, brain 1	3	13
SUMO1_HUMAN	Small ubiquitin-related modifier 1 precursor (SUMO-1)	0	0
TBA3_HUMAN	Tubulin alpha-3 chain	0	0
TBB2C_HUMAN	Tubulin beta-2C chain	0	0
TBB3_HUMAN	Tubulin beta-3 chain	0	0
TCPD_HUMAN	T-complex protein 1 subunit delta (TCP-1-delta)	0	1
TCPE_HUMAN	T-complex protein 1 subunit epsilon	1	1
TCPH_HUMAN	T-complex protein 1 subunit eta	1	3
TCPW_HUMAN	T-complex protein 1 subunit zeta-2	1	4
TCPZ_HUMAN	T-complex protein 1 subunit zeta	2	4
TIF1B_HUMAN	Transcription intermediary factor 1-beta (TIF1-beta)	2	1
XPO2_HUMAN	Exportin-2 (Exp2)	0	1

**Table 2.2. Thirteen proteins with “GG”-tag identified by mass spectrometry from cells overexpressing SUMO-1 (“GG-T95R”).** Proteins were identified by nano-LC-MS/MS from in-gel tryptic digestion followed by MASCOT search. T-complex protein 1 subunit delta and Ran GTPase-activating protein 1 are also in the common protein list (Table 2.1).

ADP-ribosylation factor 1
Cell division cycle 2-related protein kinase 7
C-jun-amino-terminal kinase-interacting protein 4
EH-domain-containing protein 1 (Testilin)
Endothelial zinc finger protein induced by tumor necrosis factor alpha (Zinc finger protein 71)
Endothelin-1 precursor (Preproendothelin-1) (PPET1)
Lethal(2) giant larvae protein homolog 1 (LLGL)
Microtubule-associated protein 1B (MAP 1B)
Protein Wnt-5b precursor
Ran GTPase-activating protein 1
Synaptonemal complex protein 1 (SCP-1)
T-complex protein 1 subunit delta (TCP-1-delta)
Tyrosine-protein kinase HCK

### **Chapter 3. The role of PDB-associated p62 mutants in NF- $\kappa$ B signaling pathway**

#### **Introduction**

PDB-associated p62 mutations are in 40% of the familiar PDB cases, and the upregulation (or defective) NF- $\kappa$ B signaling pathway is linked to PDB [7, 9]. Therefore, it is important to know the functional consequences of p62 PDB mutations [7, 9]. However, not much of the cellular impact of PDB-associated p62 mutations is known. In this Chapter, the focus is on the role of p62 PDB mutants in the NF- $\kappa$ B signaling pathway, which is related to the formation of hyperactivated osteoclasts as described in Chapter 1 [59, 67]. Specifically, we ask two important questions: (1) Do PDB-associated p62 mutations increase the NF- $\kappa$ B signaling? and (2) If so, by which mechanism do p62 PDB mutants increase the signaling?

Previous studies have reported that four mutations in p62 including P364S [79], K378X [81], P392L [79, 80] and E396X [81] increased NF- $\kappa$ B signaling. In this Chapter, whether several other mutants (M404V, G411S, D335E and A381V) also increase the NF- $\kappa$ B signaling was tested. Also, there is no report regarding how p62 PDB mutants increase the NF- $\kappa$ B signaling [9, 59]. Therefore, the possible mechanisms by which PDB-associated p62 mutants increase the NF- $\kappa$ B signaling pathway were tested.

We initiated our study on the impact of p62 PDB mutants using Raw264.7 cells, which are osteoclast-like cells and widely used in the field [170]. To study the impact of PDB-associated p62 mutants on signaling, NF- $\kappa$ B luciferase assays and I $\kappa$ B degradation assays were performed in Raw264.7 cells overexpressing WT p62 and mutant p62

induced by the GST-rRANKL [171]. Due to the high background of endogenous p62 and low transfection efficiency of Raw264.7 cells, it was challenging to draw definite conclusions. TNF $\alpha$  and RANKL belong to the same family [172]. Therefore, we subsequently studied the impact of p62 PDB mutants in TNF $\alpha$ -induced NF- $\kappa$ B signaling using p62 KO MEF cells, which have the advantage of lacking of endogenous p62.

Furthermore, previous studies have reported that p62 facilitates TRAF6 polyubiquitination, and activates the NF- $\kappa$ B signaling pathway [94]. Therefore, we firstly hypothesized that PDB-associated p62 mutants increase NF- $\kappa$ B signaling by increasing TRAF6 polyubiquitination. In this Chapter, we aim to test this hypothesis.

## **Materials and methods**

### **Cells and reagents**

Raw264.7 cells were a gift from Dr. Lisa Cassis (University of Kentucky). WT MEF and p62 KO MEF cells were kindly provided by Dr. Masaaki Komatsu at Tokyo Metropolitan Institute of Medical Science [106]. The Raw264.7 cell line stably expressing the NF- $\kappa$ B luciferase reporter was generously shared by Dr. Jiake Xu (University of Western Australia, Australia) [170, 173]. HEK 293 cells stably expressing RANK receptor was kindly provided by Dr. Sarah Rea (Sir Charles Gairdner Hospital, Australia) and Dr. Julie Crockett (University of Aberdeen, United Kingdom) [79].

Cells were cultured at 37°C with 5% CO<sub>2</sub>. HEK293 cells were cultured in Dulbecco's Modified Eagle's Medium (DMEM) supplemented with 10% fetal bovine serum (FBS), 100 units/ml penicillin and 100  $\mu$ g/ml streptomycin. WT MEF and p62 KO

MEF cells were cultured in DMEM supplemented with FBS, PS, 100 mM Sodium Pyruvate (11360-070; Invitrogen) and 10 mM Non-Essential Amino Acids (11140-050; Invitrogen). Raw264.7 cells were cultured in DMEM supplemented with FBS, PS, Sodium Pyruvate (Invitrogen), Non-Essential Amino Acids (Invitrogen) and 20 mM HEPES (15630-106; Invitrogen). For Raw264.7 cells stably expressing NF- $\kappa$ B luciferase reporter, an additional 400  $\mu$ g/ml G418 (G8168; Sigma) was required. HEK293 cells stably expressing the RANK receptor were cultured in DMEM supplemented with FBS, PS and 100  $\mu$ g/ml Hygromycin B (400053; EMD Biosciences).

Additionally, GST-rRANKL, NF- $\kappa$ B luciferase reporter and HA-RANK plasmids were generous gifts from Dr. Jiake Xu (University of Western Australia, Australia) [171, 173]. GST-rRANKL protein was purified with the help of Dr. Weimin Gong (Institute of Biophysics in Beijing, China). HA-Ub constructs including K29R, K48R and K63R were kindly shared by Dr. Marie Wooten (Auburn University). The 3xHA-Ub constructs including WT, “K48 only” and “K63 only” were gifts from Dr. Matthew Gentry (University of Kentucky). The phRL-TK (Renilla) vector used in this study was from Promega. The information of plasmids is summarized in Appendix I.

### **Plasmid construction**

The Myc-p62 (human) plasmid was a gift from Dr. Marie Wooten (Auburn University). The human p62 was amplified by PCR and was inserted among the *Eco*RI and *Kpn*I sites of the p3xFLAG-CMV10 vector (Sigma). Five PDB mutants, including D335E, A381V, P392L, M404V and G411S were generated by using the QuikChange II



Site-Directed Mutagenesis Kit (Stratagene). The details of these plasmids (Appendix I) and designed primers (Appendix II) for mutagenesis are shown in the Appendix.

### **NF- $\kappa$ B luciferase assay**

For the study of RANKL-induced NF- $\kappa$ B signaling, 70% confluent Raw264.7 cells stably expressing NF- $\kappa$ B luciferase reporter were transfected with Renilla control vector and WT p62 or p62 PDB mutants. Forty-eight hours after the transfection, cells were treated with GST-rRANKL (30ng/ml) for 7 hours. Cells were lysed with the Passive Lysis Buffer (PLB) of the Dual Luciferase Reporter Assay System (Promega). Aliquots of the cell lysates were subjected to SDS-PAGE and Western blotting using antibodies including anti-FLAG (A8592; Sigma) and anti-actin (sc-1616; Santa Cruz Biotechnology). The NF- $\kappa$ B luciferase assays were performed using the Dual Luciferase Reporter Assay System (Promega) using Optocomp I luminometer.

For the study of TNF $\alpha$ -induced NF- $\kappa$ B signaling, 70% confluent p62 KO MEF cells or WT MEF cells were transfected with Renilla vector, NF- $\kappa$ B luciferase reporter and WT p62 or p62 PDB mutants. Twenty-four hours after the transfection, cells were starved with DMEM containing only 0.1% BSA for 4 hours. Cells were then treated with 20 ng/ml mouse TNF $\alpha$  (315-01A; PeproTech, Inc.) overnight. The next day, cells were lysed in PLB. Aliquots of the cell lysates were subjected to SDS-PAGE and Western blotting using antibodies including anti-FLAG (A8592; Sigma) and anti-actin (sc-1616; Santa Cruz Biotechnology). NF- $\kappa$ B luciferase assays were performed using the Dual Luciferase Reporter Assay System (Promega).

## **Statistical analysis**

Three independent NF- $\kappa$ B luciferase assays in either p62 KO MEF cells or HEK293 cells were performed. All data were presented as mean with standard deviation (SD). The significant differences in NF- $\kappa$ B activity fold increases between control cells and cells expressing WT p62 were analyzed by *t*-test. The significant differences in NF- $\kappa$ B activity fold increases among cells expressing WT p62 and p62 PDB mutant were analyzed by one-way ANOVA, with Tukey's post-test using the software GraphPad Prism 5 Demo.

## **Monitoring the rate of I $\kappa$ B degradation**

Raw264.7 cells or p62 KO MEF cells were transfected with WT p62 or M404V p62. After 24 hours, the cells were either left untreated or were treated with GST-rRANKL (100 ng/ml) or mouse TNF $\alpha$  (30 ng/ml) for 15 or 45 minutes. Then, the cells were lysed with RIPA buffer (Millipore) supplemented with PMSF, P8340 protease inhibitor cocktail (Sigma), Na<sub>3</sub>VO<sub>4</sub> and NEM for 30 minutes. The cell lysates were centrifuged at 1000g for 10 minutes and the supernatants were boiled with 6xSDS loading buffer. Samples were subjected to SDS-PAGE, followed by Western blotting using antibodies including anti-I $\kappa$ B $\alpha$  (mAb #4812; Cell Signaling) and anti-actin (sc-1616; Santa Cruz Biotechnology).

### **P65 nuclear translocation**

Raw264.7 cells were left untreated or treated with GST-rRANKL (100 ng/ml) for 30 minutes. The cells were fixed with 4% paraformaldehyde (PFA) at 37°C for 15 minutes, permeabilized with 0.1% Triton in PBS and blocked with 3% bovine serum albumin (BSA) in PBS for 1 hour. All the primary and secondary antibodies were diluted in 3% BSA/PBS. Cells were first stained with p65 antibody (mouse, sc-8008, Santa Cruz Biotechnology, 1:50) overnight. The next day, the coverslips were washed with PBS and incubated with Hoechst (33258; Sigma, 1:1000) and secondary Alexa Fluor 488 anti-mouse antibody (A21202; Invitrogen, 1:300) for 2 hours. Finally, the coverslips were mounted using Vectashield mounting medium (Vector Laboratories). Fluorescence microscopy was performed using a confocal microscope (Olympus FluoView) with a 60x objective.

### **P62 siRNA**

Raw264.7 cells or Raw264.7 cells stably expressing NF- $\kappa$ B luciferase reporter were transfected with non-targeting siRNA (Dharmacon, D-001210-01-05) or p62 siRNA (40nM or 80nM, Dharmacon, M-047628-01) using Lipofectamine LTX transfection reagent (Invitrogen) in the Opti-MEM reduced serum medium (Invitrogen). Forty-eight hours after transfection, cells were lysed with RIPA buffer (Millipore). The cell lysates were centrifuged at 1000g for 10 minutes and the supernatants were boiled with 6xSDS loading buffer. Samples were subjected to SDS-PAGE. The knockdown efficiency was checked by Western blotting using antibodies including anti-p62 (H00008878-M01; Abnova) and anti-actin (sc-1616; Santa Cruz Biotechnology).

### **TRAF6 ubiquitination assay**

HEK293 cells were transfected with FLAG-TRAF6 and DsRed-p62 (WT or mutant) using the Lipofectamine transfection reagent (Invitrogen). Forty-eight hours after transfection, cells were lysed using either PPHB buffer (50 mM Na<sub>2</sub>HPO<sub>4</sub>, 1 mM sodium pyrophosphate, 20 mM NaF, 2 mM EDTA, 2 mM EGTA and 1% Triton X-100) or RIPA buffer (Millipore). Cells were starved for 3.5 hours and treated with human TNF $\alpha$  (30ng/ml) for 10 minutes. The cell lysates were centrifuged at 1000g for 10 minutes and pre-cleared with Sepharose 4L-CB (Sigma) beads for 1 hour. The lysates were then incubated with anti-FLAG M2 affinity beads for 2 hours at 4°C (F2426; Sigma). The beads were washed three times with lysis buffer and the immunoprecipitation (IP) products were eluted by boiling in SDS-PAGE loading buffer. The IP products and the extracts were subjected to SDS-PAGE using 4–20% ReadyGel Tris–HCl gradient gels (BioRad), followed by Western blotting with different antibodies including anti-ubiquitin (sc-8017, Santa Cruz Biotechnology), anti-FLAG (A8592; Sigma) and anti-actin (sc-1616, Santa Cruz Biotechnology).

### **Western blotting and quantification**

Nitrocellulose membrane was incubated in blocking solution, 5% milk in Tris-Buffered Saline and Tween 20 (TBST) for one hour. Then the membranes were incubated with primary antibody for more than three hours. After four washes with TBST for five minutes each, the membrane was incubated with the secondary antibody for more than

one hour. After four washes again with TBST for five minutes each, proteins of interest were visualized by either normal or dura enhanced chemiluminescent (ECL) substrate (Thermo scientific) for detection of horseradish peroxidase (HRP) enzyme (Thermo scientific). The membrane was covered with the wrapping membrane and an autoradiography film (Denville Scientific) which was exposed to the membrane. The exposure time varied from one second to 20 minutes depending on the signal intensity. Films were subsequently developed by a Kodak X- OMAT 2000 processor.

Software Image J was used for quantification of Western blotting bands on X-ray films. Since ECL signals of the Western blot were captured on X-ray films which are known to have a narrow linear range of detection, the quantification of the Western blot may be out of linear range for certain experiments. Enhanced chemofluorescence (ECF) substrate and Alkaline Phosphatase (AP)-conjugated secondary antibody are encouraged for use in the future.

## **Results**

### **Effect of the p62 PDB mutation on RANKL-induced NF- $\kappa$ B signaling in Raw264.7 cells**

We used three classical techniques, including the NF- $\kappa$ B luciferase assay, I $\kappa$ B degradation assay and p65 nuclear translocation assay, to study the impact of PDB-associated p62 mutants in the RANKL-induced NF- $\kappa$ B signaling.

#### ***(1) NF- $\kappa$ B luciferase assay***

The schematic diagram of the NF- $\kappa$ B signaling in these studies is shown in Fig. 3.1. After RANKL treatment, a significant increase of the luciferase signal was observed, suggesting that the RANKL reagent and the whole system were working (Fig. 3.2 C). It was also shown that the endogenous level of p62 was high (Fig. 3.2 A). The level of overexpressed p62 was different among WT p62 and mutant p62 (M404V, A381V and P392L) (Fig. 3.2 A). Therefore, it is reasonable to normalize the NF- $\kappa$ B luciferase data using the expression level of p62 (Fig 3.2 B). The original data of Firefly and Renilla were shown in Fig. 3.2 C. Fold increases after treatment were calculated by using the Firefly data divided by the Renilla. These increased ratios were further calibrated by using the data from the overexpressed p62 without treatment (Fig 3.2 B). Final calibrated fold increases were obtained (Fig. 3.2 D). It is shown that mutant M404V and A381V increased the NF- $\kappa$ B luciferase activity compared with WT p62 (Fig. 3.2 D). The high endogenous p62 level in Raw264.7 cells prevented us from further studying the impact of mutant p62 on signaling (Fig. 3.2 A). Also, the luciferase assay in HEK293 cells expressing the RANK receptor induced by RANKL was used, but did not produce a signal (data not shown).

## **(2) *I $\kappa$ B degradation assay***

The I $\kappa$ B degradation assay in Raw264.7 cells induced by RANKL (Fig. 3.3) was then performed. When stimulated with RANKL, I $\kappa$ B was phosphorylated, ubiquitinated and degraded by the proteasome (Fig. 1.5). Therefore, the lower I $\kappa$ B level indicates increased NF- $\kappa$ B signaling activity. The data showed that the I $\kappa$ B level in cells expressing M404V was always lower than that in cells expressing WT p62 when treated with RANKL for either 15 or 45 minutes (Fig. 3.3 B). This result indicates that M404V

p62 increased the NF- $\kappa$ B signaling. Again, due to the high endogenous p62 level in Raw264.7 cells, it is difficult to reach a definite conclusion.

### ***(3) P65 nuclear translocation***

Raw264.7 cells were either treated or untreated with RANKL for 30 minutes. P65 nuclear translocation was observed using confocal microscopy. After stimulation of RANKL in Raw264.7 cells, a significant amount of p65 was observed in the nucleus (Fig. 3.4 upper panel), whereas p65 remained in the cytoplasm without treatment (Fig. 3.4 lower panel). These results indicate that RANKL induced p65 nuclear translocation. Since the high background of p62 is an issue, comparison of the WT p62 and mutant p62 has not been done. Also, a better cell model system is needed to study the impact of p62 PDB mutants in RANKL-induced NF- $\kappa$ B signaling (see “Discussion”).

Attempts to knockdown the endogenous level of p62 of Raw264.7 cells by using the siRNA were also tried. However, the p62 siRNA (40nM and 80nM) did not decrease the endogenous p62 level (Fig. 3.5). It is possible that Raw264.7 cells have low transfection efficiency for siRNA too.

### **P62 contributes to TNF $\alpha$ -induced NF- $\kappa$ B signaling**

Firstly, this study has shown that the Firefly/Renilla ratio after TNF $\alpha$  treatment was higher in WT MEF cells compared with p62 KO MEF cells (Fig. 3.6 A and B). It is shown that overexpression of WT p62 in p62 KO MEF cells increased the signaling compared with control p62 KO MEF cells (Fig. 3.6 C and D). Altogether, this suggests that p62 contributes to TNF $\alpha$ -induced NF- $\kappa$ B signaling.

This conclusion is further supported by three independent TNF $\alpha$ -induced NF- $\kappa$ B luciferase assays in p62 KO MEF cells (Fig. 3.9 A). In order to find the best concentration of TNF $\alpha$  for measurement, cells were treated with different concentrations of TNF $\alpha$  (9 ng/ml, 18 ng/ml and 30 ng/ml) overnight. It is shown that 18 ng/ml performed best which could cause the largest difference of Firefly/Renilla signals between cells overexpressing WT p62 and control cells (Fig. 3.7). Therefore, 20ng/ml TNF $\alpha$  for the following luciferase assay for statistical study was used. It is shown that cells expressing WT p62 had higher fold increases after TNF $\alpha$  treatment compared with control cells to a statistically significant extent, with the p value 0.034 (Fig 3.9 A).

#### **P62 PDB mutants have a tendency to increase NF- $\kappa$ B signaling compared with WT p62**

Next, the impact of PDB-associated p62 mutants in TNF $\alpha$ -induced NF- $\kappa$ B signaling was examined. Firstly, it is shown that Firefly/Renilla signals were higher in p62 KO MEF cells overexpressing M404V p62 compared with WT p62, suggesting that M404V p62 increased TNF $\alpha$ -induced NF- $\kappa$ B signaling compared with WT p62 (Fig. 3.6 C and D). Then, we performed three independent TNF $\alpha$ -induced NF- $\kappa$ B luciferase assays in p62 KO MEF cells (Fig. 3.8 and 3.9). The expression level of FLAG-p62 was similar among cells overexpressing WT and mutant p62 (Fig. 3.8 A). The expression level of p62 was also used for calibration of fold increases in the analysis (Fig. 3.9 C).

Firefly/Renilla signals with or without TNF $\alpha$  in cells overexpressing WT and mutant p62 are shown in Fig. 3.8 B. The fold increases were calculated by using Firefly/Renilla (with TNF $\alpha$ ) divided by Firefly/Renilla (without TNF $\alpha$ ). The luciferase data either without considering the p62 expression level (“Non-calibrated fold increases”,



Fig. 3.9 B) or considering the p62 level (“Calibrated fold increases”, Fig. 3.9 C) was analyzed. After statistical analysis, it is shown that p62 PDB mutants including M404V, A381V and P392L all increased signaling compared with WT p62 (Fig. 3.9 B and C). However, the increase is not statistically significant with the p value larger than 0.05.

The TNF $\alpha$ -induced NF- $\kappa$ B luciferase assay was also performed in HEK293 cells. The results have shown that p62 PDB mutants had a tendency to increase the signaling compared with WT p62 (Fig. 3.10 B).

### **P62 PDB mutant suppresses its binding with polyubiquitinated proteins in HEK293 cells**

Next, we considered mechanisms by which p62 PDB mutants increased signaling. We started to study the cellular consequences of p62 PDB mutants. Because most of PDB mutations are in the UBA domain of p62, which binds the polyubiquitinated proteins [9], we want to know that whether these p62 PDB mutants have effects on the binding of polyubiquitinated proteins.

To address this question, HEK293 cells were transfected with human FLAG-p62 (WT, M404V, A381V, P392L and G411S) or mouse p62 (WT and UBA domain deleted). Forty-eight hours after transfection, FLAG-IP was performed, and it was shown that all of the mutants, especially M404V and P392L p62, impaired the binding of p62 and polyubiquitinated proteins compared with WT p62 (Fig. 3.11). Mouse p62 (UBA domain deleted) also impaired its binding with polyubiquitinated proteins compared with mouse

WT p62, suggesting the validation of negative control (Fig. 3.11). However, for the FLAG-p62 IP shown in Fig. 3.11, whether it was polyubiquitination of p62 or polyubiquitination of other proteins remains investigation.

### **Overexpression of p62 in HEK293 cells leads to TRAF6 polyubiquitination in HEK293 cells**

As mentioned above, it was found that the p62 PDB mutations abolish binding with polyubiquitinated proteins in HEK293 cells. It has also been reported that TRAF6 polyubiquitination is regulated by p62 [94]. Therefore, it is possible that p62 PDB mutations could have effects on TRAF6 polyubiquitination. To address this question, the TRAF6 ubiquitination assay in HEK293 cells overexpressing FLAG-TRAF6 and DsRed-p62 (WT, M404V, A381V and P392L) was performed.

It is shown that in the basal condition, the level of TRAF6 polyubiquitination in cells overexpressing WT p62 is much higher than control cells, indicating that overexpression of p62 in HEK293 cells leads to TRAF6 polyubiquitination (Fig. 3.12, 3.13 and 3.14). In addition, it was found that the level of TRAF6 polyubiquitination increases in proportion to the amount of p62 (Fig. 3.13). It is indicated that the level of TRAF6 polyubiquitination is dependent on p62 amount.

### **Mutant p62 impaired TRAF6 polyubiquitination compared with WT p62 in HEK293 cells**

From the TRAF6 ubiquitination assay in HEK293 cells above, it was shown that the level of TRAF6 polyubiquitination in cells overexpressing PDB-associated p62

mutants (M404V, A381V and P392L), especially M404V p62 is lower than cells overexpressing WT p62 (Fig. 3.12, 3.13 and 3.14). Therefore, p62 PDB mutants, especially M404V, impaired TRAF6 polyubiquitination compared with WT p62 in the basal condition. However, compared with control cells without overexpression of p62, cells overexpressing p62 PDB mutant still increase TRAF6 polyubiquitination (Fig. 3.12, 3.13 and 3.14), indicating that both the WT and the p62 PDB mutant could facilitate TRAF6 polyubiquitination in HEK293 cells.

### **TNF $\alpha$ did not induce TRAF6 polyubiquitination in HEK293 cells**

As mentioned above, it was shown that p62 contributes to TNF $\alpha$ -induced NF- $\kappa$ B signaling (Fig. 3.9 A). It was also shown that PDB-associated p62 mutants increased TNF $\alpha$ -induced NF- $\kappa$ B signaling (Fig. 3.9 and 3.10). Furthermore, it is shown that both WT and mutant p62 facilitate TRAF6 polyubiquitination in HEK293 cells in the basal condition (Fig. 3.12, 3.13 and 3.14). Therefore, it was of interest to determine whether WT p62 and p62 PDB mutants change TRAF6 polyubiquitination upon TNF $\alpha$  treatment compared with basal conditions. In order to address this question, TRAF6 ubiquitination assay was performed in the absence and presence of TNF $\alpha$  in HEK293 cells. It was shown that TNF $\alpha$  was effective because I $\kappa$ B was degraded after TNF $\alpha$  treatment (Fig 3.14). However, the change of TRAF6 polyubiquitination after TNF $\alpha$  treatment (Fig. 3.14) was not observed. Therefore, it is suggested TNF $\alpha$  does not play a role on TRAF6 polyubiquitination in HEK293 cells.

### **Overexpression of p62 in HEK293 cells leads to a TRAF6 polyubiquitination chain of different linkages**

Previous work has shown that p62 facilitates K63-linked polyubiquitination of TRAF6 and further activates the NF- $\kappa$ B signaling [95] (Fig. 1.5). In this study, it was found that p62 facilitates TRAF6 polyubiquitination in HEK293 cells. Therefore, is the TRAF6 polyubiquitination observed (Fig. 3.12 and Fig. 3.14) a K63-linked chain? Could the TRAF6 polyubiquitination observed activate the NF- $\kappa$ B signaling upon TNF $\alpha$  treatment?

To address these questions, HEK293 cells were transfected with FLAG-TRAF6, DsRed-p62 (WT) and a variety of different HA-Ub constructs including K29R, K48R, K63R [95], as well as “K48 only” or “K63 only” in which all the Lys of Ub are mutated to Arg except Lys48 or Lys63, respectively. If it is a K63-linked chain, the level of TRAF6 polyubiquitination should decrease in cells overexpressing HA-Ub (K63R) compared with cells overexpressing WT Ub. However, this difference (Fig. 3.15, lane 1 and 4) was not seen. There is no difference among levels of TRAF6 polyubiquitination in cells overexpressing K29R Ub, K48R Ub and K63R Ub (Fig. 3.15, lane 2-4). In addition, there is no difference between levels of TRAF6 polyubiquitination in cells overexpressing Ub (“K63 only”) and Ub (“K48 only”) (Fig. 3.15, lane 5 and 6). Altogether, it is suggested that the TRAF6 polyubiquitination observed is not a K63-linked chain, but a mixture of K48-linked, K63-linked and K29-linked chains.

Moreover, from the TRAF6 polyubiquitination assay in HEK293 cells with and without TNF $\alpha$  treatment (Fig. 3.14), it is shown that overexpression of p62 could not

activate the NF- $\kappa$ B signaling because I $\kappa$ B level is similar in the absence and presence of p62 (Fig. 3.14). Therefore, the TRAF6 polyubiquitination observed by overexpressing p62 in HEK293 cells could not activate the NF- $\kappa$ B signaling (Fig. 3.14).

## Discussion

### **Does p62 really facilitate TRAF6 to form a K63-linked polyubiquitin chain which activates NF- $\kappa$ B signaling?**

Wooten *et al.* [95] and Moscat *et al.* [93] have shown that p62 could activate the NF- $\kappa$ B signaling in HEK293 cells in the basal condition. Our study not only showed that p62 activates NF- $\kappa$ B signaling basally (Fig. 3.6 C), but also upon TNF $\alpha$  treatment to a statistically significant degree in p62 KO MEF cells (Fig. 3.9 A) and HEK293 cells (Fig. 3.10 A).

Wooten *et al.* [95] have reported that the loss of p62 completely abolishes ubiquitination of TRAF6 by performing TRAF6 immunoprecipitation from lysates of the brains from p62 WT or knock-out mice. In this study, it was shown that p62 facilitates TRAF6 polyubiquitination in HEK293 cells (Fig. 3.12 and 3.14). In their study, they have shown that the TRAF6 polyubiquitination chain is a K63-linked chain by using a variety of different Ub constructs. We also used these different Ub mutants and performed the TRAF6 ubiquitination assay as done previously [95]. However, it was found that the TRAF6 polyubiquitination chain is not K63-linked, but a mixture of K29-linked, K48-linked and K63 linked. It was further confirmed by using two other different Ub mutants, “K48 only” and “K63 only”. The contradictory results between this study and Dr.

Wooten's study might be due to the specific experiment details. In their study, although they have shown that TRAF6 polyubiquitination is a K63-linked chain, they did not show that this chain is sufficient to induce the NF- $\kappa$ B signaling. In this work, it was shown that the TRAF6 polyubiquitination observed is not sufficient to induce NF- $\kappa$ B signaling by comparing the I $\kappa$ B level in cells with and without overexpressing p62 (Fig. 3.14).

These data have shown that p62 contributes to NF- $\kappa$ B activation (Fig. 3.9 A). However, for the TRAF6 polyubiquitination assay, the I $\kappa$ B level remains similar in HEK293 cells with and without overexpressing p62, which seems to contradict that p62 contributes to NF- $\kappa$ B signaling. To clarify this point in the future, more signaling proteins such as IKK and phospho-I $\kappa$ B need to be examined.

#### **Do p62 PDB mutants impair the TRAF6 polyubiquitination upon cytokine treatment?**

In this Chapter, it was shown that M404V p62 impairs TRAF6 polyubiquitination compared with WT p62 in the basal condition (Fig. 3.12 and 3.14). Also, it has been shown that M404V p62 had a tendency to increase TNF $\alpha$ -induced NF- $\kappa$ B signaling (Fig. 3.10 B). Because TRAF6 polyubiquitination facilitates NF- $\kappa$ B signaling [125], these two pieces of data seem to be contradictory. However, it is suggested in the literature that, it is "K63 linked" polyubiquitination that facilitates NF- $\kappa$ B signaling. Was the "K63 linked" polyubiquitination chain in our FLAG-TRAF6 IP observed? Actually it did not. These data have shown that the TRAF6 polyubiquitination chain is a mixture of polyubiquitination chains which contain K29 linked, K48 linked and K63 linked chains

(Fig. 3.15). Therefore, overexpression of p62 could not facilitate TRAF6 to form the K63-linked chain.

In addition, overexpression of p62 does not appear to activate NF- $\kappa$ B signaling because the I $\kappa$ B levels were similar in the absence and presence of p62 (Fig. 3.14). It is suggested that TRAF6 K63-linked polyubiquitination might require the stimulation of cytokines, such as TNF $\alpha$  or RANKL. It has also been shown that TNF $\alpha$  did not induce the TRAF6 polyubiquitination (Fig. 3.14). Therefore, it is indicated that TRAF6 K63-linked polyubiquitination could be observed by stimulation with other cytokines, such as RANKL.

Moreover, these data showed that TNF $\alpha$  did not increase TRAF6 polyubiquitination (Fig. 3.14). Previous studies reported that TNF $\alpha$  increased TRAF2 polyubiquitination [23, 93, 135], but they did not test whether TNF $\alpha$  increased TRAF6 polyubiquitination. Thus, our study expands the knowledge of TNF $\alpha$ . In addition, Fuanakoshi-Tago *et al.* [174] have reported that TRAF6 negatively regulates TNF $\alpha$ -induced NF- $\kappa$ B signaling. They found that IKK activation and I $\kappa$ B degradation were enhanced in TRAF6-deficient MEFs compared with WT MEFs [174]. Although our data and their data are not directly related, all these studies showed at least that TNF $\alpha$ -induced NF- $\kappa$ B signaling is not activated through TRAF6.

### **Three workable cell models for studying the impact of PDB-associated p62 mutants on NF- $\kappa$ B signaling**

#### ***(1) Raw264.7 cells***

Previously, Raw264.7 cells stably expressing the NF- $\kappa$ B luciferase reporter were used as a cell model to study the effect of the p62 on the RANKL-induced NF- $\kappa$ B signaling. It was thought that Raw cells constituted a good cell model because they are osteoclast-like cells [170], which are widely used in the field studying PDB. However, for this project, the goal was to examine the effect of PDB-associated p62 mutations on NF- $\kappa$ B signaling. Because all these p62 mutations are single point mutations, it was recognized that it is very important to rule out the effect of the endogenous p62 of Raw cells. It turned out that Raw cells have a high background of endogenous p62 (Fig. 3.2 A), whereas the transfection efficiency for Raw cells are also low. The use of p62 siRNA to knockdown the endogenous p62 of Raw cells was attempted, but p62 siRNA did not work; this might also be due to the low transfection efficiency of Raw cells (Fig. 3.5). Therefore, other cell models to study the signaling were considered.

## ***(2) p62 KO MEF cells***

P62 KO MEF cells shared by Dr. Masaaki Komatsu (Japan) [106] were used for this study. The advantage of p62 KO MEF cells is that there is no endogenous p62 in this cell line. Therefore, it is advantageous to compare the effect of WT p62 and p62 PDB mutant using this p62 KO MEF cell line. The disadvantage of this cell line is that the transfection efficiency for the cell is also low. In addition, p62 KO MEF cells did not respond to the RANKL (data not shown). HA-RANK receptor (shared by Dr. Jiake Xu, Australia) was transfected into p62 KO MEF cells, and these cells again did not respond to RANKL (data not shown). However, p62 KO MEF cells did respond to TNF $\alpha$  (Fig. 3.6). Therefore, the study shifted to the effect of PDB-associated p62 mutations on TNF $\alpha$ -induced NF- $\kappa$ B signaling. The TNF $\alpha$ -induced NF- $\kappa$ B luciferase assay was



performed in p62 KO MEF cells overexpressing either WT p62 or p62 PDB mutant for more than three times (Fig. 3.8 and 3.9). These data have shown a tendency for mutant p62 to increase TNF $\alpha$ -induced NF- $\kappa$ B signaling compared with WT p62, which is not statistically significant in p62 KO MEF cells. Additionally, it is shown that even without p62, there is still basal TNF $\alpha$ -induced NF- $\kappa$ B signaling (Fig. 3.9). Also, p62 increases the TNF $\alpha$ -induced NF- $\kappa$ B signaling pathway to a statistically significant degree ( $p < 0.05$ ) (Fig. 3.9 A). Therefore, p62 PDB mutants increase NF- $\kappa$ B signaling in p62 KO MEF cells, but the increase is so subtle that it is difficult to detect with NF- $\kappa$ B luciferase assay.

### ***(3) HEK293 cells***

In addition, the TNF $\alpha$ -induced NF- $\kappa$ B assay in HEK293 cells was studied. HEK293 cells could also respond to TNF $\alpha$  signals (Fig. 3.10). In addition, the increased folds in cells expressing p62 (the number is over 50) are much higher than control cells, suggesting that it might be a good model to compare the effect of WT p62 and mutant p62 on TNF $\alpha$ -induced NF- $\kappa$ B signaling.

It appears to be challenging to study the RANKL-induced NF- $\kappa$ B signaling in this study. An ideal cell model should have little background of endogenous p62, high transfection efficiency and response after stimuli of RANKL. While it is difficult to find such a perfect cell model for study, some ways to optimize our existent cell lines are considered. The strategies are described below and summarized in Table 3.1.

#### ***(1) HEK293 cells stably expressing RANK receptor***

Rea *et al.* [79] reported that P364S and P392L increased RANKL-induced NF- $\kappa$ B signaling by NF- $\kappa$ B luciferase assay in HEK293 cells stably expressing RANK receptor.

We also obtained the above stable HEK293 cells from them. Although we tried the same assay as described in their paper, the NF- $\kappa$ B signaling induced by GST-rRANKL [171] was not detected (data not shown).

***(2) p62 KO MEF cells stably expressing HA-RANK receptor***

HA-RANK receptor was also kindly shared by Dr. Jiake Xu (Australia). We also tried transient transfection of HA-RANK into p62 KO MEF cells, but again cells did not respond to GST-rRANKL [171] (data not shown). Because currently no report regarding using p62 KO MEF cells expressing HA-RANK receptor, there is a need to change the parameters for experiment optimization. If it works in the future, this approach might generate the p62 KO MEF cells stably expressing HA-RANK receptor.

***(3) Raw264.7 cells with p62 shRNA***

Since Raw264.7 cells have low transfection efficiency, lentivirus-delivered p62 shRNA and exogenous p62 (WT or mutant) could be applied. It will be necessary to be careful about the design of p62 shRNA, which should only interfere with endogenous p62, not exogenous p62. Biosafety issues also need to be considered.

**Significance of this study and future directions**

The significance of this study in this Chapter is that this is the first example using the p62 KO MEF cells as a model for studying the effect of p62 PDB mutants on NF- $\kappa$ B signaling. Also, this is the first study to show that p62 not only increases TNF $\alpha$ -induced NF- $\kappa$ B signaling basally, but also upon TNF $\alpha$  treatments in p62 KO MEF cells, which was not reported. Moreover, these data have shown that several PDB-associated p62

mutants had tendency to increase TNF $\alpha$ -induced NF- $\kappa$ B signaling, which was not reported before. Additionally, it excluded the possibility that these p62 PDB mutants increase signaling through increasing TRAF6 polyubiquitination, suggesting the existence of other mechanisms.

Future directions include examining other possible mechanisms by which p62 PDB mutants increase TNF $\alpha$ -induced NF- $\kappa$ B signaling. Another direction is to find a better model to study the impact of PDB-associated p62 mutants on RANKL-induced NF- $\kappa$ B signaling (see Chapter 5). Additionally, previous studies have shown that p62 interacts with RIP and is involved in the TRAF2 polyubiquitination [93] in the TNF $\alpha$ -induced NF- $\kappa$ B signaling, which raises the possibility that PDB-associated p62 mutations increase TNF $\alpha$ -induced NF- $\kappa$ B signaling through increasing TRAF2 polyubiquitination. This hypothesis could be investigated in the future.

**Figure 3.1.** A schematic diagram of NF- $\kappa$ B luciferase assay.

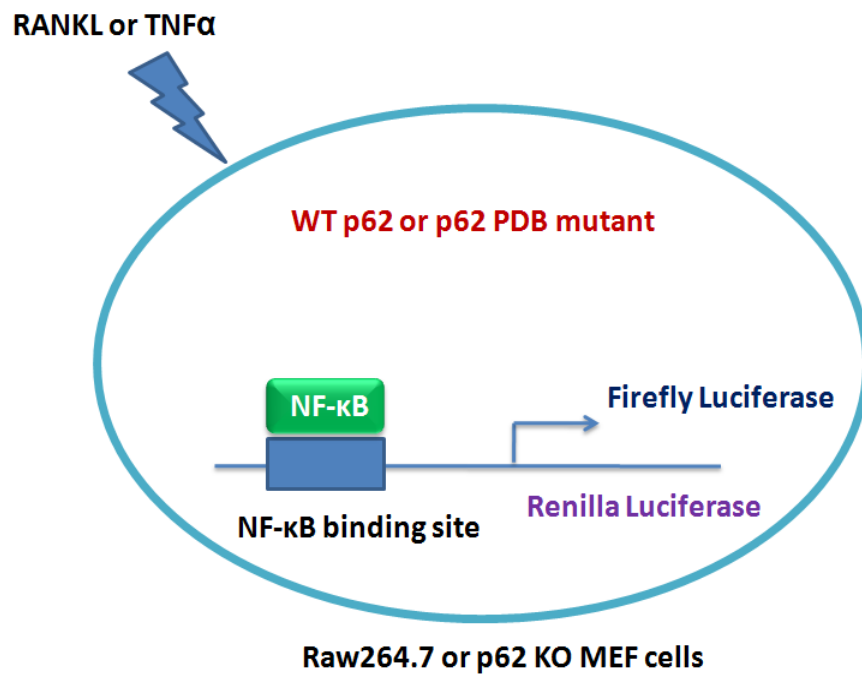
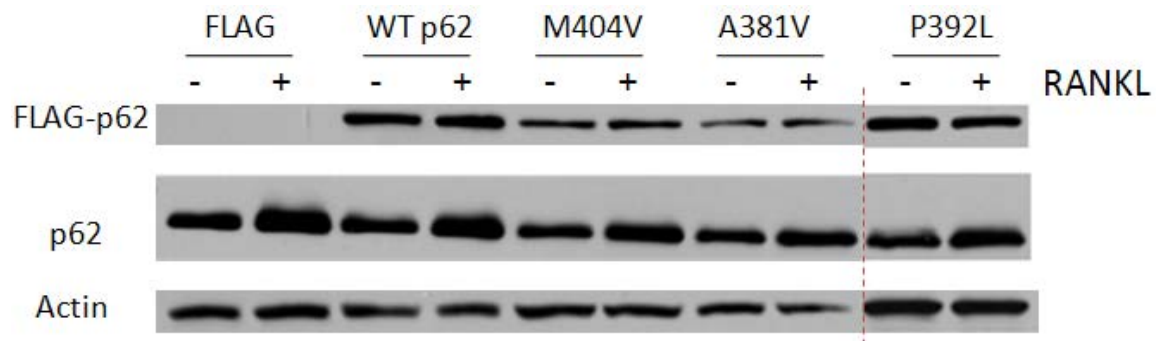
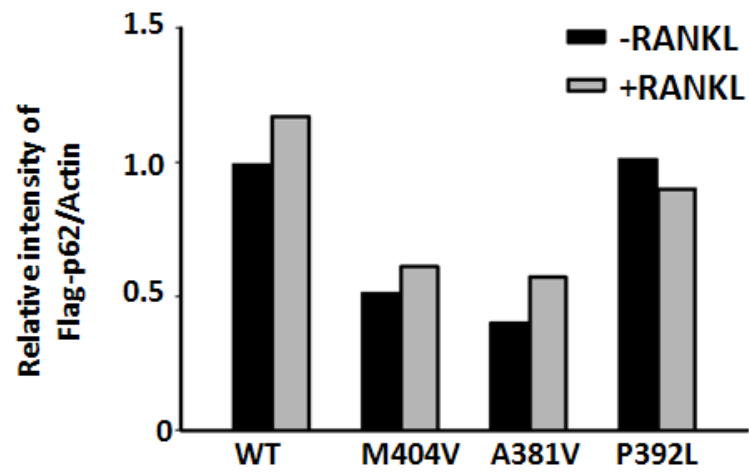


**Figure 3.2. RANKL-induced NF- $\kappa$ B luciferase assay in Raw264.7 cells expressing WT p62 and p62 PDB mutants.** Raw264.7 cells stably expressing NF- $\kappa$ B luciferase reporter were transfected with FLAG-p62 (WT, M404V, A381V and P392L) and Renilla. Forty-eight hours after transfection, cells were treated with GST-rRANKL (100ng/ml) for 7 hours. Cells were harvested with passive lysis buffer and NF- $\kappa$ B luciferase assay was performed. Cell lysates were also subjected to SDS-PAGE and Western blotting was performed using antibodies against FLAG and actin. **(A)** Western blotting of overexpressed p62 and endogenous p62. **(B)** Quantification of FLAG-p62/Actin by Image J. **(C)** Original Firefly/Renilla ratio with or without RANKL treatment. **(D)** Normalized fold increases after RANKL treatment according to the expression level of p62.

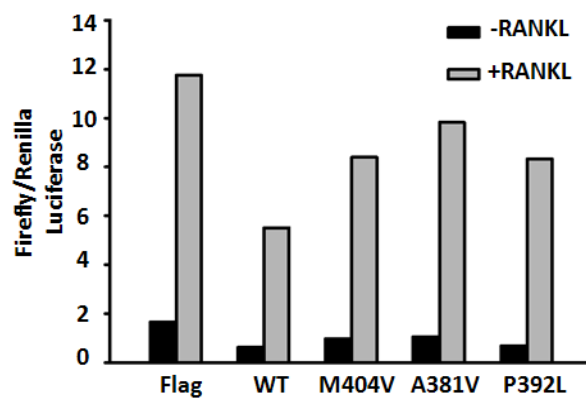
**(A)**



(B)



(C)



(D)

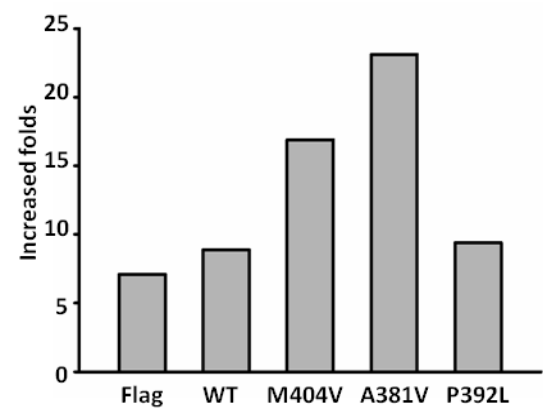
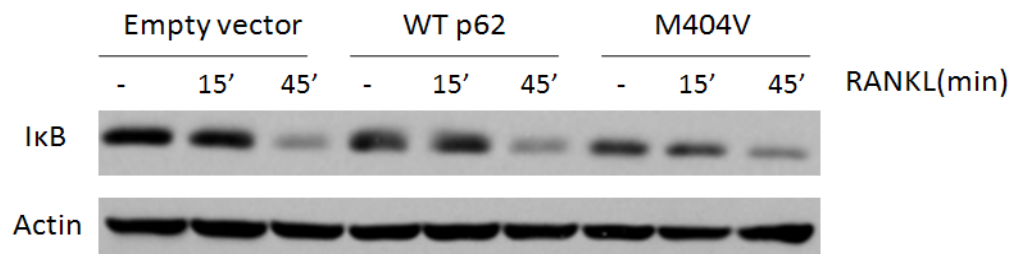


**Figure 3.3. Comparison of the rate of I $\kappa$ B degradation in Raw264.7 cells expressing WT and mutant p62 induced by GST-rRANKL. (A) I $\kappa$ B degradation in Raw264.7 cells overexpressing WT or M404V p62 induced by RANKL at 10 or 45 minutes. (B) Quantification of I $\kappa$ B/Actin by Image J software.**

**(A)**



**(B)**

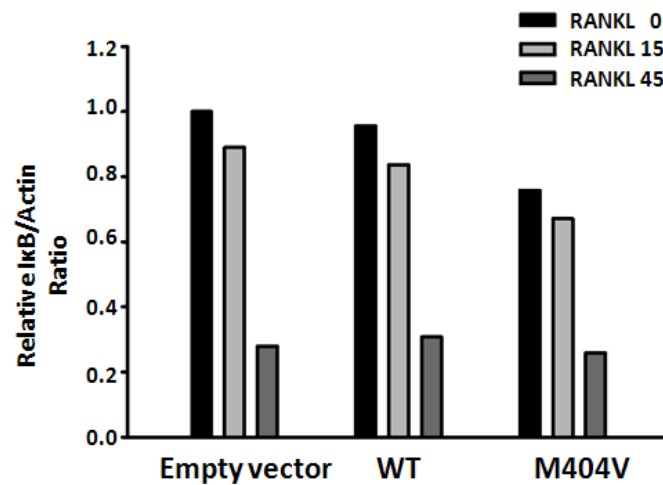


**Figure 3.4. Immunostaining of p65 in Raw264.7 cells induced by GST-rRANKL.** Raw 264.7 cells were treated with and without GST-rRANKL (100ng/ml) for 30 minutes. Cells were fixed with 4% PFA and permeabilized with 0.1% Triton. Primary antibody p65 (1:50), secondary antibody Alexa Fluoro 488 (mouse) (green, 1:300) and Hoechst (blue, 1:1000) were used. Confocal microscopy was applied for observation. Scale bars=5 $\mu$ m.

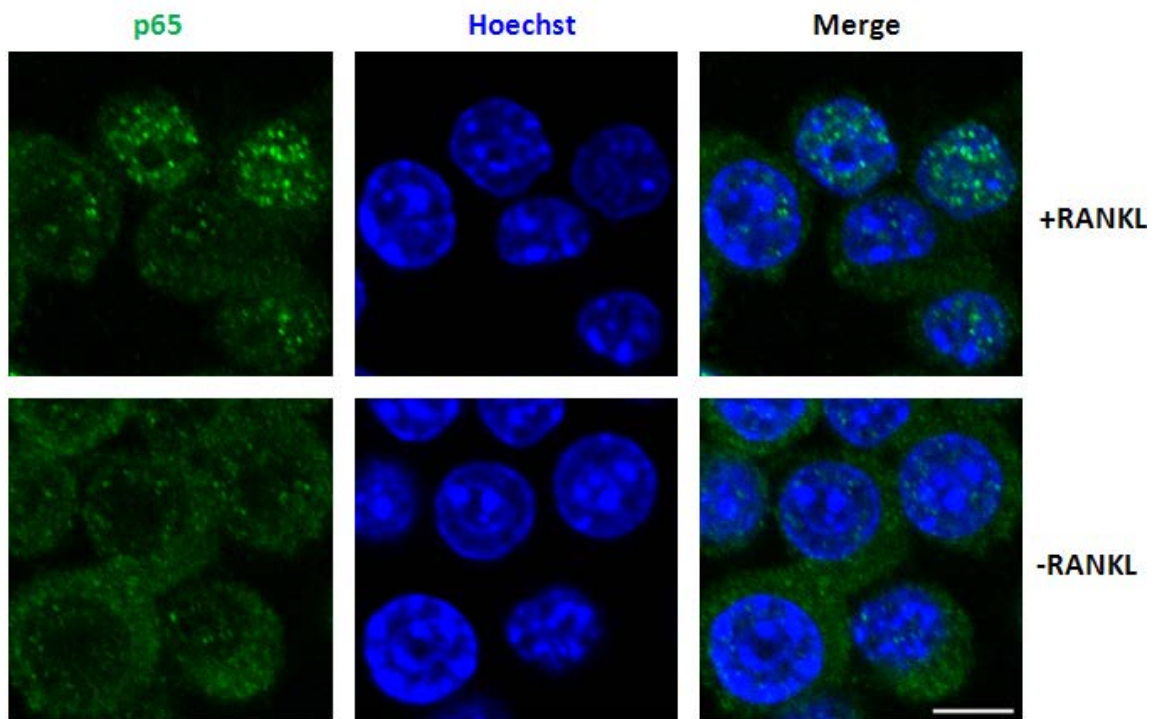




**Figure 3.5. Knockdown of the endogenous p62 in Raw264.7 cells by p62 siRNA.**

Raw264.7 cells stably expressing NF- $\kappa$ B luciferase reporter were transfected with non-targeting siRNA or p62 siRNA (40nM, 80nM) using the Lipofectamine LTX. Forty-eight hours after transfection, cells were lysed with RIPA buffer. Samples were subjected to SDS-PAGE. The knockdown efficiency was checked by Western blotting using antibodies against p62 and actin.

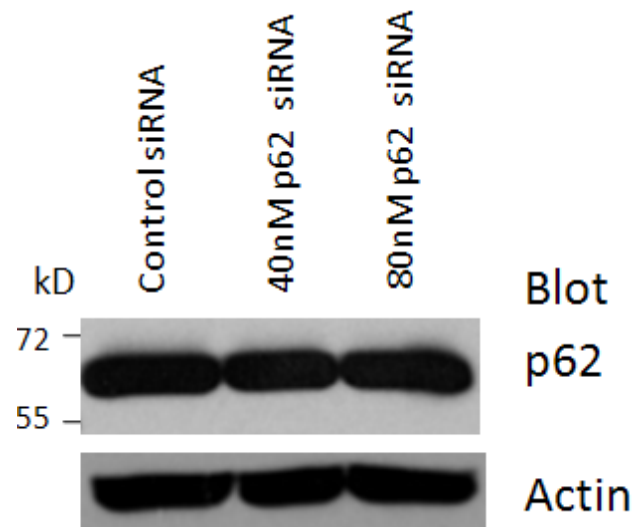
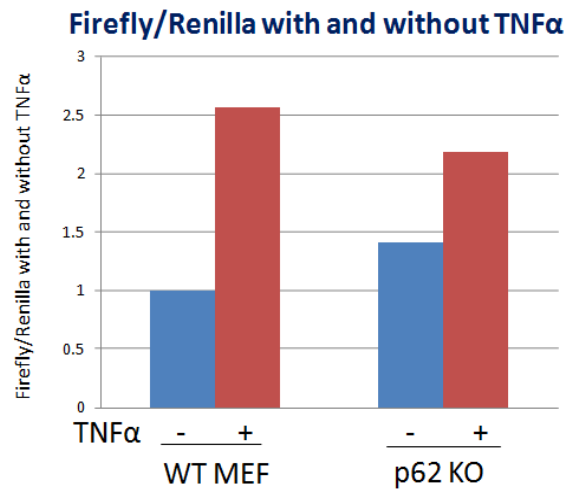
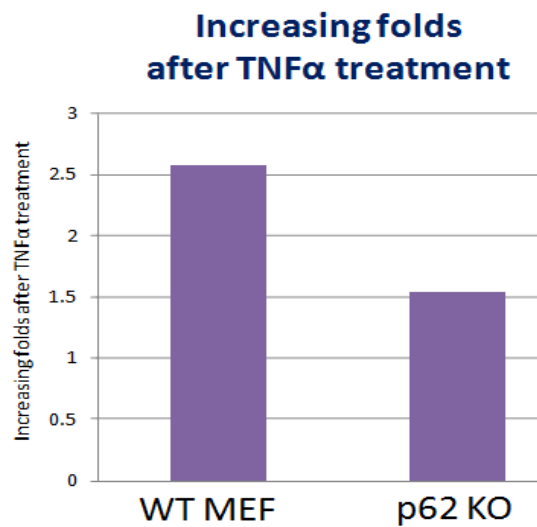


**Figure 3.6. TNF $\alpha$ -induced NF- $\kappa$ B luciferase assays in WT MEF and p62 KO MEF cells. (A) Firefly/Renilla ratio induced by TNF $\alpha$  in MEF cells. MEF cells were transfected with NF- $\kappa$ B luciferase reporter and Renilla. Cells were treated with TNF $\alpha$  (30ng/ml) for 7 hours. (B) Fold increases after TNF $\alpha$  treatment in p62 KO MEF and WT MEF cells. (C) Firefly/Renilla ratio at basal condition. MEF cells were transfected with FLAG-p62 (WT or M404V), NF- $\kappa$ B luciferase reporter and Renilla. (D) Firefly/Renilla ratio with or without TNF $\alpha$  treatment. Cells were treated with TNF $\alpha$  (30ng/ml) for 7 hours.**

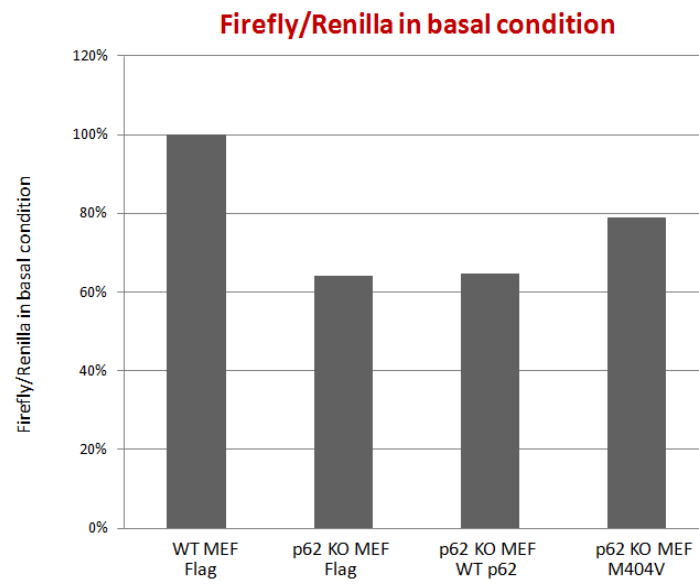
(A)



(B)



(C)



(D)

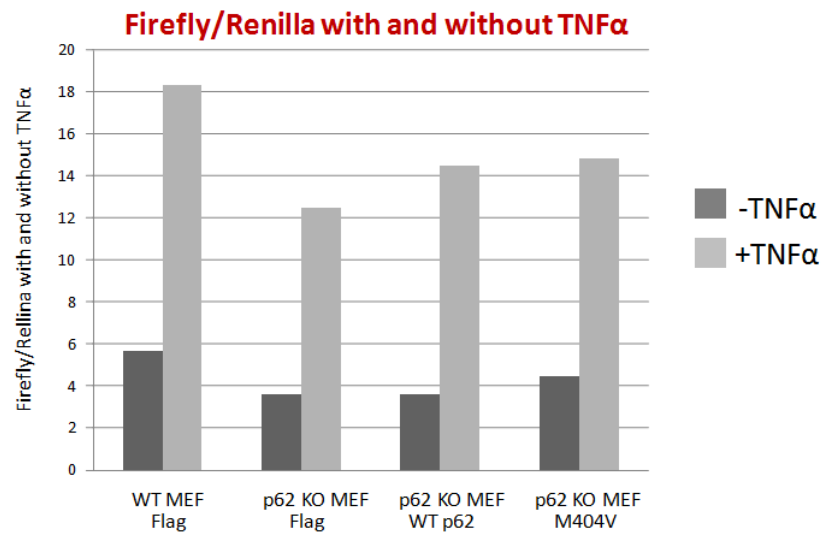
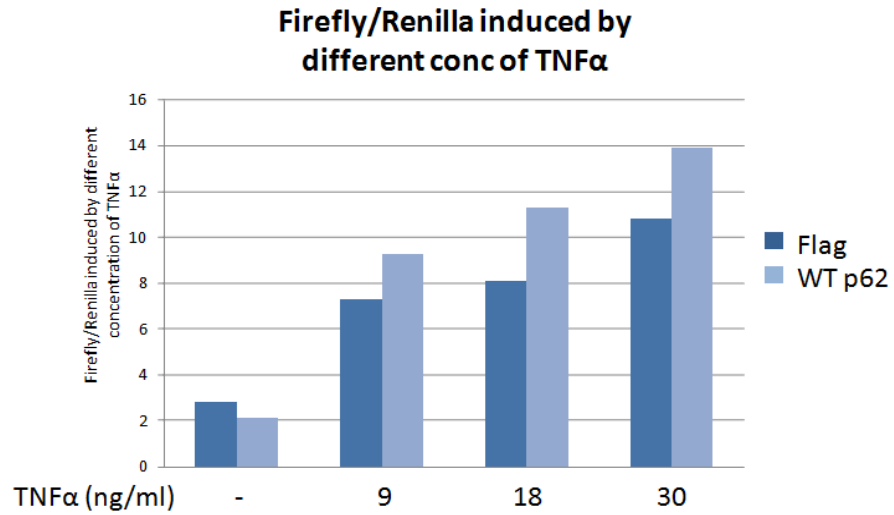


**Figure 3.7. NF- $\kappa$ B luciferase assay induced by different concentration of TNF $\alpha$  in p62 KO MEF cells. (A) The Firefly/Renilla ratio was obtained at different concentration of TNF $\alpha$  (9ng/ml, 18ng/ml and 30ng/ml). The cells were starved with DMEM (0.1% BSA) for 4 hours, and then treated with TNF $\alpha$  overnight. (B) Fold increases by different concentration of TNF $\alpha$ .**

(A)



(B)

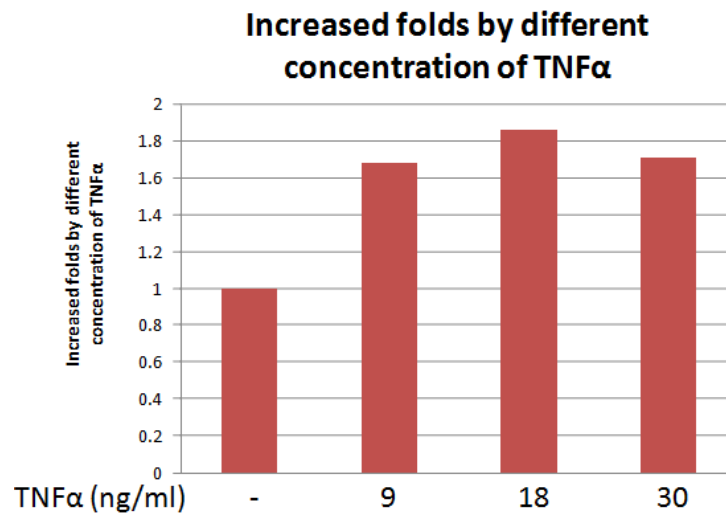
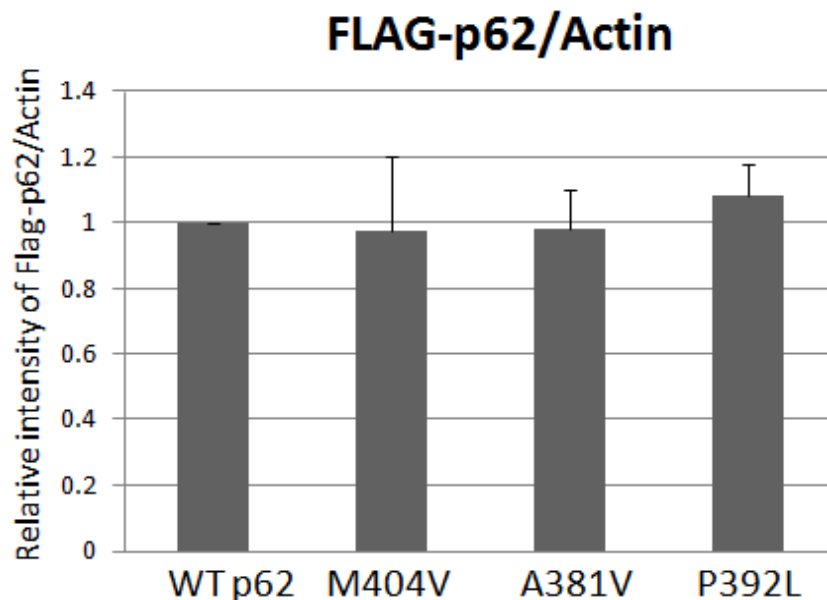
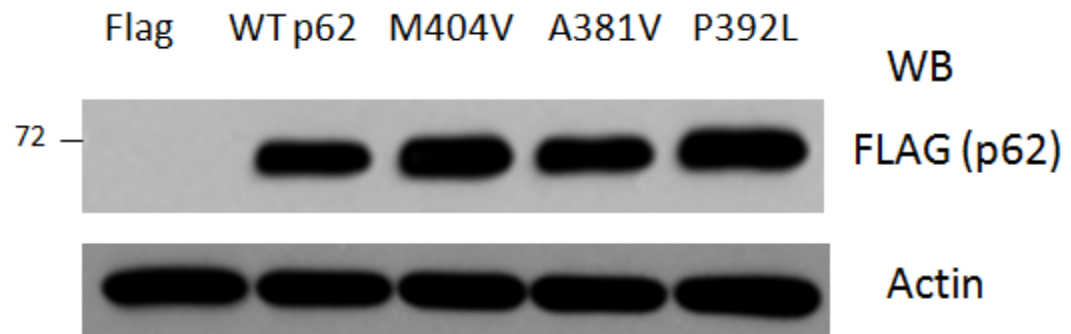


**Figure 3.8. TNF $\alpha$ -induced NF- $\kappa$ B luciferase assay in p62 KO MEF cells expressing WT p62 or p62 PDB mutants.** P62 KO MEF cells were transfected with FLAG-p62 (WT, M404V, A381V and P392L), NF- $\kappa$ B luciferase reporter and Renilla. Twenty-eight hours after transfection, cells were starved for 3.5 hours. Cells were treated with TNF $\alpha$  (20ng/ml) overnight. Cells were harvested with passive lysis buffer and NF- $\kappa$ B luciferase assay was performed. Cell lysates were also subjected to SDS-PAGE and Western blotting was performed using antibodies against FLAG and actin. Three independent experiments were performed. **(A)** Representative Western blotting of overexpressed p62 and quantification of FLAG-p62/Actin by Image J. **(B)** Representative Firefly/Renilla with and without TNF $\alpha$ .

**(A)**



(B)

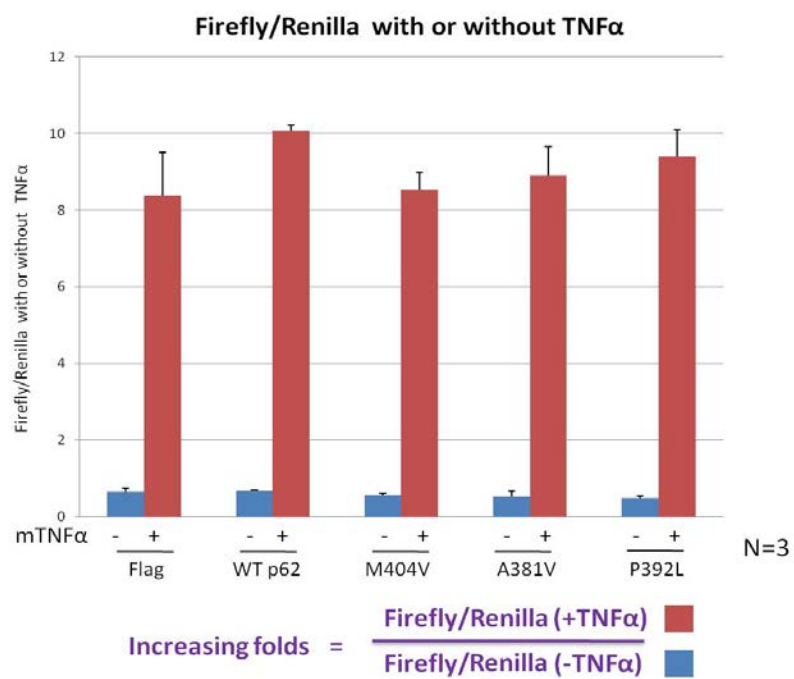
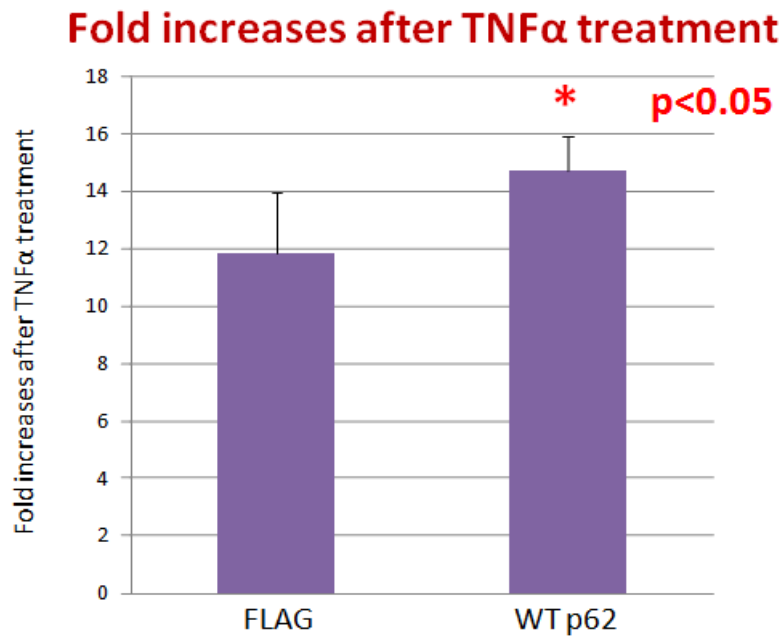
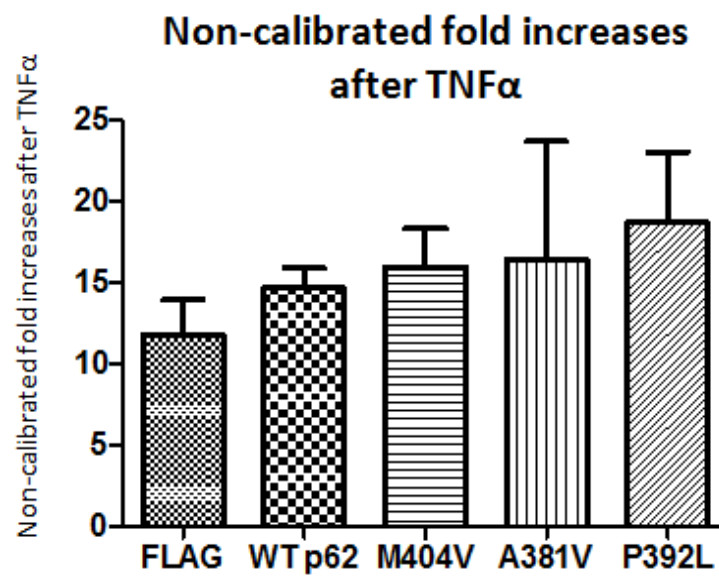


**Figure 3.9. Statistical analysis of fold increases in the TNF $\alpha$ -induced NF- $\kappa$ B luciferase assay in p62 KO MEF cells.** TNF $\alpha$ -induced NF- $\kappa$ B luciferase assay were performed three times. **(A)** Fold increases of Firefly/Renilla in control cells and cells expressing WT p62. The data were presented as mean  $\pm$  S.D., and *t*-test was used to analyze the differences between the individual experiments. \*:  $P < 0.05$ . **(B)** Fold increases of Firefly/Renilla in cells expressing WT p62 or p62 PDB mutant. The data were presented as mean  $\pm$  S.D., and one way ANOVA analysis with Tukey's test was used to analyze the differences between the individual experiments. **(C)** Fold increases of Firefly/Renilla in cells expressing WT p62 or p62 PDB mutant were calibrated according to the expression level of WT or mutant p62. The data were presented as mean  $\pm$  S.D., and one way ANOVA analysis with Tukey's test was used to analyze the differences between the individual experiments.

**(A)**



(B)



(C)

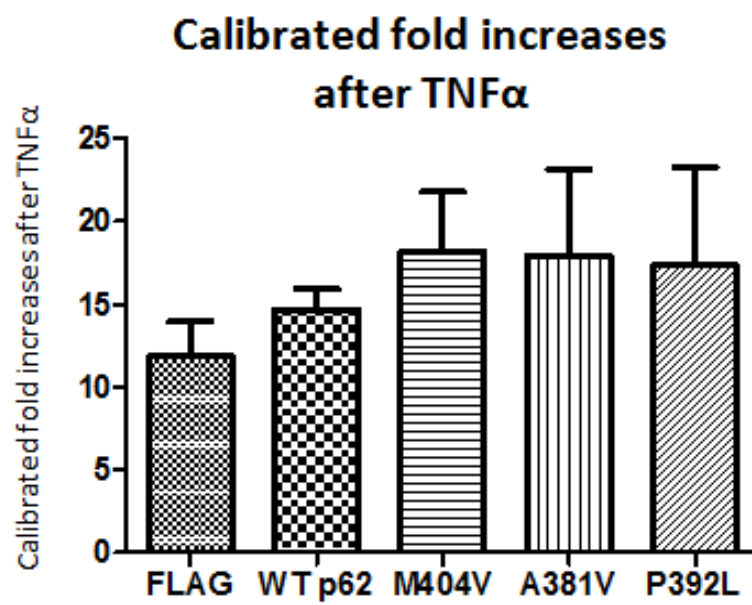
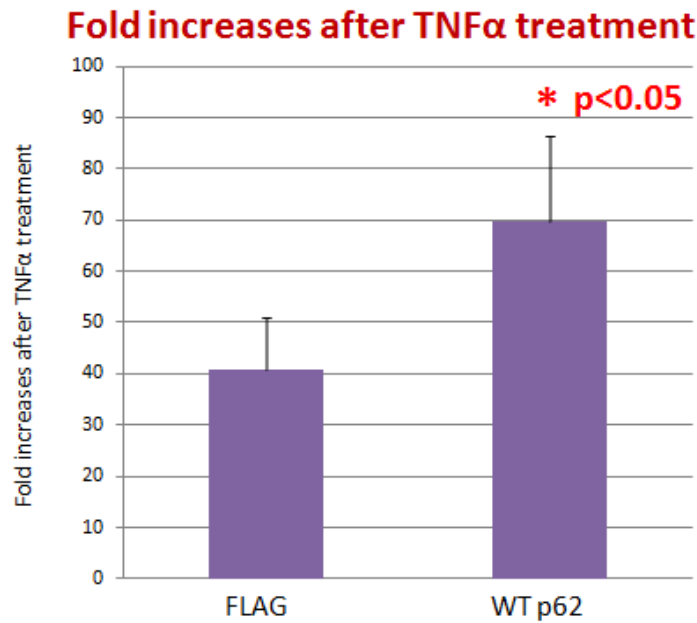




**Figure 3.10. Statistical analysis of fold increases in the TNF $\alpha$ -induced NF- $\kappa$ B luciferase assay in HEK293 cells.** TNF $\alpha$ -induced NF- $\kappa$ B luciferase assay were performed three times. HEK293 cells were transfected with FLAG-p62 (WT, M404V, A381V and P392L), NF- $\kappa$ B luciferase reporter and Renilla. Thirty hours after transfection, cells were starved overnight. Cells were treated with TNF $\alpha$  (30ng/ml) for 4 hours. **(A)** Fold increases of Firefly/Renilla in control cells and cells expressing WT p62. The data were presented as mean  $\pm$  S.D., and *t*-test was used to analyze the differences between the individual experiments. \*:  $P < 0.05$ . **(B)** Fold increases of Firefly/Renilla in cells expressing WT p62 or p62 PDB mutant. The data were presented as mean  $\pm$  S.D., and one way ANOVA analysis with Tukey's test was used to analyze the differences between the individual experiments. \*:  $P < 0.05$ .

**(A)**



(B)

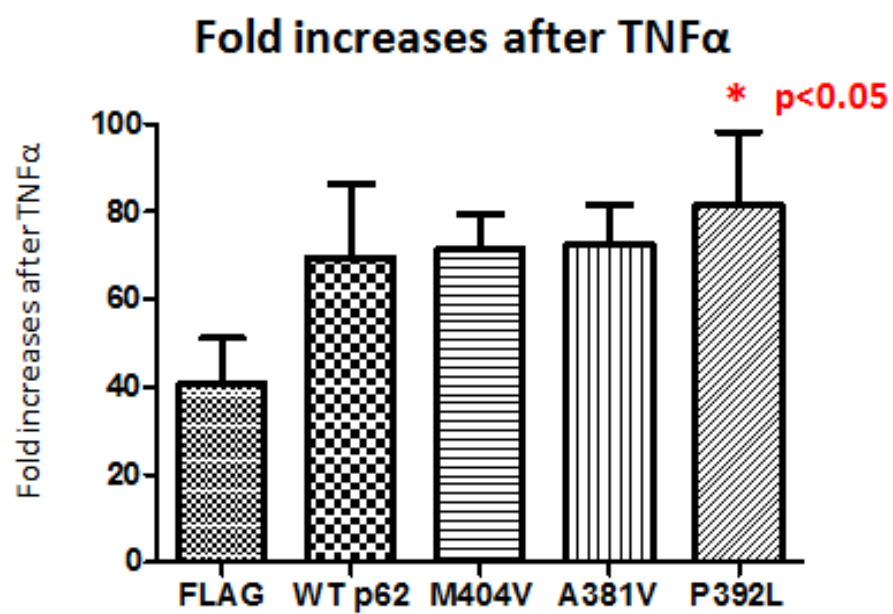


**Figure 3.11. Comparison of immunoprecipitated polyubiquitinated proteins in HEK293 cells overexpressing WT and mutant p62.** HEK293 cells were transfected with FLAG-TRAF6 (WT, A381V, P392L and M404V). Forty-eight hours after transfection, FLAG-IP was performed. Samples were subjected to 4–20% gradient gels. Western blotting was performed using antibody against Ub.

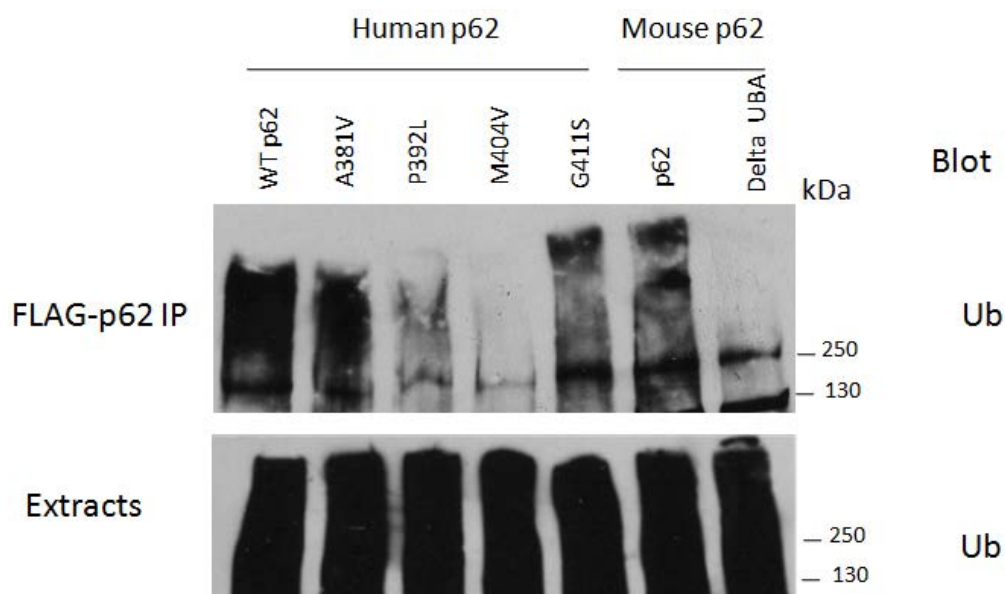


**Figure 3.12. Comparison of TRAF6 polyubiquitination in HEK293 cells overexpressing WT and mutant p62.** HEK293 cells were co-transfected with FLAG-TRAF6 and DsRed-p62 (WT, A381V, P392L or M404V). Forty-eight hours after transfection, FLAG-IP was performed. Samples were subjected to 4–20% gradient gels. Western blotting was performed using antibodies against Ub, FLAG and actin.

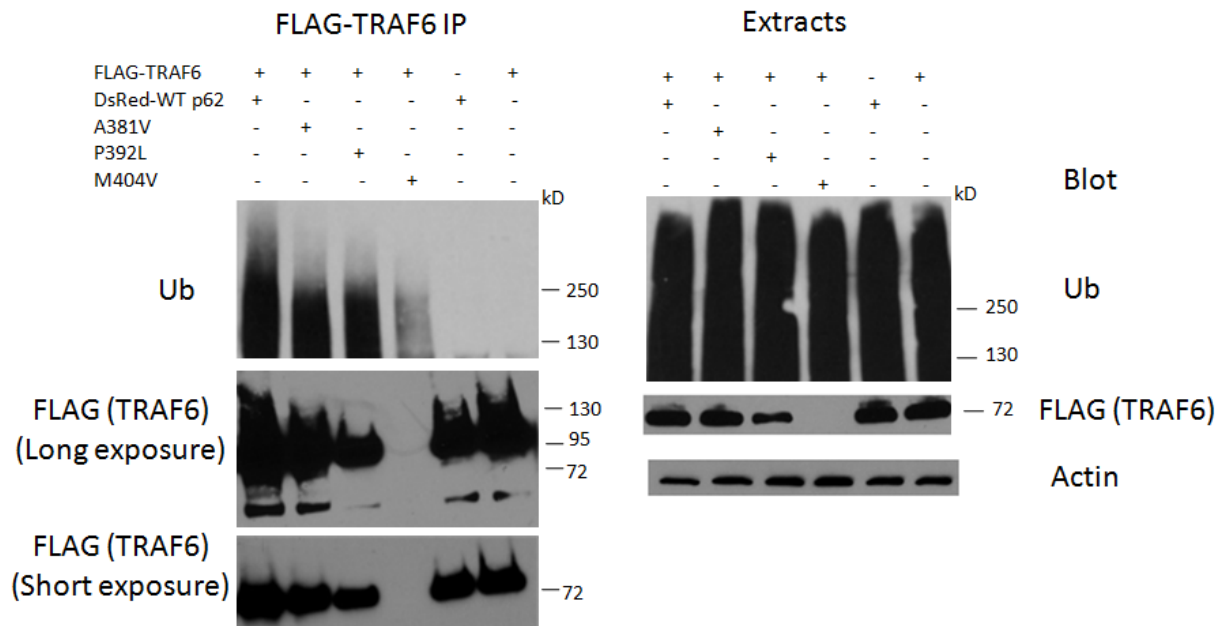


**Figure 3.13. Comparison of the level of TRAF6 polyubiquitination in HEK293 cells overexpressing different amount of p62.** HEK293 cells were co-transfected with FLAG-TRAF6 and different amounts (0.5 $\mu$ g, 0.25  $\mu$ g and 0.1  $\mu$ g) of DsRed-p62 (WT or M404V). Forty-eight hours after transfection, FLAG-IP was performed. Samples were subjected to 4–20% gradient gels. Western blotting was performed using antibodies against Ub and FLAG.

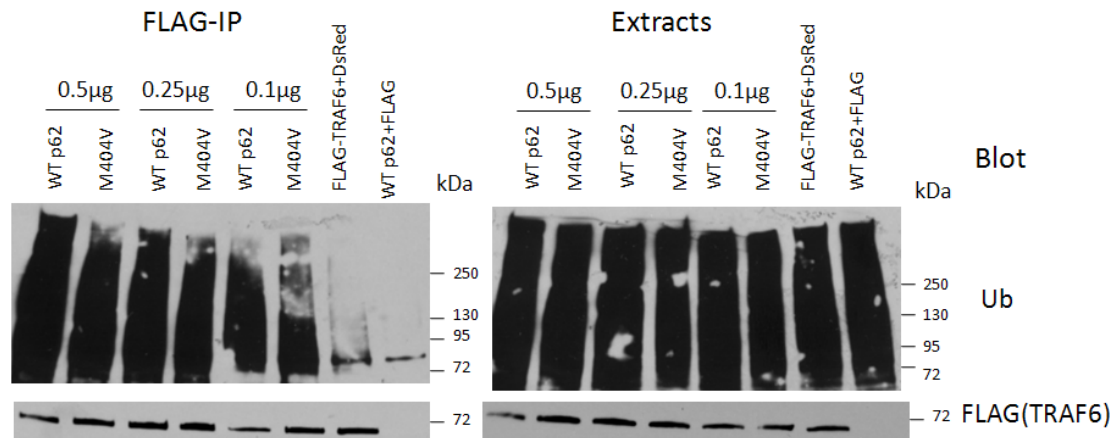


**Figure 3.14. Comparison of TRAF6 polyubiquitination in HEK293 cells overexpressing WT and mutant p62 with and without TNF $\alpha$  treatment.** HEK293 cells were co-transfected with FLAG-TRAF6 and DsRed-p62 (WT, M404V, A381V or P392L). Forty-eight hours after transfection, FLAG-IP was performed. Samples were subjected to 4–20% gradient gels. Western blotting was performed using antibodies against Ub, FLAG, I $\kappa$ B and actin.

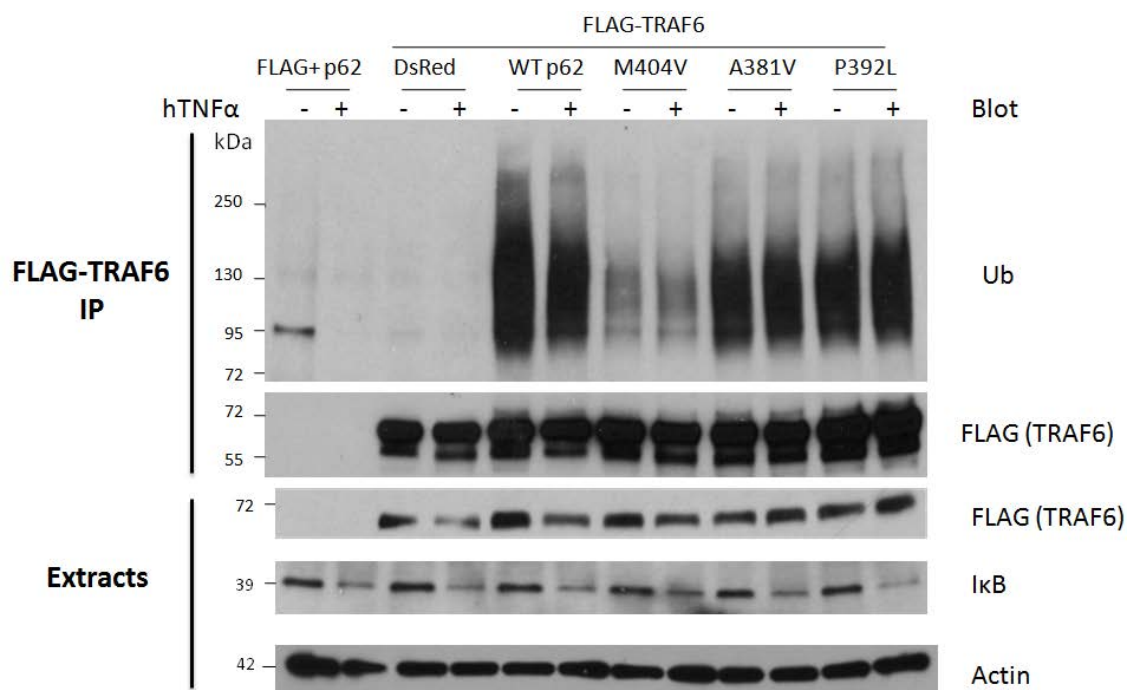


**Figure 3.15. Comparison of TRAF6 polyubiquitination in HEK293 cells overexpressing p62 and a variety of different ubiquitin constructs.** HEK293 cells were co-transfected with FLAG-TRAF6, DsRed-p62 (WT) and different HA-Ub constructs including K29R, K48R, K63R, K48 only and K63 only. Forty-eight hours after transfection, FLAG-IP was performed. Samples were subjected to 4–20% gradient gels. Western blotting was performed using antibodies against Ub, FLAG, DsRed and HA.

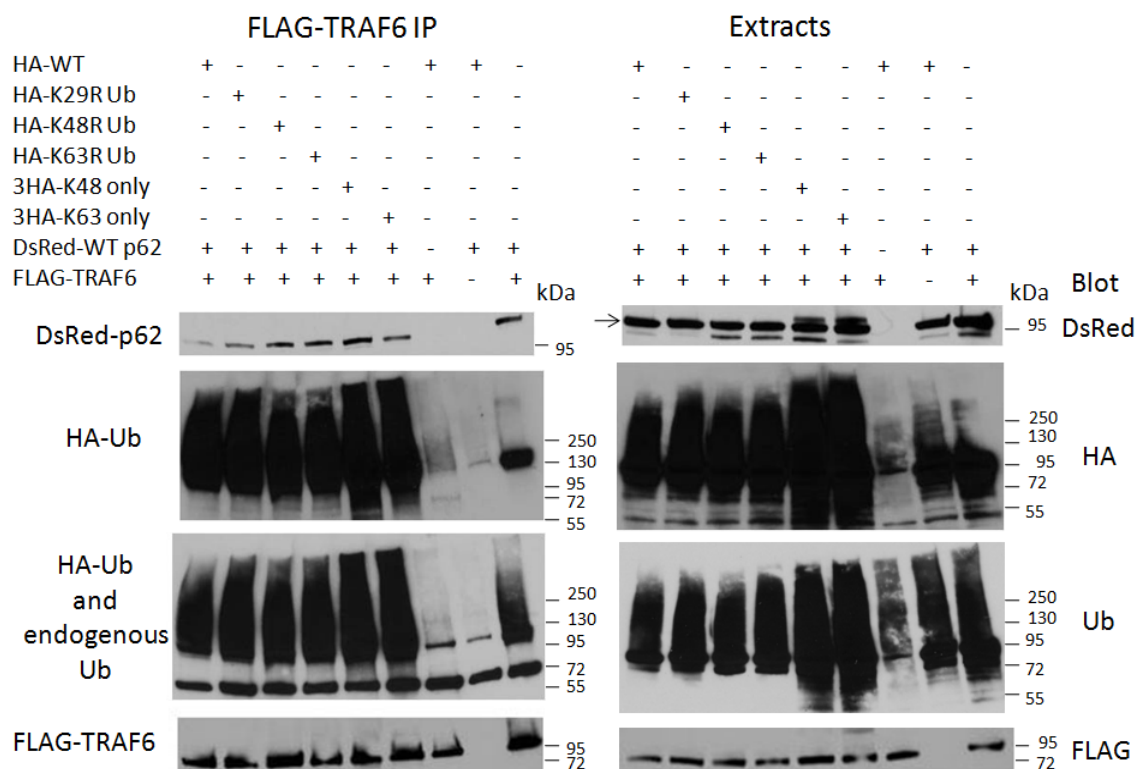


**Table 3.1. Comparison of three workable cell models for our study.**

	<b>Advantage</b>	<b>Disadvantage</b>	<b>Strategy</b>
<b>Raw cell</b>	<b>Osteoclast-like cell Have RANK receptor</b>	<b>Low transfection efficiency High background of p62</b>	<b>p62 siRNA p62 shRNA</b>
<b>p62 KO MEF</b>	<b>No p62</b>	<b>Not Osteoclast-like cell Low transfection efficiency Need to transfect RANK</b>	<b>Transfect RANK receptor</b>
<b>HEK 293</b>	<b>High transfection efficiency</b>	<b>Not Osteoclast-like cell Background of p62 Need to transfect RANK</b>	<b>p62 siRNA Transfect RANK receptor</b>



## **Chapter 4. The role of PDB-associated p62 mutants in autophagy**

### **Introduction**

It was reported that the p62 levels were elevated in PDB patients, suggesting a defect in autophagy [80, 175], which may play a role in the disease [7, 9]. Little is known, however, about the role of autophagy in PDB. As mentioned earlier, p62 mutations are linked to about 40% familial PDB cases. Therefore, the effect of PDB-associated p62 mutations in autophagy was investigated in our study.

There are two important questions regarding the role of p62 in PDB. (1) P62 is a regulator of autophagy [6, 90] , therefore do p62 PDB mutants increase or decrease autophagic activity compared with WT p62? and (2) P62 is also a substrate of autophagy [82, 150], therefore does the rate of autophagic degradation of p62 PDB mutant increase or decrease compared with WT p62?

In this Chapter, we mainly try to address the first question. We compared the effect of WT p62 and p62 PDB mutants on the interaction of LC3, a marker for autophagosome. Then, we also compared the GFP-LC3 puncta among cells overexpressing WT p62 and mutant p62. In addition, we compared the LC3-II levels after rapamycin (autophagy inducer) and/or NH<sub>4</sub>Cl (autophagy inhibitor) treatment in cells expressing WT p62 and mutant p62.

## **Methods and materials**

### **Cells and reagents**

P62 KO MEF cells were a gift from Dr. Masaaki Komatsu at Tokyo Metropolitan Institute of Medical Science [106]. Both rapamycin (autophagy inducer, R0395; Sigma) and NH<sub>4</sub>Cl (autophagy inhibitor, 254134-25G; Sigma) were used in this study.

### **Plasmids construction**

The human p62 open reading frame was amplified by PCR and was inserted among the *Eco*RI and *Kpn*I sites of the p3xFLAG-CMV10 vector (Sigma). Five PDB mutants, including D335E, A381V, P392L, M404V and G411S were generated by site-directed mutagenesis (in Chapter 3). In addition, the FLAG-p62 (WT, A381V, P392L and M404V) was inserted between the *Eco*RI and *Kpn*I sites of the pDsRed monomer C1, generating four human DsRed-p62 (WT, A381V, P392L and M404V). The mutagenic primer sequences of these DsRed-p62 constructs are listed in Appendix II.

### **Immunoprecipitation**

HEK293 cells were co-transfected with FLAG-p62 (WT, M404V, A381V and P392L) and EGFP-LC3 using the Lipofectamine reagent (Invitrogen). After 48 hours, the cells were lysed with the RIPA buffer with the PMSF (Sigma), P8340 (Sigma), Na<sub>3</sub>VO<sub>4</sub> and NEM for 30 minutes. The cell lysates were centrifuged at 1000g for 10 minutes.

Then 1000 µg cell lysates were pre-cleared with the Sepharose 4L-CB beads for 1 hour and subsequently incubated with anti-FLAG M2 affinity beads (F2426; Sigma). The beads were washed with RIPA buffer and resuspended in SDS loading buffer. The IP products and the extracts were subjected to SDS-PAGE followed by Western blotting with antibodies including anti-LC3 (PM036; MBL), anti-FLAG (A8592; Sigma) and anti-actin (sc-1616; Santa Cruz Biotechnology).

### **Immunofluorescence and confocal microscopy**

P62 KO MEF cells were transfected with FLAG-p62 (WT or M404V) and EGFP-LC3. Twenty-four hours after transfection, the cells were fixed with 4% paraformaldehyde (PFA) at 37 °C for 15 minutes, permeabilized with PBS/0.1% Triton, and blocked with 3% bovine serum albumin (BSA) in PBS for 1 hour. All the primary and secondary antibodies were diluted in 3% BSA/PBS. Cells were firstly incubated with anti-FLAG primary antibody (mouse, F3165; Sigma, 1:230) overnight. The next day, the cells on the coverslips were incubated with Hoechst (33258; Sigma, 1:1000) and Alexa Fluor 488 anti-mouse (A21202; Invitrogen, 1:300) for 2 hours. Finally, the coverslips were mounted using Vectashield mounting medium (Vector Laboratories). Confocal microscope (Olympus FluoView) was applied with a 60X objective.

### **Fractionation**

P62 KO MEF cells were transfected with FLAG-p62 (WT or M404V) using the Lipofectamine LTX (Invitrogen). The cells were treated with NH<sub>4</sub>Cl (10mM, 16 hours) or rapamycin (200nM, 16 hours). Forty-eight hours after transfection, the cells were

harvested with RIPA buffer with PMSF (Sigma), P8340 (Sigma), Na<sub>3</sub>VO<sub>4</sub> and NEM for 30 minutes. The cell lysates were centrifuged at 1000g for 10 minutes and the supernatant (S1) was collected. S1 was further centrifuged at 20,000g for 50 minutes, generating supernatant (S2) and pellet (P2). The samples were added to the 6xSDS loading buffer and subjected to the SDS-PAGE, followed by Western blotting using antibodies including anti-LC3 (PM036; MBL), anti-FLAG (A8592; Sigma) and anti-actin (sc-1616; Santa Cruz Biotechnology).

## **Results**

### **Effect of the p62 PDB mutation on interaction with LC3**

LC3-II is an active marker of the autophagosome [8], and p62 binds to LC3 through the LIR domain of p62 [83]. The effect of PDB-associated p62 mutation on this interaction was tested in this study. HEK293 cells were co-transfected with FLAG-p62 (WT, A381V, P392L and M404V) and EGFP-LC3. FLAG-IP was performed followed by SDS-PAGE and Western blotting. We used mouse LIR domain deleted p62 as a negative control, and as expected, it showed no interaction with GFP-LC3 (Fig. 4.1 A, lane 5). The p62 PDB mutation did not, however, change the interaction with LC3 (Fig. 4.1). The interaction of LC3 and p62 bearing a mutation (D335E) in LIR domain was also tested. Interestingly, this mutation also did not alter the interaction with LC3 (data not shown).

### **Effect of the p62 PDB mutation on GFP-LC3 puncta formation**

In Chapter 3, we showed that M404V p62 impaired TRAF6 polyubiquitination compared with WT p62 in HEK293 cells (Fig. 3.12 and 3.14). Therefore, we chose this mutant for the study. P62 KO MEF cells were transfected with FLAG-p62 (WT or M404V) and EGFP-LC3. After 24 hours, the cells were fixed with 4% PFA and incubated with anti-FLAG antibody (1:230) and Hoechst (1:1000). Confocal microscopy was used to observe the GFP-LC3 puncta.

It was found that WT FLAG-p62 colocalized with GFP-LC3 (Fig. 4.2), which is consistent with reports in the literature [89]. The same colocalization was found for GFP-LC3 and M404V p62 (Fig. 4.2). In addition, it was found that p62 and LC3 were exclusively located in the cytosol (Fig. 4.2). For quantification, nine Z-stack pictures for each sample were taken (data not shown). Attempts were made to count and compare the GFP-LC3 puncta in cells overexpressing WT and M404V p62 using available software. However, a larger number of cells and better software are needed for more precise quantification.

In the Fig. 4.2, it is shown that GFP-LC3 was in the nucleus. The nuclear staining of GFP-LC3 is likely due to high levels of overexpression.

#### **Effect of the p62 PDB mutant on LC3-II levels after rapamycin and NH<sub>4</sub>Cl treatment**

In Chapter 1, I introduced several available autophagy inducers and inhibitors. Here, we used rapamycin, which inhibits the mTOR pathway, and activates autophagy. Also we used NH<sub>4</sub>Cl to inhibit the fusion of lysosomes and autophagosomes, thus

inhibiting autophagy (Fig. 1.7). The level of LC3-II was monitored after treatment with these compounds.

P62 KO MEF cells were transfected with FLAG-p62 (WT or M404V). Cells were then treated with rapamycin for 16 hours. Alternatively, cells were treated with rapamycin and  $\text{NH}_4\text{Cl}$  together for 16 hours. Forty-eight hours after transfection, cells were lysed with RIPA buffer. Cell lysates were centrifuged at 1000g for 10 minutes. The supernatant (S1) was further centrifuged 20,000g for 50 minutes, generating supernatant (S2) and pellet (P2). The S1, S2 and P2 were subjected to SDS-PAGE followed by Western blotting.

Since rapamycin is an autophagy inducer, we expected to see LC3-II levels to increase after rapamycin treatment as more autophagosomes form. For cells without transfection (NT), LC3-II did increase slightly in S1 and S2, and decreased slightly in P2 after rapamycin treatment (Fig. 4.3 A, lane 1 and 5). For cells transfected with empty vector or FLAG-p62 (WT or M404V), LC3-II remained similar in S1, and slightly decreased in S2 and P2 (Fig. 4.3 A, lane 2-4 and lane 6-8). Since LC3-II decreased in P2 after rapamycin treatment in the control cells (Fig. 4.3 A, lane 2 and 6), it was indicated that rapamycin not only increased the formation of autophagosome, but also increased the enzymatic activity in the autophagolysosome, therefore more LC3-II was degraded. Based on Western blotting (Fig. 4.3 A), we quantified the LC3-II/Actin in S1 from cells overexpressing WT p62 or M404V p62 with and without rapamycin (Fig. 4.3 B). There was no significant difference between WT p62 and M404V p62 in terms of the change of LC3-II levels after rapamycin. LC3-II decreased after rapamycin in cells transfected with empty FLAG (Fig. 4.3 B), suggesting that rapamycin increased the enzymatic activity in

the autophagolysosome, thereby degrading LC3-II more rapidly. In cells overexpressing WT p62, the LC3-II levels decreased less compared with the control (7.9% vs. 23.2%) (Fig. 4.3 B), suggesting that WT p62 attenuated the autophagic activity and the rate of LC3-II degradation in the autophagolysosome. However, in cells overexpressing M404V p62, the LC3-II levels decreased more compared with cells overexpressing WT p62 (18.3% vs. 7.9%), suggesting that PDB mutant p62 (M404V p62) may increase the autophagic activity compared with WT p62 because LC3-II was degraded at a faster rate.

NH<sub>4</sub>Cl decreases autophagy by inhibiting the fusion of lysosomes and autophagosomes. We expected, therefore, to see LC3-II levels increase after NH<sub>4</sub>Cl treatment. As expected, LC3-II increased dramatically in S1, S2 and P2 after NH<sub>4</sub>Cl treatment alone (data not shown). Rapamycin was applied with NH<sub>4</sub>Cl together with the expectation that this double treatment would raise LC3-II levels even further. Treatment with both compounds (Fig. 4.3 A, lane 9-12), however, did not further increase LC3-II, suggesting LC3-II reached maximal levels after treatment with NH<sub>4</sub>Cl alone (data not shown). Based on the Western blotting (Fig. 4.3 A), we quantified the LC3-II/Actin in S1 from cells overexpressing WT p62 or M404V p62 with and without NH<sub>4</sub>Cl and rapamycin together (Fig. 4.3 C). It is shown that after double treatment, LC3-II levels in cells overexpressing WT p62 were higher than control (Fig. 4.3 C), suggesting that p62 may facilitate the autophagic activity, which appears contradictory with Fig. 4.3 B. Also, it was shown that after double treatment, LC3-II levels in cells overexpressing M404V p62 were higher than those in cells overexpressing WT p62, suggesting that M404V p62 may increase autophagic activity, which is consistent with Fig 4.3 B. However, since

LC3-II reached maximal capacity after treatment with  $\text{NH}_4\text{Cl}$ , a solid conclusion regarding the impact of p62 PDB mutant on autophagy remains unclear.

## **Discussion**

### **Challenges of current methods for studying the effect of PDB-associated p62 mutants on autophagy**

In this Chapter, we mainly used p62 KO MEF cells to study the effect of PDB-associated mutants on autophagy. We used two common methods for the study. One is comparing the GFP-LC3 puncta in cells overexpressing WT or mutant p62, the other is comparing the LC3-II levels in cells overexpressing WT or mutant p62 after treatment with an autophagy inducer and/or inhibitor.

P62 KO MEF cells have the advantage of producing no endogenous p62. However, it is not an osteoclast-like cell. For quantitative study of GFP-LC3 puncta, since there will be a large number of cells and puncta for counting, a better program or software is needed to count the puncta using the same criteria for cells over-expressing WT or mutant p62.

Another challenge is that p62 is also a substrate of autophagy. Therefore it is a little complicated to explain the regulatory role of p62. There are two possibilities. If mutant p62 increases autophagic activity, the levels of the mutant p62 will decrease with time, self limiting the stimulation of autophagy. If mutant p62 decreases autophagic activity, the levels of the mutant p62 will accumulate through the time. Thus, autophagic activity



will continue to decrease with time. The second scenario might be the case, so the central hypothesis of our study would be: PDB-associated p62 mutants impair the autophagic activity, leading to accumulation of p62, which then further impairs the autophagic activity. Meanwhile, accumulated p62 mutants further increase the NF- $\kappa$ B signaling and the formation of osteoclasts, which leads to PDB (Fig. 5.1).

### **Caution should be exercised when explaining LC3-II data**

LC3-II is widely used to estimate autophagy activity [152]. However, we need to very carefully explain LC3-II data. When autophagic activities increase, LC3-II levels increase because more autophagosomes form. However, LC3-II itself is degraded by autophagy, the increased autophagic activity also lead to more degradation of LC3-II, therefore decreasing the LC3-II levels. Therefore, it is important to measure LC3-II in the presence and absence of lysosomal protease inhibitors (e.g. E64d and pepstatin A) or inhibitors which block the fusion of lysosomes and autophagosomes (e.g. NH<sub>4</sub>Cl and Bafilomycin A1). If mutant p62 really increases the autophagic activity, we will see LC3-II levels increases after treatment of either lysosomal protease inhibitors or inhibitors blocking the formation of autophagolysosome in cells overexpressing mutant p62 compared with cells overexpressing WT p62.

In our study, we used rapamycin as an inducer of autophagy and NH<sub>4</sub>Cl as an inhibitor. We expected to see LC3-II levels increase upon rapamycin treatment because more autophagosomes form. However, LC3-II decreased in P2 in the control cells after rapamycin treatment (Fig. 4.3 A, lane 2 and 6), suggesting that while rapamycin may

increase the formation of autophagosome, this may ultimately decrease LC3-II levels through increased degradation. In addition, cells treated with  $\text{NH}_4\text{Cl}$  generated more LC3-II (Fig. 4.3 A, lane 9-12), suggesting that  $\text{NH}_4\text{Cl}$  is a good inhibitor for blocking the fusion of lysosome and autophagosome. Also, it seems that LC3-II reached maximal capacity after treatment with  $\text{NH}_4\text{Cl}$  (Fig. 4.3 A, lane 9-12). In future, it is possible that using lower  $\text{NH}_4\text{Cl}$  levels may allow useful measurements of changes in LC3-II levels.

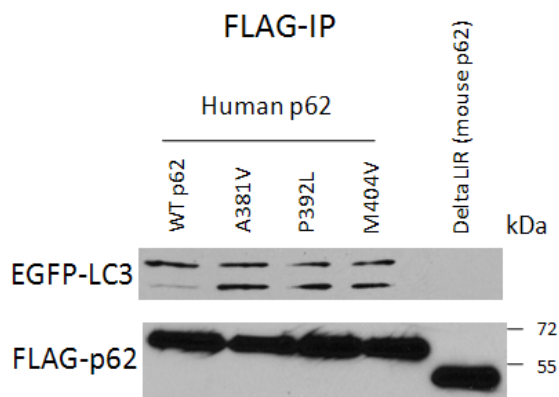
### **Significance of this study and future directions**

In this Chapter, we examined the effect of PDB-associated p62 mutants on interaction with LC3, GFP-LC3 puncta formation and LC3-II levels upon autophagy inducer and/or inhibitor treatment. Our data have shown that p62 PDB mutants did not change interaction with LC3 compared with WT p62. In addition, we speculate that mutant p62 might impair autophagic activity, leading to the accumulation of p62.

For future studies, in order to better answer whether p62 PDB mutants change autophagic activity compared with WT p62, methods must be developed to quantify GFP-LC3 puncta. Also, for the LC3-II study, other autophagy inducers (Beclin-1, starvation) and autophagy inhibitors (protease inhibitors E64d and pepstatin A) could be used. In addition, the question of whether autophagy change the rate of degradation of p62 PDB mutant compared with WT p62 has not been addressed. In order to address this question, the half life of p62 could be monitored.

**Figure 4.1. Comparison of the effect of WT p62 or PDB mutant p62 on the interaction of LC3.** (A) HEK293 cells were transfected with FLAG-p62 (WT, A381V, P392L and M404V) and EGFP-LC3. FLAG-IP was performed, followed by the SDS-PAGE. Western blotting was performed using the antibodies against the EGFP and FLAG. (B) Cell extracts of different samples.

(A)



(B)

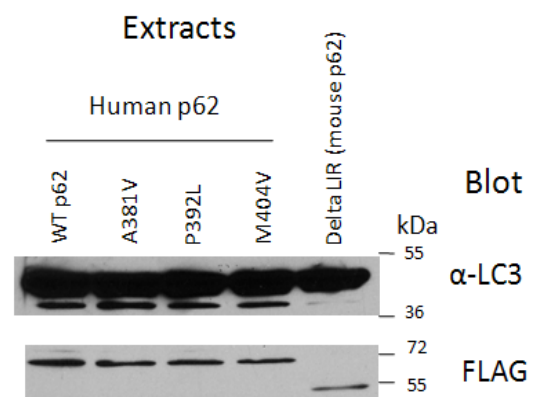


**Figure 4.2. Immunostaining of p62 and LC3 in p62 KO MEF cells overexpressing p62 and GFP-LC3.** P62 KO MEF cells were transfected with FLAG-p62 (WT or M404V) and EGFP-LC3. Twenty-four hours after transfection, cells were fixed with 4% PFA and permeabilized with 0.1% Triton. Primary antibody FLAG (1:230) and secondary antibody Hoechst (blue, 1:1000), Alexa Fluor 594 (mouse) (red, 1:300) were used. Confocal microscopy was applied for observation. Scale bars=20 $\mu$ m. The nuclear staining of GFP-LC3 is likely due to high levels of overexpression.

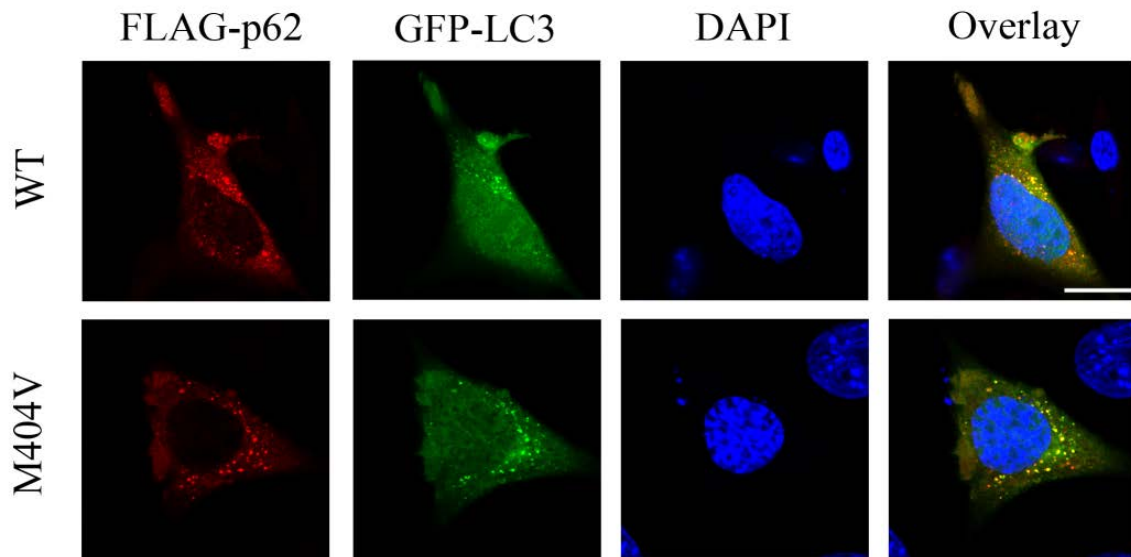
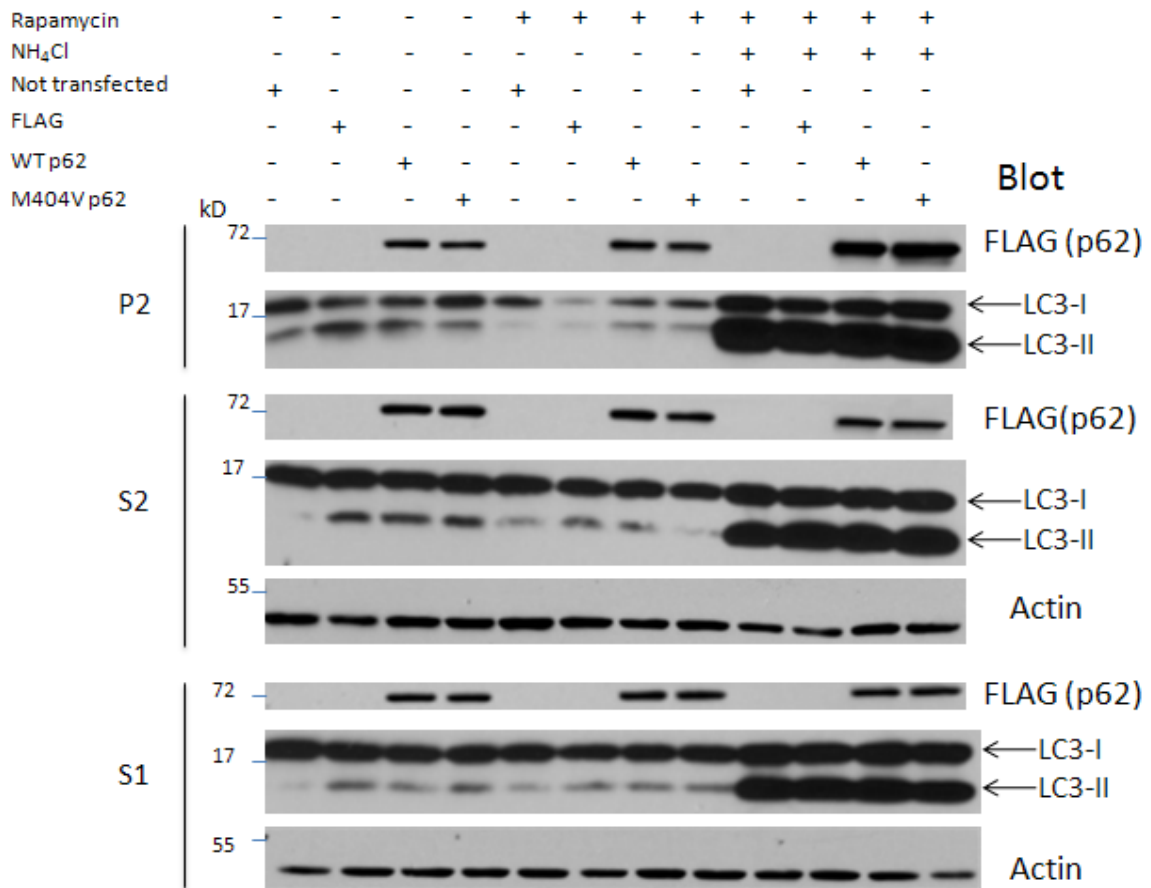
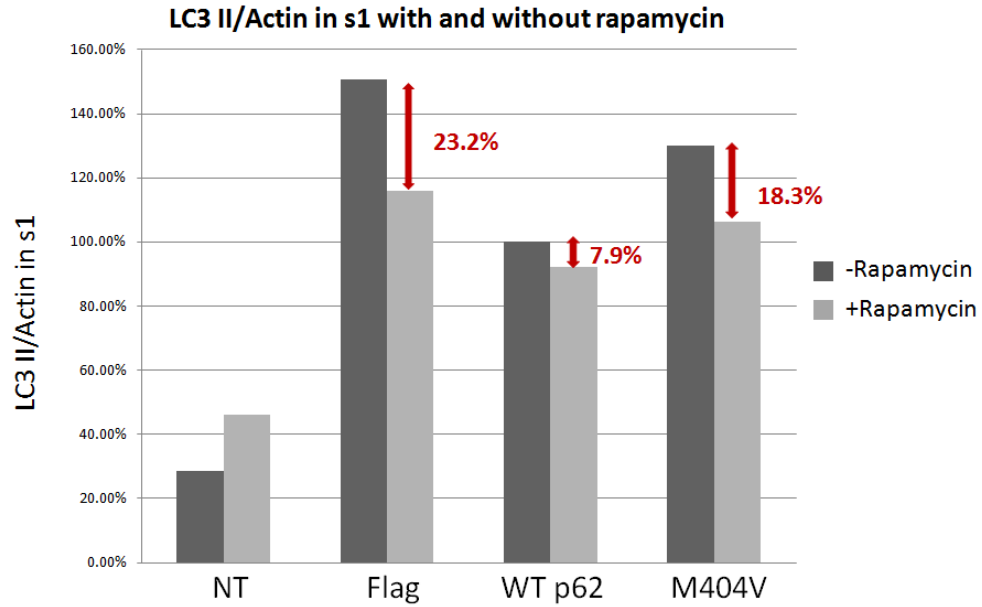


**Figure 4.3. Comparison of the effect of WT p62 and p62 PDB mutant on LC3-II level after rapamycin or rapamycin/NH<sub>4</sub>Cl treatment. (A)** Western blotting of LC3-II in S1, S2 and P2 after fractionation in p62 KO MEF cells overexpressing WT or M404V p62. P62 KO MEF cells were transfected with FLAG-p62 (WT or M404V). The cells were treated with rapamycin (200nM) alone for 16 hours or NH<sub>4</sub>Cl (10mM) and rapamycin (200nM) together for 16 hours. Forty-eight hours post transfection, the cells were harvested with RIPA buffer. The cell lysates were fractionated into S1, S2 and P2. The samples were subjected to the SDS-PAGE, followed by Western blotting using the antibodies against the LC3, FLAG and actin. NT: non-transfection. **(B)** Quantification of LC3-II/Actin in S1 treated with rapamycin alone by Image J. The value of WT p62 is normalized to 100%. Percentage of decrease after rapamycin is shown in red. **(C)** Quantification of LC3-II/Actin in S1 treated with rapamycin/NH<sub>4</sub>Cl by Image J. The value of WT p62 is normalized to 100%. Percentage of increase after rapamycin/NH<sub>4</sub>Cl is shown in red.

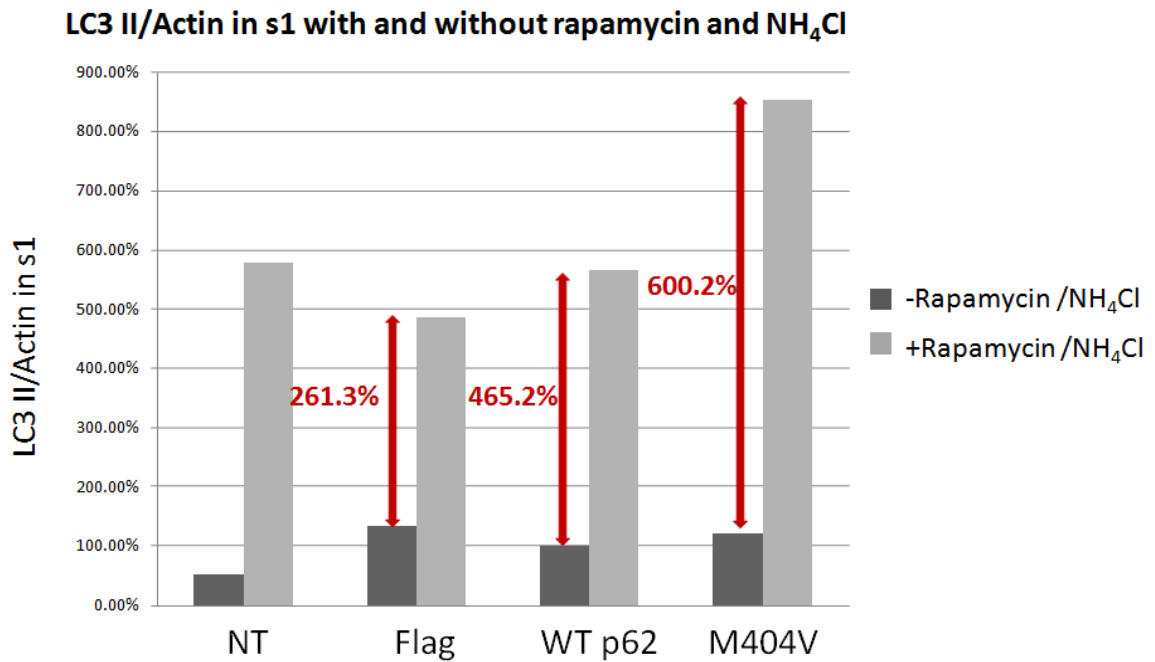
**(A)**



(B)



(C)



Copyright © Xiaoyan Liu 2012

## Chapter 5. Discussion and future perspective

### Significance of this research

In Chapter 2, we introduced a relatively simple proteomic method to identify novel SUMOylation substrates. Seventy-four SUMOylated proteins were identified by our proteomic analysis (Table 2.1). Among these proteins, Ran GTPase-activating protein 1 (RanGAP1) [12], proliferating cell nuclear antigen (PCNA) [169] and nucleophosmin (NPM) [168] have been reported to be SUMOylation substrates. In addition, 61 proteins have predicted SUMOylation sites and 40 proteins have SUMOylation consensus sequences ( $\Psi$ KXE/D) (Table 2.1). Over 50% of these proteins are nuclear proteins (Fig. 2.4), which is consistent with literature that most SUMOylation substrates are in the nucleus [2]. Altogether, this suggests that our proteomic method is applicable for identification of SUMOylated substrates.

Moreover, we are the first group to identify a novel SUMOylation substrate called Drebrin, an actin-binding protein located in the cytosol [3, 45]. We verified Drebrin SUMOylation by both FLAG and HA immunoprecipitation (Fig. 2.8 A and B). Furthermore, by using site-directed mutagenesis, we found K185, K186, K270 and K271 might be SUMOylation sites for Drebrin (Fig. 2.9 B). These lysines are conserved among vertebrate Drebrins by alignment of this region among different species (Fig. 2.7 C), suggesting that they are functionally important. At last, we observed the protrusion formation in CHO cells overexpressing Drebrin (WT and mutants) (Fig. 2.10 A), which is consistent with the literature [53, 54, 57]. However, mutation of these two sites

(K185R/K186R and K270R/K271R) in Drebrin separately did not appear to change protrusion formation (Fig. 2.10 B).

Additionally, we also identified several nuclear proteins with multiple predicted SUMOylation sites (highlighted in Table 2.1), such as general transcription factor II-I, heterogeneous nuclear ribonucleoproteins C1/C2, nucleolin and 60S ribosomal protein L24. We could further validate SUMOylation of these proteins by IP and other methods in the future.

In Chapters 3 and 4, our studies were related to “ubiquitination”, a similar modification of “SUMOylation”. We focused on an ubiquitin-binding protein, p62. We studied the effect of PDB-associated p62 mutants on NF- $\kappa$ B signaling and autophagy. In Chapter 3, we are the first group to use p62 KO MEF cells as a model for studying the effect of p62 PDB mutant on TNF $\alpha$ -induced NF- $\kappa$ B signaling. Wooten *et al.* [95] and Moscat *et al.* [93] have shown that p62 activated the NF- $\kappa$ B signaling in HEK293 cells basally. Our study not only showed that p62 activated NF- $\kappa$ B signaling basally (Fig. 3.6 C), but also upon TNF $\alpha$  treatment in p62 KO MEF cells (Fig. 3.9 A) and HEK293 cells (Fig. 3.10 A). In addition, we also have shown that p62 PDB mutants have a tendency to increase TNF $\alpha$ -induced NF- $\kappa$ B signaling compared with WT p62 in p62 KO MEF cells (Fig. 3.9 B and C) and HEK293 cells (Fig. 3.10 B). In addition, our data indicated that p62 did not increase TNF $\alpha$ -induced NF- $\kappa$ B signaling through increasing TRAF6 polyubiquitination (Fig. 3.14), suggesting other mechanisms may exist (see below).

In Chapter 4, we studied the impact of PDB-associated p62 mutants on autophagy. We found that PDB mutations did not change the interaction between p62 and the



autophagy marker protein LC3 (Fig. 4.1 A). Whether p62 PDB mutants change the autophagic activity is not certain until we optimize our experiments by using autophagy inducer/inhibitor appropriately.

In summary, my work has expanded our knowledge of the role of PDB-associated p62 mutants on NF- $\kappa$ B signaling and autophagy, as well as provided insights into several possible mechanisms, which are shown in an integrated model in Fig. 5.1.

### **Functional consequences of SUMOylation of Drebrin and other proteins**

Although we detected SUMOylation of Drebrin, the modification does not appear to be involved in protrusion formation in CHO cells (Fig. 2.10 B). So what are the functional consequences of Drebrin SUMOylation? In Chapter 1, we introduced that SUMOylation modification of certain protein could bind other proteins only when SUMOylation is present. For example, only SUMOylated Ran-GAP1 binds RanBP2 [12]. Therefore, we hypothesized that Drebrin SUMOylation might also bind some proteins only when SUMOylation is present. So how to identify these target proteins which bind SUMOylated Drebrin, not non-SUMOylated Drebrin? We could take advantage of mass spectrometry to do the quantification for Drebrin interacting proteins from cells overexpressing WT Drebrin and mutant Drebrin. We will expect to see the amounts of some Drebrin interacting proteins are significantly higher in cells overexpressing WT Drebrin than Drebrin mutants, which impair Drebrin SUMOylation. These proteins are potential Drebrin interacting proteins only when Drebrin is SUMOylated. We will further verify their interaction by immunoprecipitation and Western blotting.

In addition, we could further validate the SUMOylation of proteins with higher predicted SUMOylation sites, which are highlighted in Table 2.1 by IP and other methods. We could also study the functional consequences of these proteins in the future.

### **Mechanisms that PDB-associated p62 mutations increase NF- $\kappa$ B signaling**

In Chapter 3, we have shown that PDB-associated p62 mutations (M404V, A381V and P392L) had a tendency to increase TNF $\alpha$ -induced NF- $\kappa$ B signaling in p62 KO MEF cells (Fig. 3.9) and HEK293 cells (Fig. 3.10). Previously, we hypothesized that p62 PDB mutant increased TNF $\alpha$ -induced NF- $\kappa$ B signaling through increasing TRAF6 polyubiquitination. However, we showed that TNF $\alpha$  did not increase TRAF6 polyubiquitination in HEK293 cells overexpressing WT and mutant p62 (Fig. 3.14), which did not support our hypothesis. Therefore, by what other mechanisms do p62 PDB mutants increase NF- $\kappa$ B signaling? Several possibilities are described below and summarized in Fig. 5.1.

#### ***(1) TRAFs or RIP polyubiquitination***

Moscat *et al.* [93] showed that p62 could interact with RIP. They also showed that p62 interacted with TRAF2 in the presence of RIP by immunoprecipitation experiment in HEK293 cells transfected with p62, RIP and TRAF2 constructs. In their study, they also showed that upon TNF $\alpha$  treatment, p62 and RIP could be co-immunoprecipitated with TNF-R1. This suggested that the interaction of p62 and RIP plays a role in the TNF $\alpha$ -induced NF- $\kappa$ B signaling. In Chapter 1, we also introduced that upon TNF $\alpha$  treatment,

TRAF2 undergoes auto-polyubiquitination (K63-linked), which catalyzes RIP K63-linked polyubiquitination and activates the TNF $\alpha$  signaling [93] (Fig. 1.5). Our data showed that p62 contributed to TNF $\alpha$ -induced NF- $\kappa$ B signaling in p62 KO MEF cells (Fig. 3.9 A) and HEK293 cells (Fig. 3.10 A) by luciferase assay. Therefore, we hypothesize that WT p62 increases TNF $\alpha$ -induced NF- $\kappa$ B signaling by increasing TRAF2 or RIP polyubiquitination. Based on our data that p62 PDB mutants had a tendency to increase TNF $\alpha$ -induced NF- $\kappa$ B signaling (Fig. 3.9 and 3.10), we also hypothesize that p62 PDB mutant increases TNF $\alpha$ -induced NF- $\kappa$ B signaling by increasing TRAF2 or RIP polyubiquitination compared with WT p62.

In order to test our hypothesis, we should first set up a model system in which TRAF2 or RIP polyubiquitination increases upon TNF $\alpha$ , and the signaling proteins IKK increase, I $\kappa$ B decreases, phospho-I $\kappa$ B increases after TNF $\alpha$  treatment. Then, we will test whether TRAF2 or RIP polyubiquitination increases in the presence of p62. If so, we will have demonstrated that p62 involves in TRAF2 and RIP polyubiquitination. Next, we will compare the effect of WT p62 and p62 PDB mutant on TRAF2 and RIP polyubiquitination, see if mutant p62 could further increase polyubiquitination. If these experiments have results as expected, we could further examine TRAF2 or RIP polyubiquitination using a variety of different Ub constructs. If we find that TRAF2 or RIP polyubiquitination is a mixed linkage polyubiquitin chain, not a K63-linked polyubiquitin chain as we found for TRAF6 (Fig. 3.15), it will be a new finding to the field, that the mixed linkage polyubiquitin chain could also successfully activate the signaling.

In addition, when the model for studying RANKL-induced NF- $\kappa$ B signaling is available in the future, we could test whether PDB-associated p62 mutations increase RANKL-induced NF- $\kappa$ B signaling through increasing TRAF6 polyubiquitination.

## (2) *aPKC*

In the NF- $\kappa$ B signaling pathway (Fig. 1.5), it is shown that p62 directly interacts with aPKC through its PB1 domain, and further activates IKK, leading to NF- $\kappa$ B activation. Therefore, we propose that PDB-associated p62 mutants increase the interaction with aPKC or increase the activity of aPKC compared with WT p62, and activate the signaling.

Duran *et al.* [77] demonstrated RANKL ligand-dependent interactions between p62 and aPKC by immunoprecipitating endogenous p62 in Raw264.7 cells. However, they did not show negative controls in their IP. In our study, we performed the same experiment as they did, however our negative control was not working, since HA antibody could also pull down the endogenous aPKC in the absence and presence of RANKL (data not shown). Also, the IP efficiency is only about 13%. In the long run, we could use better IP buffer or better HA antibody to improve the IP efficiency and diminish the effect of non-specific interaction. We could also use fusion protein p62 or aPKC (GST, GFP, Myc, FLAG, or DsRed tagged protein) to study the interaction. Once the experiment is set up, we could introduce WT p62 and p62 PDB mutants, and test if interactions with aPKC are changed. We could also monitor signaling proteins, such as IKK, I $\kappa$ B and phospho-I $\kappa$ B, and see if the activity of aPKC increases in the presence of mutant p62.

### (3) *CYLD*

Jin *et al.* [176] reported that a deubiquitinating enzyme, *CYLD*, negatively regulates osteoclastogenesis and RANK signaling. They have shown that RANKL induced a much higher number of osteoclasts from the bone marrow-derived macrophages (BMDMs) in *CYLD* knockout mice than control mice. They also showed that ubiquitinated TRAF6 was accumulated in BMDMs from *CYLD* knockout mice. In addition, they showed that *CYLD* could interact with WT p62, but not UBA-deleted p62 by IP, indicating that the interaction requires the UBA domain. Also, they showed that the interaction of *CYLD* and TRAF6 is dependent on p62 and its UBA domain by IP.

In light of their work, we hypothesized that p62 PDB UBA mutant decreases interaction with *CYLD*, leading to decreased deubiquitination of polyubiquitinated TRAF6, further increasing NF- $\kappa$ B signaling. To test this hypothesis, HEK293 cells were transfected with human HA-*CYLD* [177] and human FLAG-p62 (WT and mutants) or mouse p62 (WT and UBA domain deleted). Forty-eight hours after transfection, FLAG-p62 IP was performed. In contrast to Jin *et al.* [176], we found that *CYLD* co-immunoprecipitated with mouse UBA-deleted p62 (data not shown). In their study, they used the EGFP-p62, and we used FLAG-p62 in our study. In the future, to rule out non-specific interactions, we could further change other tags (GST, GFP, Myc and DsRed), or use the human UBA-deleted p62, not mouse, as a better negative control.

A recent study reported that the de-ubiquitination enzyme *CYLD* interacted with wild-type and a non-UBA mutant A381V p62 in osteoclast progenitor cells, but not to the UBA mutant P392L p62 [178]. Expression of p62 P392L also resulted in increased levels

of polyubiquitinated TRAF6 and phospho-I $\kappa$ B during osteoclast differentiation. These findings suggest that at least some p62 PDB mutations might perturb NF- $\kappa$ B signaling by altering CYLD activity and TRAF6 polyubiquitination.

#### ***(4) Other signaling proteins***

Our data showed that p62 PDB mutants (M404V, P392L and G411S) suppressed its association with polyubiquitinated proteins (Fig. 3.11). Layfield *et al.* [116] also reported that p62 PDB mutants impaired K48-linked polyubiquitin binding *in vitro*. In Chapter 1, we introduced that p62 could bind polyubiquitinated proteins and target them for degradation by both UPS and autophagy (Fig. 1.6) [8]. Therefore, p62 PDB mutations may impair their binding with polyubiquitinated proteins that are active signal proteins in the NF- $\kappa$ B signaling pathway, leading to decreased protein degradation of these proteins, which might increase the NF- $\kappa$ B signaling. To test this hypothesis in the future, mass spectrometry could be applied for identification of these important targeting signaling proteins. In detail, we could use mass spectrometry to do the quantification for the amount of proteins in cells overexpressing WT p62 and p62 PDB mutant (Fig. 3.11). We will expect to see that the amounts of some signaling proteins are significantly higher in cells overexpressing p62 PDB mutant than WT p62. These proteins could be candidate signaling proteins regulated by p62. When these certain proteins are polyubiquitinated, p62 PDB mutants fail to bind with these polyubiquitinated proteins, leading to less capable of sequestering these proteins for degradation. We would confirm these proteins by IP in cells overexpressing Ub and individual candidate proteins. In addition, p62 PDB

mutants could also impair autophagy activity leading to accumulation of important signaling proteins, and further activating NF- $\kappa$ B signaling (see below).

## **Autophagy in PDB**

In a recent autophagy review, it is suggested that autophagy may be related to the development of bone diseases, although the physiological roles of autophagy in bone are still mostly unknown [85]. In addition, the presence of inclusion bodies in osteoclasts seems to link PDB to autophagy [7]. Moreover, it is found that p62 colocalizes with Autophagy-Linked FYVE-domain containing protein (ALFY) in osteoclasts [7]. While this suggests that autophagy is linked to PDB [179], little is known about the role of autophagy in PDB so far. Therefore, the role of autophagy is clearly an area that merits investigation in the future.

Here, I offer some speculation of the role of autophagy based on the literature and our preliminary data in Chapter 4. P62 accumulation has been reported in French PDB patients with and without p62 mutations [175], suggesting that autophagy is impaired in PDB since p62 is a substrate for autophagy [147]. If impairment of autophagy is confirmed in a large number of PDB patients, what are the mechanisms?

Defective autophagy in PDB patients could be related to PDB-associated p62 mutants. As described in Chapter 1, p62 mutations are found in about 40% of familial PDB [7]. Additionally, p62 is both a substrate and regulator of autophagy [8], therefore do PDB-associated p62 mutations contribute to the impairment of autophagy in PDB? In Chapter 4, we tried to use p62 KO MEF cells and several autophagy inducers and/or

inhibitors to test this hypothesis (Fig. 4.3). In preliminary experiments with cells overexpressing WT p62, the LC3-II level decreased less than the control (7.90% vs. 23.20%) after rapamycin treatment (Fig. 4.3 B), suggesting that overexpression of WT p62 attenuates the autophagic activity. Here, we propose that p62 PDB mutants could decrease the autophagic activity compared with WT p62, leading to accumulation of p62, which will further decrease the autophagic activity. In the future, this hypothesis could be tested by better experiment design, including better software to analyze the GFP-LC3 puncta, more effective and appropriate usage of autophagy inducer and/or inhibitor and monitoring the endogenous and exogenous p62 levels as indicators of autophagy.

A recent review paper Goode *et al.* [9] suggests that defective autophagy and dysregulated NF- $\kappa$ B signaling in PDB may be linked. A number of signaling intermediaries of the RANKL-induced NF- $\kappa$ B signaling, such as IKK, are targets of ubiquitination [9, 62], which might be degraded by autophagy. Therefore, it would be interesting to determine the effect of PDB mutations on p62-mediated autophagic protein degradation of signaling intermediaries in the NF- $\kappa$ B signaling. In order to address this question, we could monitor the signaling proteins, including IKK, I $\kappa$ B and phospho-I $\kappa$ B, in cells treated with autophagy inhibitor/inducer in the absence and presence of RANK or TNF $\alpha$ .

Considering our findings of p62 PDB mutant on NF- $\kappa$ B signaling, a new proposed model showing that PDB-associated p62 mutants increase NF- $\kappa$ B signaling by several of the mechanisms is described in Fig. 5.1. P62 PDB mutants could also impair autophagy activity leading to accumulation of important signaling proteins, and further activating NF- $\kappa$ B signaling. Meanwhile, defective autophagy could lead to accumulation



of mutant p62, which would further impair autophagy and upregulate the NF- $\kappa$ B signaling, creating a feed-forward pathological cycle. This combined model is presented in Fig. 5.1.

### **Other methods and models for studying the PDB**

In Chapter 3, we compared cell models for studying the impact of PDB-associated p62 mutants on NF- $\kappa$ B signaling (Table 3.1). Among them, Raw264.7 cells might be the best one since they are osteoclast-like cells [170]. The main technique we used is the NF- $\kappa$ B luciferase assay.

Aside from Raw264.7 cells and NF- $\kappa$ B luciferase assays, people used other methods and materials for studying PDB [80, 170]. Additional methods include bone resorption pit assay [80, 170], *in vitro* osteoclastogenesis assay [170], osteoclast apoptosis [80] and others. In addition, besides NF- $\kappa$ B luciferase assays, people used other methods to examine the NF- $\kappa$ B signaling. These methods include electrophoretic mobility shift assay (EMSA) [180, 181], nuclear:cytoplasmic ratios of NF- $\kappa$ B [182], monitoring the rate of I $\kappa$ B degradation [80] and p65 nuclear translocation [183]. In our study, we monitored the rate of I $\kappa$ B degradation (Fig. 3.3). However, our assay needs to be optimized by co-transfection of HA-I $\kappa$ B (or other tags) with the FLAG-p62, in order to monitor the I $\kappa$ B in cells expressing FLAG-p62 only. In addition, we also tried p65 nuclear translocation in our study (Fig. 3.4). Again, we need to determine how to quantify p65 nuclear translocation between cells expressing WT p62 and mutant p62 in the future.

Mouse models including mice expressing human P392L p62 [184] and P394L mutant mice [185] were reported previously. Isolated bone marrow macrophages (BMM) from WT and p62 mutant mice [170], isolated osteoclast precursors from healthy donors and PDB patients [184], cord blood monocyte (CBM) and peripheral blood mononuclear cells (PBMC) isolated from blood provided by healthy donors and PDB patients [80] were also applied in other people's work.

Compared with our mutant p62 overexpressing in cells, using cells from PDB patient has its advantage of natural background of the PDB-associated p62 mutants. In the future, we may learn from these other methods and models.

### **SUMOylation and NF- $\kappa$ B signaling**

In Chapter 2, we mainly focused on identification of novel SUMOylation substrates. In Chapter 3, we investigated the PDB-associated p62 mutants in NF- $\kappa$ B signaling, which involves TRAFs polyubiquitination. The linkage of Chapter 2 and Chapter 3 seems to be that both SUMOylation and ubiquitination are important post-translational modifications which also share similarities [2].

In addition, several signaling proteins in the NF- $\kappa$ B signaling pathway are reported to be SUMOylation substrates, such as TNF-R1 [35], I $\kappa$ B [30] and NF- $\kappa$ B essential modulator (NEMO) [186], the IKK regulatory subunit. Therefore, does SUMOylation play a role in the NF- $\kappa$ B signaling related to PDB? What is the interplay of SUMOylation and ubiquitination in the NF- $\kappa$ B signaling related to PDB? Could SUMOylation be

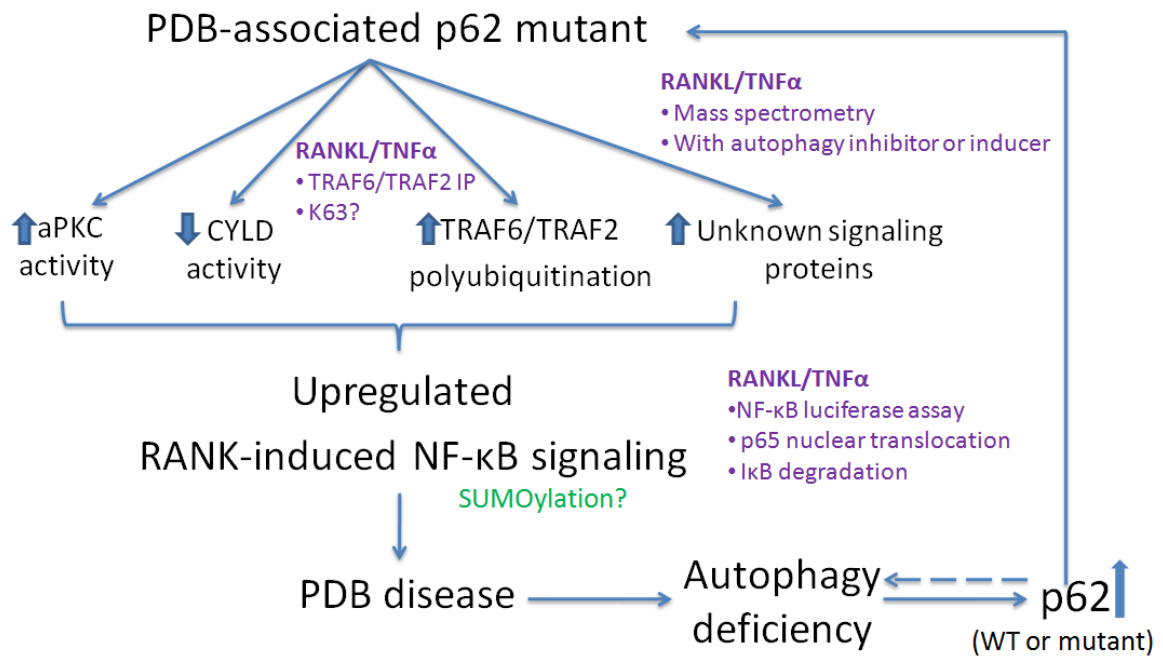
involved in the mechanisms of PDB? We could expand our knowledge of PDB by answering these questions.

### **An integrated model: speculation about the role of PDB-associated p62 mutation**

In light of a recent review paper Goode *et al.* [9], as well as our work and the literature, I proposed a model integrating the role of PDB-associated p62 mutants on both NF- $\kappa$ B signaling and autophagy (Fig. 5.1).

PDB-associated p62 mutants increase NF- $\kappa$ B signaling through several mechanisms including increasing aPKC activity, decreasing CYLD activity, increasing TRAF6/TRAF2 polyubiquitination, as well as increasing activity of unknown signaling proteins. Autophagy deficiency was detected in PDB patients, leading to the accumulation of mutant p62, which is proposed to further impair autophagy (dash line). P62 accelerates disease progression by upregulating NF- $\kappa$ B signaling through one or several of the mechanisms. Therefore, PDB-associated p62 mutants play a synergistic role in disease progression by affecting both NF- $\kappa$ B signaling and autophagy. The impairment of autophagy in PDB patient results in accumulation of mutant p62, which accelerates disease progression by increasing the NF- $\kappa$ B signaling. SUMOylation was found on several NF- $\kappa$ B signaling proteins including I $\kappa$ B [30], TNF-R1[35] and NEMO [186]. SUMOylation would therefore be involved in other mechanisms of PDB.

**Figure 5.1. A proposed model for the role of PDB mutant p62 in NF- $\kappa$ B signaling and autophagy.** PDB-associated p62 mutants increase NF- $\kappa$ B signaling through several mechanisms including increasing aPKC activity, decreasing CYLD activity, increasing TRAF6/TRAFF2 polyubiquitination, as well as increasing activity of unknown signaling proteins. Autophagy deficiency was detected in PDB patients, leading to the accumulation of mutant p62, which is proposed to further impair autophagy (dash line). P62 accelerates disease progression by upregulating NF- $\kappa$ B signaling through several mechanisms. Therefore, PDB-associated p62 mutants play a synergistic role in disease progression by affecting both NF- $\kappa$ B signaling and autophagy. The impairment of autophagy in PDB patient results in accumulation of mutant p62, which accelerates disease progression by increasing the NF- $\kappa$ B signaling. In addition, SUMOylation would be involved in other mechanisms of PDB.



## APPENDICES

### Appendix I: List of all constructs

<i>Plasmid</i>	<i>Insert</i>	<i>Vector</i>	<i>Reference</i>
p3xFLAG-CMV10	N/A	p3xFLAG-CMV10	Sigma
pDsRed <sup>M</sup> = pDsRed-monomer C1	N/A	pDsRed-monomer C1	Clontech
p3xHA-CMV10	N/A	The 3xFLAG tag of p3xFLAG-CMV10 replaced with 3xHA tag	Chapter 2, made by Dr. Jozsef Gal
p3xFLAG-SUMO1(FL)	N/A	p3xFLAG-CMV10	Chapter 2
p3xFLAG-SUMO1(GG)		p3xFLAG-CMV10	Chapter 2
p3xFLAG-SUMO1(FL-T95R)	T95R	p3xFLAG-CMV10	Chapter 2
p3xFLAG-SUMO1(GG-T95R)		p3xFLAG-CMV10	Chapter 2
pDrebrin		pCMV	Chapter 2 Dr. Tomas Brdicka [165]
p3xHA-Drebrin	Human full-length, WT Drebrin	p3xHA-CMV10	Chapter 2
p3xHA-Drebrin, K185R	Human Drebrin K185R	p3xHA-CMV10	Chapter 2
p3xHA-Drebrin, K186R	Human Drebrin K186R	p3xHA-CMV10	Chapter 2
p3xHA-Drebrin, K192R	Human Drebrin K192R	p3xHA-CMV10	Chapter 2
p3xHA-Drebrin, K270R	Human Drebrin K270R	p3xHA-CMV10	Chapter 2
p3xHA-Drebrin, K271R	Human Drebrin K271R	p3xHA-CMV10	Chapter 2
p3xHA-Drebrin, K185R/K186R	Human Drebrin K185R/K186R	p3xHA-CMV10	Chapter 2
p3xHA-Drebrin, K270R/K271R	Human Drebrin K270R/K271R	p3xHA-CMV10	Chapter 2
Contd.			

p3xHA-Drebrin, RRRRR	Human Drebrin K185R/K186R/K192R/K270 R/K271R	p3xHA-CMV10	Chapter 2
pMYC-p62 (human)	Human full-length, WT p62	pcDNA-MYC	Dr. Marie Wooten
p3xFLAG-p62 (human)	Human full-length, WT p62	p3xFLAG-CMV10	Chapter 3, 4 and 5
p3xFLAG-p62, D335E	Human p62 D335E	p3xFLAG-CMV10	Chapter 3, 4 and 5
p3xFLAG-p62, A381V	Human p62 A381V	p3xFLAG-CMV10	Chapter 3, 4 and 5
p3xFLAG-p62, P392L	Human p62 P392L	p3xFLAG-CMV10	Chapter 3, 4 and 5
p3xFLAG-p62, M404V	Human p62 M404V	p3xFLAG-CMV10	Chapter 3, 4 and 5
p3xFLAG-p62, G411S	Human p62 G411S	p3xFLAG-CMV10	Chapter 3, 4 and 5
pDsRed <sup>M</sup> -p62	Human full-length, WT p62	pDsRed- monomerC1	Chapter 3, 4 and 5
pDsRed <sup>M</sup> -p62, A381V	Human p62 A381V	pDsRed- monomerC1	Chapter 3, 4 and 5
pDsRed <sup>M</sup> -p62, P392L	Human p62 P392L	pDsRed- monomerC1	Chapter 3, 4 and 5
pDsRed <sup>M</sup> -p62, M404V	Human p62 M404V	pDsRed- monomerC1	Chapter 3, 4 and 5
p3xFLAG- p62 (mouse)	WT, full-length mouse p62	p3xFLAG-CMV10	Chapter 3,made by Dr. Jozsef Gal [83]
p3xFLAG- p62 (mouse), delta UBA	Mouse p62, A2-T352	p3xFLAG-CMV10	Chapter 4, made by Dr. Jozsef Gal [83]
p3xFLAG-TRAF6	Full-length, WT mouse TRAF6	p3xFLAG-CMV10	Chapter 3 and 4 Made by Dr. Jozsef Gal
NF-κB luciferase reporter		pCMV	Chapter 3 and 4, Dr. Jiake Xu [170, 173].
GST-rRANKL		pCMV	Chapter 3, Dr. Jiake Xu [171]
phRL-TK			Promega
p3xHA-Ub		p3xHA	Chapter 3, Dr. Matthew Gentry
Contd.			

p3xHA-Ub, K48 only	K6R/ K11R/ K27R/ K29R/ K33R/ K63R	p3xHA	Chapter 3, Dr. Matthew Gentry
p3xHA-Ub, K63 only	K6R/K11R/ K27R/K29R/ K33R/K48R	p3xHA	Chapter 3, Dr. Matthew Gentry
pHA-Ub		pcDNA-HA	Chapter 3, Dr. Marie Wooten
pHA-Ub, K29R	K29R	pcDNA-HA	Chapter 3, Dr. Marie Wooten
pHA-Ub, K48R	K48R	pcDNA-HA	Chapter 3, Dr. Marie Wooten
pHA-Ub, K63R	K63R	pcDNA-HA	Chapter 3, Dr. Marie Wooten
pGFP-LC3	Mouse LC3B, P2-V125	pEGFP-C1	Chapter 5, Made by Dr. Jozsef Gal
HA-CYLD	Human full-length, WT CYLD	pDEST-HA	Addgene Plasmid 15506 [177].

## Appendix II: List of amplification primers and mutagenic primer sequences.

<i>Number</i>	<i>Name</i>	<i>Primer sequences</i>
GJ464	T375A reversion primer in the Wooten human p62 clone	5'-CCTTCAGCCCTGTGGGTCCCTCCTG-3'
GJ465	T375A reversion primer in the Wooten human p62 clone	5'-CAGGAGGGACCCACAGGGCTGAAGG-3'
GJ468	Human p62 upstream for N-terminal tagging ( <i>EcoRI</i> )	5'-GCTGGAATTCGCGTCGCTCACCGTGAAG-3'
GJ469	Human p62 downstream, cont. STOP ( <i>KpnI</i> )	5'-CGTCGGTACCTCACAACGGCGGGGGATG-3'
GJ470	Human p62 internal seq. primer	5'-TGGTTGCCTTTTCCAGTGAC-3'
GJ471	Human p62 D335E QuikchangeII primer, upper strand	5'-ACTGTTTCAGGAGGAGAAGATGACTGGACCCATC-3'
GJ472	Human p62 D335E QuikchangeII primer, lower strand	5'-GATGGGTCCAGTCATCTTCTCCTCCTGAACAGT-3'
GJ473	Human p62 A381V QuikchangeII primer, upper strand	5'-GGCTGAAGGAAGCCGTCTTGTACCCACATCT-3'
GJ474	Human p62 A381V QuikchangeII primer, lower strand	5'-AGATGTGGGTACAAGACGGCTTCCTTCAGCC-3'
GJ475	Human p62 P392L QuikchangeII primer, upper strand	5'-CCAGAGGCTGACCTGCGGCTGATTGAG-3'
GJ476	Human p62 P392L QuikchangeII primer, lower strand	5'-CTCAATCAGCCGCAGGTCAGCCTCTGG-3'
GJ477	Human p62 M404V QuikchangeII primer, upper strand	5'-TCCCAGATGCTGTCCGTGGGCTTCTCTGATG-3'
GJ478	Human p62 M404V QuikchangeII primer, lower strand	5'-CATCAGAGAAGCCCACGGACAGCATCTGGGA-3'
GJ479	Human p62 G411S QuikchangeII primer, upper strand	5'-TCTCTGATGAAGGCAGCTGGCTCACCAGG-3'

Contd.



GJ480	Human p62 G411S QuikchangeII primer, lower strand	5'-CCTGGTGAGCCAGCTGCCTTCATCAGAGA-3'
GJ757	hDrebrin Quikchange Multi, K185R K186R, upper strand	5'-GTTCTGGGAGCAGGCCAGGAGGGAAGAAGAGCTGC-3'
GJ758	hDrebrin Quikchange Multi, K185R K186R, lower strand	5'-GCAGCTCTTCTTCCCTCCTGGCCTGCTCCCAGAAC-3'
GJ759	hDrebrin Quikchange Multi, K192R, upper	5'-AGAAGAGCTGCGGAGGGAGGAGGAGCG-3'
GJ760	hDrebrin Quikchange Multi, K192R, lower strand	5'-CGCTCCTCCTCCCTCCGCAGCTCTTCT-3'
GJ761	hDrebrin Quikchange Multi, K270R K271R, upper strand	5'-GAAGAGACCCACATGAGGAGGTCAGAGTCGGAGGTG-3'
GJ762	hDrebrin Quikchange Multi, K270R K271R, lower strand	5'-CACCTCCGACTCTGACCTCCTCATGTGGGTCTCTTC-3'
GJ763	hDrebrin internal sequencing primer	5'-AAGACGGATGCAGCTGTGGA-3'
GJ764	hDrebrin, upstream primer for p3xHA- CMV10 ( <i>EcoRI</i> )	5'-CGTCGAATTCGCCGGCGTCAGCTTCAG-3'
GJ765	hDrebrin, downstream primer for p3xHA-CMV10 ( <i>BamHI</i> )	5'-CGTCGGATCCCTAATCACCACCCTCGAAGC-3'
GJ769	hDrebrin K185R Quikchange II, upper strand	5'-CTGGGAGCAGGCCAGGAAGGAAGAAGAGC-3'
GJ770	hDrebrin K185R Quikchange II, lower strand	5'-GCTCTTCTTCCTTCCTGGCCTGCTCCCAG-3'
GJ771	hDrebrin K186R Quikchange II, upper strand	5'-TGGGAGCAGGCCAAGAGGGAAGAAGAGCTG-3'
GJ772	hDrebrin K186R Quikchange II, lower	5'-CAGCTCTTCTTCCCTCTTGGCCTGCTCCCA-3'
GJ773	hDrebrin K270R Quikchange II, upper strand	5'-GAAGAGACCCACATGAGGAAGTCAGAGTCGGAG-3'
GJ774	hDrebrin K270R Quikchange II, lower strand	5'-CTCCGACTCTGACTTCCTCATGTGGGTCTCTTC-3'
GJ775	hDrebrin K271R Quikchange II, upper strand	5'-GAGACCCACATGAAGAGGTCAGAGTCGGAGGTG-3'

Contd.

---

GJ776	hDrebrin K271R Quikchange II, lower strand	5'-CACCTCCGACTCTGACCTCTTCATGTGGGTCTC-3'
-------	--	---

---

### **Appendix III: List of abbreviations**

ALS: Amyotrophic lateral sclerosis  
aPKC: atypical protein kinase C  
CHO: Chinese hamster ovary  
Drebrin: Developmentally regulated brain protein  
EMSA: Electrophoretic mobility shift assay  
ERK: Extracellular responsive kinase  
FL: Full-length  
GFP: Green fluorescent protein  
HA: Hemagglutinin  
HEK: Human embryonic kidney  
HRP: Horseradish peroxidase  
hSUMO-1: human SUMO-1  
IKK: I $\kappa$ B kinase  
I $\kappa$ B: Inhibitor of NF- $\kappa$ B  
KO: Knockout  
LC3: Microtubule-associated protein light chain 3  
LIR: LC3 interaction region  
MEK5: MAPK/ERK kinase 5  
MEF: Mouse Fibroblast  
NBR1: Neighbor of BRCA1 gene 1  
NEMO: NF- $\kappa$ B essential modulator  
NF- $\kappa$ B: Nuclear factor  $\kappa$ B  
NPC: Nuclear pore complex  
IP: Immunoprecipitation  
PDB: Paget's disease of bone

PB1 domain: Phox and Bem1 domain

PE: Phosphatidylethanolamine

PML: Promyelocytic leukemia

RANK: Receptor Activator of Nuclear Factor  $\kappa$ B

Ran-GAP1: Ran-GTPase-activating protein 1

RIP: Receptor-interacting protein

SDS-PAGE: Sodium dodecyl sulfate polyacrylamide gel electrophoresis

SENP: Sentrin/SUMO-specific protease

SUMO: Small Ubiquitin-like Modifier protein

TB domain: TRAF6 binding domain

TBST: Tris-Buffered Saline and Tween 20

TNF $\alpha$ : Tumor Necrosis Factor- $\alpha$

TRADD: TNFR1-associated death domain protein

TRAF6: TNF receptor associated factor 6

TrkA: Tropomyosin-receptor- kinase

UBA domain: Ubiquitin-association domain

UPS: Ubiquitin-proteasom system

WT: Wild-type

## REFERENCES

1. Wilkinson, K.A. and J.M. Henley, *Mechanisms, regulation and consequences of protein SUMOylation*. Biochem J, 2010. **428**(2): p. 133-45.
2. Zhao, J., *Sumoylation regulates diverse biological processes*. Cell Mol Life Sci, 2007. **64**(23): p. 3017-33.
3. Shirao, T., N. Kojima, Y. Kato, and K. Obata, *Molecular cloning of a cDNA for the developmentally regulated brain protein, drebrin*. Brain Res, 1988. **464**(1): p. 71-4.
4. Babu, J.R., T. Geetha, and M.W. Wooten, *Sequestosome 1/p62 shuttles polyubiquitinated tau for proteasomal degradation*. J Neurochem, 2005. **94**(1): p. 192-203.
5. Moscat, J., M.T. Diaz-Meco, and M.W. Wooten, *Signal integration and diversification through the p62 scaffold protein*. Trends Biochem Sci, 2007. **32**(2): p. 95-100.
6. Seibenhener, M.L., T. Geetha, and M.W. Wooten, *Sequestosome 1/p62--more than just a scaffold*. FEBS Lett, 2007. **581**(2): p. 175-9.
7. Helfrich, M.H. and L.J. Hocking, *Genetics and aetiology of Pagetic disorders of bone*. Arch Biochem Biophys, 2008. **473**(2): p. 172-82.
8. Komatsu, M. and Y. Ichimura, *Physiological significance of selective degradation of p62 by autophagy*. FEBS Lett, 2010. **584**(7): p. 1374-8.
9. Goode, A. and R. Layfield, *Recent advances in understanding the molecular basis of Paget disease of bone*. J Clin Pathol, 2010. **63**(3): p. 199-203.
10. Wimmer, P., S. Schreiner, and T. Dobner, *Human pathogens and the host cell SUMOylation system*. J Virol, 2012. **86**(2): p. 642-54.
11. Mahajan, R., C. Delphin, T. Guan, L. Gerace, and F. Melchior, *A small ubiquitin-related polypeptide involved in targeting RanGAP1 to nuclear pore complex protein RanBP2*. Cell, 1997. **88**(1): p. 97-107.
12. Matunis, M.J., E. Coutavas, and G. Blobel, *A novel ubiquitin-like modification modulates the partitioning of the Ran-GTPase-activating protein RanGAP1 between the cytosol and the nuclear pore complex*. J Cell Biol, 1996. **135**(6 Pt 1): p. 1457-70.
13. Marx, J., *Cell biology. SUMO wrestles its way to prominence in the cell*. Science, 2005. **307**(5711): p. 836-9.
14. Sarge, K.D. and O.K. Park-Sarge, *Sumoylation and human disease pathogenesis*. Trends Biochem Sci, 2009. **34**(4): p. 200-5.
15. Bohren, K.M., K.H. Gabbay, and D. Owerbach, *Affinity chromatography of native SUMO proteins using His-tagged recombinant UBC9 bound to Co2+-charged talon resin*. Protein Expr Purif, 2007. **54**(2): p. 289-94.
16. Wang, Y. and M. Dasso, *SUMOylation and deSUMOylation at a glance*. J Cell Sci, 2009. **122**(Pt 23): p. 4249-52.
17. Muller, S., C. Hoege, G. Pyrowolakis, and S. Jentsch, *SUMO, ubiquitin's mysterious cousin*. Nat Rev Mol Cell Biol, 2001. **2**(3): p. 202-10.
18. Melchior, F., *SUMO--nonclassical ubiquitin*. Annu Rev Cell Dev Biol, 2000. **16**: p. 591-626.
19. Bayer, P., A. Arndt, S. Metzger, R. Mahajan, F. Melchior, R. Jaenicke, and J. Becker, *Structure determination of the small ubiquitin-related modifier SUMO-1*. J Mol Biol, 1998. **280**(2): p. 275-86.
20. Johnson, E.S., *Protein modification by SUMO*. Annu Rev Biochem, 2004. **73**: p. 355-82.
21. Gill, G., *SUMO and ubiquitin in the nucleus: different functions, similar mechanisms?* Genes Dev, 2004. **18**(17): p. 2046-59.

22. Jentsch, S., *The ubiquitin-conjugation system*. Annu Rev Genet, 1992. **26**: p. 179-207.
23. Wertz, I.E. and V.M. Dixit, *Signaling to NF-kappaB: regulation by ubiquitination*. Cold Spring Harb Perspect Biol, 2010. **2**(3): p. a003350.
24. Hay, R.T., *SUMO: a history of modification*. Mol Cell, 2005. **18**(1): p. 1-12.
25. Ulrich, H.D., *SUMO modification: wrestling with protein conformation*. Curr Biol, 2005. **15**(7): p. R257-9.
26. Yeh, E.T., *SUMOylation and De-SUMOylation: wrestling with life's processes*. J Biol Chem, 2009. **284**(13): p. 8223-7.
27. Sampson, D.A., M. Wang, and M.J. Matunis, *The small ubiquitin-like modifier-1 (SUMO-1) consensus sequence mediates Ubc9 binding and is essential for SUMO-1 modification*. J Biol Chem, 2001. **276**(24): p. 21664-9.
28. Rodriguez, M.S., C. Dargemont, and R.T. Hay, *SUMO-1 conjugation in vivo requires both a consensus modification motif and nuclear targeting*. J Biol Chem, 2001. **276**(16): p. 12654-9.
29. Gocke, C.B., H. Yu, and J. Kang, *Systematic identification and analysis of mammalian small ubiquitin-like modifier substrates*. J Biol Chem, 2005. **280**(6): p. 5004-12.
30. Desterro, J.M., M.S. Rodriguez, and R.T. Hay, *SUMO-1 modification of IkappaBalpha inhibits NF-kappaB activation*. Mol Cell, 1998. **2**(2): p. 233-9.
31. Zhang, Y.Q. and K.D. Sarge, *Sumoylation of amyloid precursor protein negatively regulates Abeta aggregate levels*. Biochem Biophys Res Commun, 2008. **374**(4): p. 673-8.
32. Maul, G.G., D. Negorev, P. Bell, and A.M. Ishov, *Review: properties and assembly mechanisms of ND10, PML bodies, or PODs*. J Struct Biol, 2000. **129**(2-3): p. 278-87.
33. Potts, P.R. and H. Yu, *Human MMS21/NSE2 is a SUMO ligase required for DNA repair*. Mol Cell Biol, 2005. **25**(16): p. 7021-32.
34. Verger, A., J. Perdomo, and M. Crossley, *Modification with SUMO. A role in transcriptional regulation*. EMBO Rep, 2003. **4**(2): p. 137-42.
35. Okura, T., L. Gong, T. Kamitani, T. Wada, I. Okura, C.F. Wei, H.M. Chang, and E.T. Yeh, *Protection against Fas/APO-1- and tumor necrosis factor-mediated cell death by a novel protein, sentrin*. J Immunol, 1996. **157**(10): p. 4277-81.
36. Geiss-Friedlander, R. and F. Melchior, *Concepts in sumoylation: a decade on*. Nat Rev Mol Cell Biol, 2007. **8**(12): p. 947-56.
37. Matunis, M.J., J. Wu, and G. Blobel, *SUMO-1 modification and its role in targeting the Ran GTPase-activating protein, RanGAP1, to the nuclear pore complex*. J Cell Biol, 1998. **140**(3): p. 499-509.
38. Harder, Z., R. Zunino, and H. McBride, *Sumo1 conjugates mitochondrial substrates and participates in mitochondrial fission*. Curr Biol, 2004. **14**(4): p. 340-5.
39. Yang, S.H. and A.D. Sharrocks, *SUMO promotes HDAC-mediated transcriptional repression*. Mol Cell, 2004. **13**(4): p. 611-7.
40. Gill, G., *Something about SUMO inhibits transcription*. Curr Opin Genet Dev, 2005. **15**(5): p. 536-41.
41. Hay, R.T., *Role of ubiquitin-like proteins in transcriptional regulation*. Ernst Schering Res Found Workshop, 2006(57): p. 173-92.
42. Hong, Y., R. Rogers, M.J. Matunis, C.N. Mayhew, M.L. Goodson, O.K. Park-Sarge, and K.D. Sarge, *Regulation of heat shock transcription factor 1 by stress-induced SUMO-1 modification*. J Biol Chem, 2001. **276**(43): p. 40263-7.
43. Sarge, K.D. and O.K. Park-Sarge, *SUMO and its role in human diseases*. Int Rev Cell Mol Biol, 2011. **288**: p. 167-83.
44. Dun, X.P. and J.K. Chilton, *Control of cell shape and plasticity during development and disease by the actin-binding protein Drebrin*. Histol Histopathol, 2010. **25**(4): p. 533-40.

45. Majoul, I., T. Shirao, Y. Sekino, and R. Duden, *Many faces of drebrin: from building dendritic spines and stabilizing gap junctions to shaping neurite-like cell processes*. Histochem Cell Biol, 2007. **127**(4): p. 355-61.
46. Shirao, T. and K. Obata, *Two acidic proteins associated with brain development in chick embryo*. J Neurochem, 1985. **44**(4): p. 1210-6.
47. Kojima, N., T. Shirao, and K. Obata, *Molecular cloning of a developmentally regulated brain protein, chicken drebrin A and its expression by alternative splicing of the drebrin gene*. Brain Res Mol Brain Res, 1993. **19**(1-2): p. 101-14.
48. Shirao, T. and K. Obata, *Immunohistochemical homology of 3 developmentally regulated brain proteins and their developmental change in neuronal distribution*. Brain Res, 1986. **394**(2): p. 233-44.
49. Kojima, N., Y. Kato, T. Shirao, and K. Obata, *Nucleotide sequences of two embryonic drebrins, developmentally regulated brain proteins, and developmental change in their mRNAs*. Brain Res, 1988. **464**(3): p. 207-15.
50. Lappalainen, P., M.M. Kessels, M.J. Cope, and D.G. Drubin, *The ADF homology (ADF-H) domain: a highly exploited actin-binding module*. Mol Biol Cell, 1998. **9**(8): p. 1951-9.
51. Foa, L. and R. Gasperini, *Developmental roles for Homer: more than just a pretty scaffold*. J Neurochem, 2009. **108**(1): p. 1-10.
52. Saha, S., M.M. Mundia, F. Zhang, R.W. Demers, F. Korobova, T. Svitkina, A.A. Perieteanu, J.F. Dawson, and A. Kashina, *Arginylation regulates intracellular actin polymer level by modulating actin properties and binding of capping and severing proteins*. Mol Biol Cell, 2010. **21**(8): p. 1350-61.
53. Hayashi, K. and T. Shirao, *Change in the shape of dendritic spines caused by overexpression of drebrin in cultured cortical neurons*. J Neurosci, 1999. **19**(10): p. 3918-25.
54. Shirao, T., K. Hayashi, R. Ishikawa, K. Isa, H. Asada, K. Ikeda, and K. Uyemura, *Formation of thick, curving bundles of actin by drebrin A expressed in fibroblasts*. Exp Cell Res, 1994. **215**(1): p. 145-53.
55. Shirao, T., N. Kojima, and K. Obata, *Cloning of drebrin A and induction of neurite-like processes in drebrin-transfected cells*. Neuroreport, 1992. **3**(1): p. 109-12.
56. Hayashi, K., R. Ishikawa, R. Kawai-Hirai, T. Takagi, A. Taketomi, and T. Shirao, *Domain analysis of the actin-binding and actin-remodeling activities of drebrin*. Exp Cell Res, 1999. **253**(2): p. 673-80.
57. Mizui, T., H. Takahashi, Y. Sekino, and T. Shirao, *Overexpression of drebrin A in immature neurons induces the accumulation of F-actin and PSD-95 into dendritic filopodia, and the formation of large abnormal protrusions*. Mol Cell Neurosci, 2005. **30**(1): p. 149-57.
58. Keon, B.H., P.T. Jedrzejewski, D.L. Paul, and D.A. Goodenough, *Isoform specific expression of the neuronal F-actin binding protein, drebrin, in specialized cells of stomach and kidney epithelia*. J Cell Sci, 2000. **113 Pt 2**: p. 325-36.
59. Layfield, R., *The molecular pathogenesis of Paget disease of bone*. Expert Rev Mol Med, 2007. **9**(27): p. 1-13.
60. Laurin, N., J.P. Brown, A. Lemainque, A. Duchesne, D. Huot, Y. Lacourciere, G. Drapeau, J. Verreault, V. Raymond, and J. Morissette, *Paget disease of bone: mapping of two loci at 5q35-qter and 5q31*. Am J Hum Genet, 2001. **69**(3): p. 528-43.
61. Michou, L. and J.P. Brown, *Emerging strategies and therapies for treatment of Paget's disease of bone*. Drug Des Devel Ther, 2011. **5**: p. 225-39.
62. Layfield, R. and B. Shaw, *Ubiquitin-mediated signalling and Paget's disease of bone*. BMC Biochem, 2007. **8 Suppl 1**: p. S5.

63. van Staa, T.P., P. Selby, H.G. Leufkens, K. Lyles, J.M. Sprafka, and C. Cooper, *Incidence and natural history of Paget's disease of bone in England and Wales*. J Bone Miner Res, 2002. **17**(3): p. 465-71.
64. Huvos, A.G., *Osteogenic sarcoma of bones and soft tissues in older persons. A clinicopathologic analysis of 117 patients older than 60 years*. Cancer, 1986. **57**(7): p. 1442-9.
65. Xu, J., H.F. Wu, E.S. Ang, K. Yip, M. Woloszyn, M.H. Zheng, and R.X. Tan, *NF-kappaB modulators in osteolytic bone diseases*. Cytokine Growth Factor Rev, 2009. **20**(1): p. 7-17.
66. Ralston, S.H., *Pathogenesis of Paget's disease of bone*. Bone, 2008. **43**(5): p. 819-25.
67. Teitelbaum, S.L. and F.P. Ross, *Genetic regulation of osteoclast development and function*. Nat Rev Genet, 2003. **4**(8): p. 638-49.
68. Wong, B.R., J. Rho, J. Arron, E. Robinson, J. Orlinick, M. Chao, S. Kalachikov, E. Cayani, F.S. Bartlett, 3rd, W.N. Frankel, S.Y. Lee, and Y. Choi, *TRANCE is a novel ligand of the tumor necrosis factor receptor family that activates c-Jun N-terminal kinase in T cells*. J Biol Chem, 1997. **272**(40): p. 25190-4.
69. Anderson, D.M., E. Maraskovsky, W.L. Billingsley, W.C. Dougall, M.E. Tometsko, E.R. Roux, M.C. Teepe, R.F. DuBose, D. Cosman, and L. Galibert, *A homologue of the TNF receptor and its ligand enhance T-cell growth and dendritic-cell function*. Nature, 1997. **390**(6656): p. 175-9.
70. Yasuda, H., N. Shima, N. Nakagawa, K. Yamaguchi, M. Kinoshita, S. Mochizuki, A. Tomoyasu, K. Yano, M. Goto, A. Murakami, E. Tsuda, T. Morinaga, K. Higashio, N. Udagawa, N. Takahashi, and T. Suda, *Osteoclast differentiation factor is a ligand for osteoprotegerin/osteoclastogenesis-inhibitory factor and is identical to TRANCE/RANKL*. Proc Natl Acad Sci U S A, 1998. **95**(7): p. 3597-602.
71. Lacey, D.L., E. Timms, H.L. Tan, M.J. Kelley, C.R. Dunstan, T. Burgess, R. Elliott, A. Colombero, G. Elliott, S. Scully, H. Hsu, J. Sullivan, N. Hawkins, E. Davy, C. Capparelli, A. Eli, Y.X. Qian, S. Kaufman, I. Sarosi, V. Shalhoub, G. Senaldi, J. Guo, J. Delaney, and W.J. Boyle, *Osteoprotegerin ligand is a cytokine that regulates osteoclast differentiation and activation*. Cell, 1998. **93**(2): p. 165-76.
72. Verstrepen, L., T. Bekaert, T.L. Chau, J. Tavernier, A. Chariot, and R. Beyaert, *TLR-4, IL-1R and TNF-R signaling to NF-kappaB: variations on a common theme*. Cell Mol Life Sci, 2008. **65**(19): p. 2964-78.
73. Li, J., I. Sarosi, X.Q. Yan, S. Morony, C. Capparelli, H.L. Tan, S. McCabe, R. Elliott, S. Scully, G. Van, S. Kaufman, S.C. Juan, Y. Sun, J. Tarpley, L. Martin, K. Christensen, J. McCabe, P. Kostenuik, H. Hsu, F. Fletcher, C.R. Dunstan, D.L. Lacey, and W.J. Boyle, *RANK is the intrinsic hematopoietic cell surface receptor that controls osteoclastogenesis and regulation of bone mass and calcium metabolism*. Proc Natl Acad Sci U S A, 2000. **97**(4): p. 1566-71.
74. Reddy, S.V., *Etiologic factors in Paget's disease of bone*. Cell Mol Life Sci, 2006. **63**(4): p. 391-8.
75. Lever, J.H., *Paget's disease of bone in Lancashire and arsenic pesticide in cotton mill wastewater: a speculative hypothesis*. Bone, 2002. **31**(3): p. 434-6.
76. Watts, G.D., J. Wymer, M.J. Kovach, S.G. Mehta, S. Mumm, D. Darvish, A. Pestronk, M.P. Whyte, and V.E. Kimonis, *Inclusion body myopathy associated with Paget disease of bone and frontotemporal dementia is caused by mutant valosin-containing protein*. Nat Genet, 2004. **36**(4): p. 377-81.
77. Duran, A., M. Serrano, M. Leitges, J.M. Flores, S. Picard, J.P. Brown, J. Moscat, and M.T. Diaz-Meco, *The atypical PKC-interacting protein p62 is an important mediator of RANK-activated osteoclastogenesis*. Dev Cell, 2004. **6**(2): p. 303-9.



78. Najat, D., T. Garner, T. Hagen, B. Shaw, P.W. Sheppard, A. Falchetti, F. Marini, M.L. Brandi, J.E. Long, J.R. Cavey, M.S. Searle, and R. Layfield, *Characterization of a non-UBA domain missense mutation of sequestosome 1 (SQSTM1) in Paget's disease of bone*. J Bone Miner Res, 2009. **24**(4): p. 632-42.
79. Rea, S.L., J.P. Walsh, L. Ward, A.L. Magno, B.K. Ward, B. Shaw, R. Layfield, G.N. Kent, J. Xu, and T. Ratajczak, *Sequestosome 1 mutations in Paget's disease of bone in Australia: prevalence, genotype/phenotype correlation, and a novel non-UBA domain mutation (P364S) associated with increased NF-kappaB signaling without loss of ubiquitin binding*. J Bone Miner Res, 2009. **24**(7): p. 1216-23.
80. Chamoux, E., J. Couture, M. Bisson, J. Morissette, J.P. Brown, and S. Roux, *The p62 P392L mutation linked to Paget's disease induces activation of human osteoclasts*. Mol Endocrinol, 2009. **23**(10): p. 1668-80.
81. Rea, S.L., J.P. Walsh, L. Ward, K. Yip, B.K. Ward, G.N. Kent, J.H. Steer, J. Xu, and T. Ratajczak, *A novel mutation (K378X) in the sequestosome 1 gene associated with increased NF-kappaB signaling and Paget's disease of bone with a severe phenotype*. J Bone Miner Res, 2006. **21**(7): p. 1136-45.
82. Seibenhener, M.L., J.R. Babu, T. Geetha, H.C. Wong, N.R. Krishna, and M.W. Wooten, *Sequestosome 1/p62 is a polyubiquitin chain binding protein involved in ubiquitin proteasome degradation*. Mol Cell Biol, 2004. **24**(18): p. 8055-68.
83. Gal, J., A.L. Strom, D.M. Kwinter, R. Kilty, J. Zhang, P. Shi, W. Fu, M.W. Wooten, and H. Zhu, *Sequestosome 1/p62 links familial ALS mutant SOD1 to LC3 via an ubiquitin-independent mechanism*. J Neurochem, 2009. **111**(4): p. 1062-73.
84. Moscat, J. and M.T. Diaz-Meco, *p62 at the crossroads of autophagy, apoptosis, and cancer*. Cell, 2009. **137**(6): p. 1001-4.
85. Mizushima, N. and M. Komatsu, *Autophagy: renovation of cells and tissues*. Cell, 2011. **147**(4): p. 728-41.
86. Inami, Y., S. Waguri, A. Sakamoto, T. Kouno, K. Nakada, O. Hino, S. Watanabe, J. Ando, M. Iwade, M. Yamamoto, M.S. Lee, K. Tanaka, and M. Komatsu, *Persistent activation of Nrf2 through p62 in hepatocellular carcinoma cells*. J Cell Biol, 2011. **193**(2): p. 275-84.
87. Mizuno, Y., M. Amari, M. Takatama, H. Aizawa, B. Mihara, and K. Okamoto, *Immunoreactivities of p62, an ubiquitin-binding protein, in the spinal anterior horn cells of patients with amyotrophic lateral sclerosis*. J Neurol Sci, 2006. **249**(1): p. 13-8.
88. Zatloukal, K., C. Stumptner, A. Fuchsichler, H. Heid, M. Schnoelzer, L. Kenner, R. Kleinert, M. Prinz, A. Aguzzi, and H. Denk, *p62 Is a common component of cytoplasmic inclusions in protein aggregation diseases*. Am J Pathol, 2002. **160**(1): p. 255-63.
89. Bjorkoy, G., T. Lamark, A. Brech, H. Outzen, M. Perander, A. Overvatn, H. Stenmark, and T. Johansen, *p62/SQSTM1 forms protein aggregates degraded by autophagy and has a protective effect on huntingtin-induced cell death*. J Cell Biol, 2005. **171**(4): p. 603-14.
90. Moscat, J., M.T. Diaz-Meco, and M.W. Wooten, *Of the atypical PKCs, Par-4 and p62: recent understandings of the biology and pathology of a PBI-dominated complex*. Cell Death Differ, 2009. **16**(11): p. 1426-37.
91. Wilson, M.I., D.J. Gill, O. Perisic, M.T. Quinn, and R.L. Williams, *PBI domain-mediated heterodimerization in NADPH oxidase and signaling complexes of atypical protein kinase C with Par6 and p62*. Mol Cell, 2003. **12**(1): p. 39-50.
92. Lamark, T., M. Perander, H. Outzen, K. Kristiansen, A. Overvatn, E. Michaelsen, G. Bjorkoy, and T. Johansen, *Interaction codes within the family of mammalian Phox and Bem1p domain-containing proteins*. J Biol Chem, 2003. **278**(36): p. 34568-81.
93. Sanz, L., P. Sanchez, M.J. Lallena, M.T. Diaz-Meco, and J. Moscat, *The interaction of p62 with RIP links the atypical PKCs to NF-kappaB activation*. EMBO J, 1999. **18**(11): p. 3044-53.

94. Geetha, T., J. Jiang, and M.W. Wooten, *Lysine 63 polyubiquitination of the nerve growth factor receptor TrkA directs internalization and signaling*. Mol Cell, 2005. **20**(2): p. 301-12.
95. Wooten, M.W., T. Geetha, M.L. Seibenhener, J.R. Babu, M.T. Diaz-Meco, and J. Moscat, *The p62 scaffold regulates nerve growth factor-induced NF-kappaB activation by influencing TRAF6 polyubiquitination*. J Biol Chem, 2005. **280**(42): p. 35625-9.
96. Martin, P., M.T. Diaz-Meco, and J. Moscat, *The signaling adapter p62 is an important mediator of T helper 2 cell function and allergic airway inflammation*. EMBO J, 2006. **25**(15): p. 3524-33.
97. Pankiv, S., T.H. Clausen, T. Lamark, A. Brech, J.A. Bruun, H. Outzen, A. Overvatn, G. Bjorkoy, and T. Johansen, *p62/SQSTM1 binds directly to Atg8/LC3 to facilitate degradation of ubiquitinated protein aggregates by autophagy*. J Biol Chem, 2007. **282**(33): p. 24131-45.
98. Falchetti, A., M. Di Stefano, F. Marini, S. Ortolani, M.F. Ulivieri, S. Bergui, L. Masi, C. Cepollaro, M. Benucci, O. Di Munno, M. Rossini, S. Adami, A. Del Puente, G. Isaia, F. Torricelli, and M.L. Brandi, *Genetic epidemiology of Paget's disease of bone in Italy: sequestosome1/p62 gene mutational test and haplotype analysis at 5q35 in a large representative series of sporadic and familial Italian cases of Paget's disease of bone*. Calcif Tissue Int, 2009. **84**(1): p. 20-37.
99. Ciani, B., R. Layfield, J.R. Cavey, P.W. Sheppard, and M.S. Searle, *Structure of the ubiquitin-associated domain of p62 (SQSTM1) and implications for mutations that cause Paget's disease of bone*. J Biol Chem, 2003. **278**(39): p. 37409-12.
100. Vadlamudi, R.K., I. Joung, J.L. Strominger, and J. Shin, *p62, a phosphotyrosine-independent ligand of the SH2 domain of p56lck, belongs to a new class of ubiquitin-binding proteins*. J Biol Chem, 1996. **271**(34): p. 20235-7.
101. Geetha, T., M.L. Seibenhener, L. Chen, K. Madura, and M.W. Wooten, *p62 serves as a shuttling factor for TrkA interaction with the proteasome*. Biochem Biophys Res Commun, 2008. **374**(1): p. 33-7.
102. Korolchuk, V.I., F.M. Menzies, and D.C. Rubinsztein, *Mechanisms of cross-talk between the ubiquitin-proteasome and autophagy-lysosome systems*. FEBS Lett, 2010. **584**(7): p. 1393-8.
103. Kuusisto, E., A. Salminen, and I. Alafuzoff, *Ubiquitin-binding protein p62 is present in neuronal and glial inclusions in human tauopathies and synucleinopathies*. Neuroreport, 2001. **12**(10): p. 2085-90.
104. Nagaoka, U., K. Kim, N.R. Jana, H. Doi, M. Maruyama, K. Mitsui, F. Oyama, and N. Nukina, *Increased expression of p62 in expanded polyglutamine-expressing cells and its association with polyglutamine inclusions*. J Neurochem, 2004. **91**(1): p. 57-68.
105. Kuusisto, E., A. Salminen, and I. Alafuzoff, *Early accumulation of p62 in neurofibrillary tangles in Alzheimer's disease: possible role in tangle formation*. Neuropathol Appl Neurobiol, 2002. **28**(3): p. 228-37.
106. Komatsu, M., S. Waguri, M. Koike, Y.S. Sou, T. Ueno, T. Hara, N. Mizushima, J. Iwata, J. Ezaki, S. Murata, J. Hamazaki, Y. Nishito, S. Iemura, T. Natsume, T. Yanagawa, J. Uwayama, E. Warabi, H. Yoshida, T. Ishii, A. Kobayashi, M. Yamamoto, Z. Yue, Y. Uchiyama, E. Kominami, and K. Tanaka, *Homeostatic levels of p62 control cytoplasmic inclusion body formation in autophagy-deficient mice*. Cell, 2007. **131**(6): p. 1149-63.
107. Yue, Z., *Regulation of neuronal autophagy in axon: implication of autophagy in axonal function and dysfunction/degeneration*. Autophagy, 2007. **3**(2): p. 139-41.
108. Shvets, E., E. Fass, R. Scherz-Shouval, and Z. Elazar, *The N-terminus and Phe52 residue of LC3 recruit p62/SQSTM1 into autophagosomes*. J Cell Sci, 2008. **121**(Pt 16): p. 2685-95.

109. Ichimura, Y., T. Kumanomidou, Y.S. Sou, T. Mizushima, J. Ezaki, T. Ueno, E. Kominami, T. Yamane, K. Tanaka, and M. Komatsu, *Structural basis for sorting mechanism of p62 in selective autophagy*. J Biol Chem, 2008. **283**(33): p. 22847-57.
110. Layfield, R., B. Ciani, S.H. Ralston, L.J. Hocking, P.W. Sheppard, M.S. Searle, and J.R. Cavey, *Structural and functional studies of mutations affecting the UBA domain of SQSTM1 (p62) which cause Paget's disease of bone*. Biochem Soc Trans, 2004. **32**(Pt 5): p. 728-30.
111. Layfield, R. and L.J. Hocking, *SQSTM1 and Paget's disease of bone*. Calcif Tissue Int, 2004. **75**(5): p. 347-57.
112. Johnson-Pais, T.L., J.H. Wisdom, K.S. Weldon, J.D. Cody, M.F. Hansen, F.R. Singer, and R.J. Leach, *Three novel mutations in SQSTM1 identified in familial Paget's disease of bone*. J Bone Miner Res, 2003. **18**(10): p. 1748-53.
113. Laurin, N., J.P. Brown, J. Morissette, and V. Raymond, *Recurrent mutation of the gene encoding sequestosome 1 (SQSTM1/p62) in Paget disease of bone*. Am J Hum Genet, 2002. **70**(6): p. 1582-8.
114. Hocking, L.J., G.J. Lucas, A. Daroszewska, J. Mangion, M. Olavesen, T. Cundy, G.C. Nicholson, L. Ward, S.T. Bennett, W. Wuyts, W. Van Hul, and S.H. Ralston, *Domain-specific mutations in sequestosome 1 (SQSTM1) cause familial and sporadic Paget's disease*. Hum Mol Genet, 2002. **11**(22): p. 2735-9.
115. Hocking, L.J., G.J. Lucas, A. Daroszewska, T. Cundy, G.C. Nicholson, J. Donath, J.P. Walsh, C. Finlayson, J.R. Cavey, B. Ciani, P.W. Sheppard, M.S. Searle, R. Layfield, and S.H. Ralston, *Novel UBA domain mutations of SQSTM1 in Paget's disease of bone: genotype phenotype correlation, functional analysis, and structural consequences*. J Bone Miner Res, 2004. **19**(7): p. 1122-7.
116. Cavey, J.R., S.H. Ralston, P.W. Sheppard, B. Ciani, T.R. Gallagher, J.E. Long, M.S. Searle, and R. Layfield, *Loss of ubiquitin binding is a unifying mechanism by which mutations of SQSTM1 cause Paget's disease of bone*. Calcif Tissue Int, 2006. **78**(5): p. 271-7.
117. Falchetti, A., M. Di Stefano, F. Marini, F. Del Monte, C. Mavilia, D. Strigoli, M.L. De Feo, G. Isaia, L. Masi, A. Amedei, F. Cioppi, V. Ghinai, S.M. Bongi, G. Di Fede, C. Sferrazza, G.B. Rini, D. Melchiorre, M. Matucci-Cerinic, and M.L. Brandi, *Two novel mutations at exon 8 of the Sequestosome 1 (SQSTM1) gene in an Italian series of patients affected by Paget's disease of bone (PDB)*. J Bone Miner Res, 2004. **19**(6): p. 1013-7.
118. Fecto, F., J. Yan, S.P. Vemula, E. Liu, Y. Yang, W. Chen, J.G. Zheng, Y. Shi, N. Siddique, H. Arrat, S. Donkervoort, S. Ajroud-Driss, R.L. Sufit, S.L. Heller, H.X. Deng, and T. Siddique, *SQSTM1 mutations in familial and sporadic amyotrophic lateral sclerosis*. Arch Neurol, 2011. **68**(11): p. 1440-6.
119. Giuliani, C., G. Napolitano, I. Bucci, V. Montani, and F. Monaco, *[Nf-kB transcription factor: role in the pathogenesis of inflammatory, autoimmune, and neoplastic diseases and therapy implications]*. Clin Ter, 2001. **152**(4): p. 249-53.
120. Gilmore, T.D., *Introduction to NF-kappaB: players, pathways, perspectives*. Oncogene, 2006. **25**(51): p. 6680-4.
121. Dolcet, X., D. Llobet, J. Pallares, and X. Matias-Guiu, *NF-kB in development and progression of human cancer*. Virchows Arch, 2005. **446**(5): p. 475-82.
122. Perkins, N.D., *Integrating cell-signalling pathways with NF-kappaB and IKK function*. Nat Rev Mol Cell Biol, 2007. **8**(1): p. 49-62.
123. Jimi, E., K. Aoki, H. Saito, F. D'Acquisto, M.J. May, I. Nakamura, T. Sudo, T. Kojima, F. Okamoto, H. Fukushima, K. Okabe, K. Ohya, and S. Ghosh, *Selective inhibition of NF-kappa B blocks osteoclastogenesis and prevents inflammatory bone destruction in vivo*. Nat Med, 2004. **10**(6): p. 617-24.

124. Darnay, B.G., A. Besse, A.T. Poblenz, B. Lamothe, and J.J. Jacoby, *TRAFs in RANK signaling*. Adv Exp Med Biol, 2007. **597**: p. 152-9.
125. Lamothe, B., W.K. Webster, A. Gopinathan, A. Besse, A.D. Campos, and B.G. Darnay, *TRAF6 ubiquitin ligase is essential for RANKL signaling and osteoclast differentiation*. Biochem Biophys Res Commun, 2007. **359**(4): p. 1044-9.
126. Deng, L., C. Wang, E. Spencer, L. Yang, A. Braun, J. You, C. Slaughter, C. Pickart, and Z.J. Chen, *Activation of the I $\kappa$ B kinase complex by TRAF6 requires a dimeric ubiquitin-conjugating enzyme complex and a unique polyubiquitin chain*. Cell, 2000. **103**(2): p. 351-61.
127. de Bie, P. and A. Ciechanover, *Ubiquitination of E3 ligases: self-regulation of the ubiquitin system via proteolytic and non-proteolytic mechanisms*. Cell Death Differ, 2011. **18**(9): p. 1393-402.
128. Yang, W.L., X. Zhang, and H.K. Lin, *Emerging role of Lys-63 ubiquitination in protein kinase and phosphatase activation and cancer development*. Oncogene, 2010. **29**(32): p. 4493-503.
129. Wang, C., L. Deng, M. Hong, G.R. Akkaraju, J. Inoue, and Z.J. Chen, *TAK1 is a ubiquitin-dependent kinase of MKK and IKK*. Nature, 2001. **412**(6844): p. 346-51.
130. Cundy, T. and M. Bolland, *Paget disease of bone*. Trends Endocrinol Metab, 2008. **19**(7): p. 246-53.
131. Baud'huin, M., F. Lamoureux, L. Duplomb, F. Redini, and D. Heymann, *RANKL, RANK, osteoprotegerin: key partners of osteoimmunology and vascular diseases*. Cell Mol Life Sci, 2007. **64**(18): p. 2334-50.
132. Van Antwerp, D.J., S.J. Martin, I.M. Verma, and D.R. Green, *Inhibition of TNF-induced apoptosis by NF-kappa B*. Trends Cell Biol, 1998. **8**(3): p. 107-11.
133. Heyninck, K. and R. Beyaert, *Crosstalk between NF-kappaB-activating and apoptosis-inducing proteins of the TNF-receptor complex*. Mol Cell Biol Res Commun, 2001. **4**(5): p. 259-65.
134. Aggarwal, B.B., *Signalling pathways of the TNF superfamily: a double-edged sword*. Nat Rev Immunol, 2003. **3**(9): p. 745-56.
135. Wu, Y. and B.P. Zhou, *TNF-alpha/NF-kappaB/Snail pathway in cancer cell migration and invasion*. Br J Cancer, 2010. **102**(4): p. 639-44.
136. Funderburk, S.F., B.K. Marcellino, and Z. Yue, *Cell "self-eating" (autophagy) mechanism in Alzheimer's disease*. Mt Sinai J Med, 2010. **77**(1): p. 59-68.
137. Korolchuk, V.I., A. Mansilla, F.M. Menzies, and D.C. Rubinsztein, *Autophagy inhibition compromises degradation of ubiquitin-proteasome pathway substrates*. Mol Cell, 2009. **33**(4): p. 517-27.
138. Cheung, Z.H. and N.Y. Ip, *Autophagy deregulation in neurodegenerative diseases - recent advances and future perspectives*. J Neurochem, 2011. **118**(3): p. 317-25.
139. Fujita, N. and T. Yoshimori, *Ubiquitination-mediated autophagy against invading bacteria*. Curr Opin Cell Biol, 2011. **23**(4): p. 492-7.
140. Ichimura, Y. and M. Komatsu, *Pathophysiological role of autophagy: lesson from autophagy-deficient mouse models*. Exp Anim, 2011. **60**(4): p. 329-45.
141. Kim, P.K., D.W. Hailey, R.T. Mullen, and J. Lippincott-Schwartz, *Ubiquitin signals autophagic degradation of cytosolic proteins and peroxisomes*. Proc Natl Acad Sci U S A, 2008. **105**(52): p. 20567-74.
142. Yoshikawa, Y., M. Ogawa, T. Hain, M. Yoshida, M. Fukumatsu, M. Kim, H. Mimuro, I. Nakagawa, T. Yanagawa, T. Ishii, A. Kakizuka, E. Sztul, T. Chakraborty, and C. Sasakawa, *Listeria monocytogenes ActA-mediated escape from autophagic recognition*. Nat Cell Biol, 2009. **11**(10): p. 1233-40.

143. Zheng, Y.T., S. Shahnazari, A. Brech, T. Lamark, T. Johansen, and J.H. Brumell, *The adaptor protein p62/SQSTM1 targets invading bacteria to the autophagy pathway*. J Immunol, 2009. **183**(9): p. 5909-16.
144. Kimmelman, A.C., *The dynamic nature of autophagy in cancer*. Genes Dev, 2011. **25**(19): p. 1999-2010.
145. Ding, W.X., S. Manley, and H.M. Ni, *The emerging role of autophagy in alcoholic liver disease*. Exp Biol Med (Maywood), 2011. **236**(5): p. 546-56.
146. Hara, T., K. Nakamura, M. Matsui, A. Yamamoto, Y. Nakahara, R. Suzuki-Migishima, M. Yokoyama, K. Mishima, I. Saito, H. Okano, and N. Mizushima, *Suppression of basal autophagy in neural cells causes neurodegenerative disease in mice*. Nature, 2006. **441**(7095): p. 885-9.
147. Mizushima, N., T. Yoshimori, and B. Levine, *Methods in mammalian autophagy research*. Cell, 2010. **140**(3): p. 313-26.
148. Singh, R. and A.M. Cuervo, *Autophagy in the cellular energetic balance*. Cell Metab, 2011. **13**(5): p. 495-504.
149. Kabeya, Y., N. Mizushima, T. Ueno, A. Yamamoto, T. Kirisako, T. Noda, E. Kominami, Y. Ohsumi, and T. Yoshimori, *LC3, a mammalian homologue of yeast Apg8p, is localized in autophagosome membranes after processing*. EMBO J, 2000. **19**(21): p. 5720-8.
150. Mizushima, N. and B. Levine, *Autophagy in mammalian development and differentiation*. Nat Cell Biol, 2010. **12**(9): p. 823-30.
151. Nedelsky, N.B., P.K. Todd, and J.P. Taylor, *Autophagy and the ubiquitin-proteasome system: collaborators in neuroprotection*. Biochim Biophys Acta, 2008. **1782**(12): p. 691-9.
152. Mizushima, N. and T. Yoshimori, *How to interpret LC3 immunoblotting*. Autophagy, 2007. **3**(6): p. 542-5.
153. Johansen, T. and T. Lamark, *Selective autophagy mediated by autophagic adapter proteins*. Autophagy, 2011. **7**(3): p. 279-96.
154. Klionsky, D.J., H. Abeliovich, P. Agostinis, D.K. Agrawal, G. Aliev, D.S. Askew, M. Baba, E.H. Baehrecke, B.A. Bahr, A. Ballabio, B.A. Bamber, D.C. Bassham, E. Bergamini, X. Bi, M. Biard-Piechaczyk, J.S. Blum, D.E. Bredesen, J.L. Brodsky, J.H. Brumell, U.T. Brunk, W. Bursch, N. Camougrand, E. Cebollero, F. Cecconi, Y. Chen, L.S. Chin, A. Choi, C.T. Chu, J. Chung, P.G. Clarke, R.S. Clark, S.G. Clarke, C. Clave, J.L. Cleveland, P. Codogno, M.I. Colombo, A. Coto-Montes, J.M. Cregg, A.M. Cuervo, J. Debnath, F. Demarchi, P.B. Dennis, P.A. Dennis, V. Deretic, R.J. Devenish, F. Di Sano, J.F. Dice, M. Difiglia, S. Dinesh-Kumar, C.W. Distelhorst, M. Djavaheri-Mergny, F.C. Dorsey, W. Droge, M. Dron, W.A. Dunn, Jr., M. Duszenko, N.T. Eissa, Z. Elazar, A. Esclatine, E.L. Eskelinen, L. Fesus, K.D. Finley, J.M. Fuentes, J. Fueyo, K. Fujisaki, B. Galliot, F.B. Gao, D.A. Gewirtz, S.B. Gibson, A. Gohla, A.L. Goldberg, R. Gonzalez, C. Gonzalez-Estevez, S. Gorski, R.A. Gottlieb, D. Haussinger, Y.W. He, K. Heidenreich, J.A. Hill, M. Hoyer-Hansen, X. Hu, W.P. Huang, A. Iwasaki, M. Jaattela, W.T. Jackson, X. Jiang, S. Jin, T. Johansen, J.U. Jung, M. Kadowaki, C. Kang, A. Kelekar, D.H. Kessel, J.A. Kiel, H.P. Kim, A. Kimchi, T.J. Kinsella, K. Kiselyov, K. Kitamoto, E. Knecht, M. Komatsu, E. Kominami, S. Kondo, A.L. Kovacs, G. Kroemer, C.Y. Kuan, R. Kumar, M. Kundu, J. Landry, M. Laporte, W. Le, H.Y. Lei, M.J. Lenardo, B. Levine, A. Lieberman, K.L. Lim, F.C. Lin, W. Liou, L.F. Liu, G. Lopez-Berestein, C. Lopez-Otin, B. Lu, K.F. Macleod, W. Malorni, W. Martinet, K. Matsuoka, J. Mautner, A.J. Meijer, A. Melendez, P. Michels, G. Miotto, W.P. Mistiaen, N. Mizushima, B. Mograbi, I. Monastyrska, M.N. Moore, P.I. Moreira, Y. Moriyasu, T. Motyl, C. Munz, L.O. Murphy, N.I. Naqvi, T.P. Neufeld, I. Nishino, R.A. Nixon, T. Noda, B. Nurnberg, M. Ogawa, N.L. Oleinick, L.J. Olsen, B. Ozpolat, S. Paglin, G.E. Palmer, I. Papassideri, M. Parkes, D.H. Perlmuter, G.

- Perry, M. Piacentini, R. Pinkas-Kramarski, M. Prescott, T. Proikas-Cezanne, N. Raben, A. Rami, F. Reggiori, B. Rohrer, D.C. Rubinsztein, K.M. Ryan, J. Sadoshima, H. Sakagami, Y. Sakai, M. Sandri, C. Sasakawa, M. Sass, C. Schneider, P.O. Seglen, O. Seleverstov, J. Settleman, J.J. Shacka, I.M. Shapiro, A. Sibirny, E.C. Silva-Zacarin, H.U. Simon, C. Simone, A. Simonsen, M.A. Smith, K. Spanel-Borowski, V. Srinivas, M. Steeves, H. Stenmark, P.E. Stromhaug, C.S. Subauste, S. Sugimoto, D. Sulzer, T. Suzuki, M.S. Swanson, I. Tabas, F. Takeshita, N.J. Talbot, Z. Talloczy, K. Tanaka, K. Tanaka, I. Tanida, G.S. Taylor, J.P. Taylor, A. Terman, G. Tettamanti, C.B. Thompson, M. Thumm, A.M. Tolkovsky, S.A. Tooze, R. Truant, L.V. Tumanovska, Y. Uchiyama, T. Ueno, N.L. Uzcategui, I. van der Klei, E.C. Vaquero, T. Vellai, M.W. Vogel, H.G. Wang, P. Webster, J.W. Wiley, Z. Xi, G. Xiao, J. Yahalom, J.M. Yang, G. Yap, X.M. Yin, T. Yoshimori, L. Yu, Z. Yue, M. Yuzaki, O. Zabirnyk, X. Zheng, X. Zhu and R.L. Deter, *Guidelines for the use and interpretation of assays for monitoring autophagy in higher eukaryotes*. Autophagy, 2008. **4**(2): p. 151-75.
155. Ishii, T., T. Yanagawa, T. Kawane, K. Yuki, J. Seita, H. Yoshida, and S. Bannai, *Murine peritoneal macrophages induce a novel 60-kDa protein with structural similarity to a tyrosine kinase p56lck-associated protein in response to oxidative stress*. Biochem Biophys Res Commun, 1996. **226**(2): p. 456-60.
  156. Jain, A., T. Lamark, E. Sjøttem, K.B. Larsen, J.A. Awuh, A. Overvatn, M. McMahon, J.D. Hayes, and T. Johansen, *p62/SQSTM1 is a target gene for transcription factor NRF2 and creates a positive feedback loop by inducing antioxidant response element-driven gene transcription*. J Biol Chem, 2010. **285**(29): p. 22576-91.
  157. Kuusisto, E., T. Suuronen, and A. Salminen, *Ubiquitin-binding protein p62 expression is induced during apoptosis and proteasomal inhibition in neuronal cells*. Biochem Biophys Res Commun, 2001. **280**(1): p. 223-8.
  158. Kirkin, V., D.G. McEwan, I. Novak, and I. Dikic, *A role for ubiquitin in selective autophagy*. Mol Cell, 2009. **34**(3): p. 259-69.
  159. Fujita, K. and S.M. Srinivasula, *Ubiquitination and TNFR1 signaling*. Results Probl Cell Differ, 2009. **49**: p. 87-114.
  160. Bettermann, K., M. Benesch, S. Weis, and J. Haybaeck, *SUMOylation in carcinogenesis*. Cancer Lett, 2012. **316**(2): p. 113-25.
  161. Andersen, J.S., I. Matic, and A.C. Vertegaal, *Identification of SUMO target proteins by quantitative proteomics*. Methods Mol Biol, 2009. **497**: p. 19-31.
  162. Vertegaal, A.C., J.S. Andersen, S.C. Ogg, R.T. Hay, M. Mann, and A.I. Lamond, *Distinct and overlapping sets of SUMO-1 and SUMO-2 target proteins revealed by quantitative proteomics*. Mol Cell Proteomics, 2006. **5**(12): p. 2298-310.
  163. Knuesel, M., H.T. Cheung, M. Hamady, K.K. Barthel, and X. Liu, *A method of mapping protein sumoylation sites by mass spectrometry using a modified small ubiquitin-like modifier 1 (SUMO-1) and a computational program*. Mol Cell Proteomics, 2005. **4**(10): p. 1626-36.
  164. Wilkinson, K.A., Y. Nakamura, and J.M. Henley, *Targets and consequences of protein SUMOylation in neurons*. Brain Res Rev, 2010. **64**(1): p. 195-212.
  165. Vaskova, M., M. Kovac, P. Volna, P. Angelisova, E. Mejstrikova, J. Zuna, T. Brdicka, and O. Hrusak, *High expression of cytoskeletal protein drebrin in TEL/AML1pos B-cell precursor acute lymphoblastic leukemia identified by a novel monoclonal antibody*. Leuk Res, 2011. **35**(8): p. 1111-3.
  166. Kirkpatrick, D.S., C. Denison, and S.P. Gygi, *Weighing in on ubiquitin: the expanding role of mass-spectrometry-based proteomics*. Nat Cell Biol, 2005. **7**(8): p. 750-7.
  167. Denis, N.J., J. Vasilescu, J.P. Lambert, J.C. Smith, and D. Figeys, *Tryptic digestion of ubiquitin standards reveals an improved strategy for identifying ubiquitinated proteins by mass spectrometry*. Proteomics, 2007. **7**(6): p. 868-74.

168. Liu, X., Z. Liu, S.W. Jang, Z. Ma, K. Shinmura, S. Kang, S. Dong, J. Chen, K. Fukasawa, and K. Ye, *Sumoylation of nucleophosmin/B23 regulates its subcellular localization, mediating cell proliferation and survival*. Proc Natl Acad Sci U S A, 2007. **104**(23): p. 9679-84.
169. Pfander, B., G.L. Moldovan, M. Sacher, C. Hoege, and S. Jentsch, *SUMO-modified PCNA recruits Srs2 to prevent recombination during S phase*. Nature, 2005. **436**(7049): p. 428-33.
170. Ang, E., N.J. Pavlos, S.L. Rea, M. Qi, T. Chai, J.P. Walsh, T. Ratajczak, M.H. Zheng, and J. Xu, *Proteasome inhibitors impair RANKL-induced NF-kappaB activity in osteoclast-like cells via disruption of p62, TRAF6, CYLD, and IkappaBalpha signaling cascades*. J Cell Physiol, 2009. **220**(2): p. 450-9.
171. Xu, J., J.W. Tan, L. Huang, X.H. Gao, R. Laird, D. Liu, S. Wysocki, and M.H. Zheng, *Cloning, sequencing, and functional characterization of the rat homologue of receptor activator of NF-kappaB ligand*. J Bone Miner Res, 2000. **15**(11): p. 2178-86.
172. Zou, W., A. Amcheslavsky, S. Takeshita, H. Drissi, and Z. Bar-Shavit, *TNF-alpha expression is transcriptionally regulated by RANK ligand*. J Cell Physiol, 2005. **202**(2): p. 371-8.
173. Wang, C., J.H. Steer, D.A. Joyce, K.H. Yip, M.H. Zheng, and J. Xu, *12-O-tetradecanoylphorbol-13-acetate (TPA) inhibits osteoclastogenesis by suppressing RANKL-induced NF-kappaB activation*. J Bone Miner Res, 2003. **18**(12): p. 2159-68.
174. Funakoshi-Tago, M., N. Kamada, T. Shimizu, Y. Hashiguchi, K. Tago, Y. Sonoda, and T. Kasahara, *TRAF6 negatively regulates TNFalpha-induced NF-kappaB activation*. Cytokine, 2009. **45**(2): p. 72-9.
175. Collet, C., L. Michou, M. Audran, S. Chasseigneaux, P. Hilliquin, T. Bardin, I. Lemaire, F. Cornelis, J.M. Launay, P. Orcel, and J.L. Laplanche, *Paget's disease of bone in the French population: novel SQSTM1 mutations, functional analysis, and genotype-phenotype correlations*. J Bone Miner Res, 2007. **22**(2): p. 310-7.
176. Jin, W., M. Chang, E.M. Paul, G. Babu, A.J. Lee, W. Reiley, A. Wright, M. Zhang, J. You, and S.C. Sun, *Deubiquitinating enzyme CYLD negatively regulates RANK signaling and osteoclastogenesis in mice*. J Clin Invest, 2008. **118**(5): p. 1858-66.
177. Stegmeier, F., M.E. Sowa, G. Nalepa, S.P. Gygi, J.W. Harper, and S.J. Elledge, *The tumor suppressor CYLD regulates entry into mitosis*. Proc Natl Acad Sci U S A, 2007. **104**(21): p. 8869-74.
178. Sundaram, K., S. Shanmugarajan, D.S. Rao, and S.V. Reddy, *Mutant p62P392L stimulation of osteoclast differentiation in Paget's disease of bone*. Endocrinology, 2011. **152**(11): p. 4180-9.
179. Ju, J.S. and C.C. Weihl, *Inclusion body myopathy, Paget's disease of the bone and fronto-temporal dementia: a disorder of autophagy*. Hum Mol Genet, 2010. **19**(R1): p. R38-45.
180. Li, Y., J.C. Tharappel, S. Cooper, M. Glenn, H.P. Glauert, and B.T. Spear, *Expression of the hydrogen peroxide-generating enzyme fatty acyl CoA oxidase activates NF-kappaB*. DNA Cell Biol, 2000. **19**(2): p. 113-20.
181. Dhar, S.K., Y. Xu, and D.K. St Clair, *Nuclear factor kappaB- and specificity protein 1-dependent p53-mediated bi-directional regulation of the human manganese superoxide dismutase gene*. J Biol Chem, 2010. **285**(13): p. 9835-46.
182. Ponce, C., M. Torres, C. Galleguillos, H. Sovino, M.A. Boric, A. Fuentes, and M.C. Johnson, *Nuclear factor kappaB pathway and interleukin-6 are affected in eutopic endometrium of women with endometriosis*. Reproduction, 2009. **137**(4): p. 727-37.
183. Ewins, B.A., M. Vassiliadou, A.M. Minihaue, G.H. Rimbach, and P.D. Weinberg, *Techniques for quantifying effects of dietary antioxidants on transcription factor translocation and nitric oxide production in cultured cells*. Genes Nutr, 2006. **1**(2): p. 125-31.

184. Kurihara, N., Y. Hiruma, H. Zhou, M.A. Subler, D.W. Dempster, F.R. Singer, S.V. Reddy, H.E. Gruber, J.J. Windle, and G.D. Roodman, *Mutation of the sequestosome 1 (p62) gene increases osteoclastogenesis but does not induce Paget disease*. J Clin Invest, 2007. **117**(1): p. 133-42.
185. Daroszewska, A., R.J. van 't Hof, J.A. Rojas, R. Layfield, E. Landao-Basonga, L. Rose, K. Rose, and S.H. Ralston, *A point mutation in the ubiquitin-associated domain of SQSTM1 is sufficient to cause a Paget's disease-like disorder in mice*. Hum Mol Genet, 2011. **20**(14): p. 2734-44.
186. Mabb, A.M., S.M. Wuerzberger-Davis, and S. Miyamoto, *PIASy mediates NEMO sumoylation and NF-kappaB activation in response to genotoxic stress*. Nat Cell Biol, 2006. **8**(9): p. 986-93.



## **VITA**

**NAME:** Xiaoyan Liu

**DATE AND PLACE OF BIRTH:** June 10, 1983, Wuhan City, Hubei Province, China.

### **EDUCATION**

2007.5- Present Research Assistant, Department of Molecular and Cellular Biochemistry, University of Kentucky

2006.8-2007.5 Research Assistant, Integrated Biomedical Sciences (IBS), University of Kentucky

2002.9-2006.6 B.S. Biotechnology, Huazhong University of Science and Technology, Wuhan, Hubei, China

1999.9-2002.6 NO.1 Middle School Attached to Central China Normal University, Wuhan, Hubei, China

1995.9-1999.6 NO. 45 Middle School of Hubei Province, Wuhan, Hubei, China

### **HONORS AND AWARDS**

#### **Graduate**

2009 Molecular and Cellular Biochemistry Department's Research Challenge Trust Fund Award

#### **Undergraduate**

2006 Second Prize Thesis Award. (Title: "The expression of fluorescent sensors", Mentor: Prof. Tao Xu.)

2004 "Excellent Academic Students" for NO.1 student in my grade. 3000 RMB

2003 "Excellent Academic Students" for NO.1 student in my grade. 3000 RMB

### **PUBLICATIONS**

#### **Graduate**

**Xiaoyan Liu**, Jozsef Gal and Haining Zhu. P62/Sequestosome 1: A multi-domain protein with multi-faceted functions. *Frontiers in Biology*, 2012. DOI: 10.1007/s11515-012-1217-z (in press).

Ping Shi, Jozsef Gal, David Kwinter, **Xiaoyan Liu**, Haining Zhu. Mitochondrial dysfunction in amyotrophic lateral sclerosis. *Biochim Biophys Acta*, 2010. 1802(1): p. 45-51.

Jianjun Zhai, **Xiaoyan Liu**, Zhenyu Huang, and Haining Zhu. RABA (Reductive Alkylation By Acetone): A Novel Stable Isotope Labeling Approach for Quantitative Proteomics. *J Am Soc Mass Spectrom*, 2009. 20(7): p. 1366-77.

**Xiaoyan Liu**, Fujian Zhang, Jianjun Zhai and Haining Zhu. Identification of novel SUMOylated proteins in mammalian cells (ready to submit).

**Xiaoyan Liu**, Jozsef Gal, Jiake Xu, Weimin Gong and Haining Zhu. Analysis of the role of p62 mutants in NF- $\kappa$ B signaling pathway related to Paget's disease of bone (in preparation).

### **Undergraduate**

Xingfu Liu, Yuanxi Wu, Longjiang Yu and **Xiaoyan Liu**. "On the cultivation of "little teacher's" ability in experimental biochemistry teaching reform." *Experimental Technology and Management*, 2005. 22(2):102-105.

Ying Xiong, **Xiaoyan Liu** and Chang-Guo Zhan. "Molecular docking and molecular dynamics simulation on cocaine binding with antibody 15A10", *Journal of Central China Normal University (Natural Science)*, 2005. 39(2): 205-207.

### **TEACHING**

2008 Spring Semester

Biochemistry 401G FUNDAMENTALS OF BIOCHEMISTRY: DNA Replication, Repair and Recombination (undergraduate)

### **ACTIVITY**

- Chairperson of oral presentation sessions for five years at Biochemistry Departmental Retreat (2007-2011)  
2007-2008 Pine Mtn. State Resort Park, Pineville, Kentucky  
2009-2011 Cumberland Falls State Park, Corbin, Kentucky
- Organizer for the Ice Cream Social for Biochemistry Department, July, 2010
- Organizer for the Holiday Food Drive Donation (2009, 2011)

## **MEMBERSHIP**

2010-Present Member of American Society for Mass Spectrometry (ASMS)

## **PRESENTATIONS**

### **One invited talk**

**Xiaoyan Liu**, Jianjun Zhai, Zhenyu Huang, Haining Zhu. “Novel Stable Isotope Labeling for Quantitative Proteomics.” American Chemical Society Central Regional Meeting; Covington KY; May, 2007.

### **Four student seminars of department**

**Xiaoyan Liu**, Bennett E.J. *et al.* (2007) Global changes to the ubiquitin system in Huntington's disease. *Nature* 448, 704-708. BBSRB 202A, Feb 6<sup>th</sup>, 2008

**Xiaoyan Liu**, Wang *et al.* (2009) Oncogenic Function of ATDC in Pancreatic Cancer through Wnt Pathway Activation and  $\beta$ -Catenin Stabilization. *Cancer Cell* 15, 207-219. BBSRB 202A, Apr 9<sup>th</sup>, 2009

**Xiaoyan Liu**, Shin, O.H. *et al.* (2010) Munc13 C<sub>2</sub>B domain is an activity-dependent Ca<sup>2+</sup> regulator of synaptic exocytosis. *Nat Struct Mol Biol* 17, 280-288. BBSRB 202A, Mar 25<sup>th</sup>, 2010

**Xiaoyan Liu**, The role of p62 mutants in NF- $\kappa$ B signaling pathway related to Paget's Disease of Bone. BBSRB 202A, Mar 3<sup>rd</sup>, 2011

### **One invited data club**

**Xiaoyan Liu**, Data Club. BBSRB B231, Feb 27<sup>th</sup>, 2009

### **Five posters in the department summer retreat**

**Xiaoyan Liu**, Jianjun Zhai, Zhenyu Huang, Haining Zhu. “Proteomic Studies of Amyotrophic Lateral Sclerosis (ALS).” Pine Mtn. State Resort Park, Pineville, KY; August, 2007.

**Xiaoyan Liu**, Jianjun Zhai, Anna-Lena Britt Ström, Haining Zhu. Proteomic Characterization of Proteins Associated with Axonal Transport Machinery. Pine Mtn. State Resort Park, Pineville, KY; July, 2008.

**Xiaoyan Liu**, Jozsef Gal and Haining Zhu. Analysis of the role of p62 mutants in Paget's

disease of bone. Cumberland Falls State Park, Corbin, Kentucky; May, 2009.

**Xiaoyan Liu**, Jozsef Gal and Haining Zhu. Analysis of the role of p62 mutants in NF- $\kappa$ B signaling pathway related to Paget's disease of bone. Cumberland Falls State Park, Corbin, Kentucky; May, 2010.

**Xiaoyan Liu**, Jozsef Gal and Haining Zhu. The role of p62 mutants in NF- $\kappa$ B signaling pathway related to Paget's disease of bone. Cumberland Falls State Park, Corbin, Kentucky; May, 2011.

#### **Six posters in the conferences**

**Xiaoyan Liu**, Jianjun Zhai, Zhenyu Huang, Haining Zhu. "A Novel Stable Isotope Labeling for Quantitative Proteomics." 55th ASMS Conference on Mass Spectrometry and Allied Topics, Indianapolis IN; June, 2007.

**Xiaoyan Liu**, Fujian Zhang, Haining Zhu. Proteomic Analysis of SUMOylated Protein in Mammalian Cells. ASBMB Conference, San Diego, California; April, 2008.

**Xiaoyan Liu**, Fujian Zhang, Jianjun Zhai, Haining Zhu. Proteomic Analysis of SUMOylated Proteins in Mammalian Cells. 57th ASMS Conference on Mass Spectrometry and Allied Topics, Philadelphia PA; June, 2009.

Zhenyu Huang, Ravi Akundi, Lisa Boock, **Xiaoyan Liu**, Haining Zhu and Hansruedi Bueler<sup>1</sup>. Generation and initial characterization of cells and mice lacking the recessive parkinsonism-associated gene pink1. "2009 Center for Clinical and Translational Science Spring conference", Lexington, KY, April 23, 2009.

Ravi Akundi<sup>1</sup>, Zhenyu Huang, Lisa Boock, **Xiaoyan Liu**, Haining Zhu, Hansruedi Bueler<sup>1</sup>. Generation and characterization of cells and mice lacking the recessive Parkinsonism-associated gene PINK1. "Society for Neuroscience" annual conference , October 17-21, Chicago, IL, 2009.

Ravi Akundi, Zhenyu Huang, Lisa Boock, **Xiaoyan Liu**, Haining Zhu, Hansruedi Bueler<sup>1</sup>. Generation and characterization of cells and mice lacking the recessive Parkinsonism-associated gene PINK1. Third Annual Postdoctoral Poster Session. BBSRB Atrium. December 9, 2009.